Effects of ocean acidification on reef-building corals: Understanding variability and projecting population-level impacts

Neil Ching Siang Chan

March 2015

For the degree of Doctor of Philosophy

in the College of Marine and Environmental Sciences

James Cook University

STATEMENT OF ACCESS

I, the undersigned, the author of this thesis, understand that James Cook University will make this thesis available for use within the University Library and via the Australia Digital Theses network (unless granted any exemption) for use elsewhere.

I understand that, as an unpublished work, a thesis has significant protection under the Copyright Act and;

I wish this work to be embargoed until March 2016.

_____ _____

Signature Date

ELECTRONIC COPY OF THESIS

I, the undersigned, the author of this work, declare that the electronic copy of this thesis provided to the James Cook University Library is an accurate copy of the print thesis submitted, within the limits of the technology available.

_____ _____

Signature Date

STATEMENT OF SOURCES

I, declare that this thesis is my own work and has not been submitted in any other form for another degree or diploma at any university or other institution of tertiary education. Information derived from the published or unpublished work of others has been acknowledged in the text and a list of references is given.

_____ _____

Signature Date

STATEMENT ON THE CONTRIBUTION OF OTHERS

CONTRIBUTION OF ALL AUTHORS TO CO-AUTHORED ACCOMPANYING PAPERS

Chapter 2

Neil Chan co-conceived the project, co-designed the analysis, collected the data and performed the meta-analysis, and led writing of the paper.

Sean Connolly co-conceived the project, co-designed the analysis, and made suggestions on and edits to multiple drafts of the paper

Chapter 3

Neil Chan co-conceived the project, designed, constructed and parameterized the model, ran simulations with the model, and led writing of the paper.

Sean Connolly co-conceived the project, provided advice about data analysis, and made suggestions on and edits to multiple drafts of the paper.

Chapter 4

Neil Chan conceived the project, designed the experiment, contributed reagents/materials/analysis tools, performed the experiment, analysed the data, and led writing of the paper.

Sean Connolly contributed reagents/materials/analysis tools, provided advice about data analysis, and made suggestions on and edits to multiple drafts of the paper.

Ken Anthony provided advice about experimental design and equipment set up, contributed reagents/materials/analysis tools, and made suggestions on and edits to multiple drafts of the paper.

Chapter 5

Neil Chan conceived the project, designed and constructed the model, co-designed the experiments, co-performed the experiments, analysed the data, and led writing of the paper.

Daniel Wangpraseurt[1] co-designed the experiments, co-performed the experiments, provided advice about data analysis, and made suggestions on and edits to multiple drafts of the paper

Sean Connolly contributed materials/analysis tools, provided advice about data analysis, and made suggestions on and edits to multiple drafts of the paper

Michael Kühl[1,2,3] contributed materials/analysis tools, provided advice on data analysis and result interpretation, and reviewed a draft of the paper

1. Plant Functional Biology and Climate Change Cluster, University of Technology Sydney, Sydney, NSW 2007 Australia

2. Marine Biology Section, Department of Biology, University of Copenhagen, DK-3000 Helsingor, Denmark

3. Singapore Centre on Environmental Life Sciences Engineering, School of Biological Sciences, Nanyang Technology University, 639798 Singapore

OTHER CONTRIBUTIONS

Mia Hoogenboom[1] provided invaluable insights into the interpretation of results with respect to flow, photosynthesis and feeding (Chapter 2 & 4) and also some parameter estimates for the model (Chapter 3)

Sue-Anne Watson[1] provided technical assistance with the use of the titrator (Chapter 4)

David Suggett[2] (Chapter 2), Jess Hopf[1] (Chapter 3) and anonymous reviewers (Chapter 2 & 4) provided comments and suggestions that improved the chapters

1. College of Marine and Environmental Sciences, James Cook University, Townsville, Queensland 4811 Australia

2. Plant Functional Biology and Climate Change Cluster, University of Technology Sydney, Sydney, NSW 2007 Australia

ACKNOWLEDGEMENTS

First and foremost, I'd like to express my sincere appreciation to my supervisors, Professor Sean Connolly and Dr. Ken Anthony. Thank you Sean for your intellectual guidance, support and patience throughout my PhD candidature. And Ken, thank you for sharing your practical and experimental skills.

I would like to thank all the people who provided field and lab support for this works. Thanks to Ross Barrett and Greg Napier for constructing my flow tanks. Sue-Anne Watson for answering my never-ending questions about using the titrator, pH scales and standards. To all the guys at Reef HQ who helped make the experiments there run smoothly, Stephen Menzies, Michael Shanahan, Chris Benstead and Andrea Severati among others, a heartfelt thank you. Thanks also go to Thomas Roberts, Chris Benstead, Shane Blowes, Martin van der Meer and Jessica Nowicki for assisting me on coral collecting trips. I would also like to thank Isobel Cummings for sharing her acidified seawater for the experiments at UTS.

A huge thank you to Mia Hoogenboom for all your invaluable advice on everything flow and photosynthesis related and for the helpful discussions that guided many of the projects. I am grateful also to all the people who have been members of JCU's Theoretical Ecology Lab over the years. Thank you Mia, Shane, Mizue, Loic, Jess, Martino, Jordan, Paulina, Theo, Mariana, Ben, Ed, Erin and Stephen for sitting through countless presentations of my research but always having honest and constructive feedback.

Finally, thanks to Mum and Dad for giving me the opportunity and support to reach my dreams, I can never thank you enough. And to all the friends and family who have been patient with me through one of the longest PhDs ever!

ABSTRACT

Understanding the long-term ecosystem level impacts of ocean acidification on marine environments is critical to informing national and international policies on carbon emission targets. However, key to understanding such long-term impacts is the ability of projection models to scale up short-term physiological responses to long-term ecosystem-level impacts. This thesis aims to improve upon previous models projecting the impacts of ocean acidification on coral reefs by incorporating the effects of ocean acidification on every stage of the coral life cycle, and also by deepening our understanding of how flow potentially influences the effects of ocean acidification on calcification.

Experimental studies investigating the effects of ocean acidification on calcification have produced a wide range of responses. However, as yet there have been no attempts to produce a summary response that can be used in projection models. Thus in Chapter 2, I use regression-based meta-analysis to produce a quantitative summary of the effect of ocean acidification on calcification from all existing experimental studies. I also test several factors that may explain significant amounts of variability in experimental results so far. The effect of ocean acidification on calcification was found to be less sensitive than originally thought, ~15% per unit change in aragonite saturation state (Ω_{Arag}). I also found that studies employing buoyant weighting found significantly smaller decreases in calcification per unit Ω_{Arag} (~10%), compared to studies using the alkalinity anomaly technique (~25%).

Despite recent studies suggesting that coral recruitment (when including the effects on crustose coralline algae) is very sensitive to ocean acidification, projection models to date have yet to take into account the effects of ocean acidification on pre- and post-settlement stages of corals. In Chapter 3, I used the quantitative summary from Chapter 2, combined

with a similar meta-analysis of recruitment, in an integral projection model to evaluate the effects of ocean acidification on growth and recruitment on long-term population growth. I found that the effects of ocean acidification on recruitment potentially exert more influence on long-term population growth rate than the effects of ocean acidification on growth, although there is substantial uncertainty associated with recruitment-mediated effects, due to the comparative paucity of studies of effects of ocean acidification on this aspect of the life cycle.

The meta-analysis of the effects of ocean acidification on calcification also revealed that among-study variation is large. It had been suggested that interactions between ocean acidification and other factors might account for a proportion of the variability between experimental results. One potential interacting factor that has not received any attention is flow, despite its long recognized role in shaping reefs through its influence on mass-transfer rates. In Chapter 4, I show, using flume experiments, that flow, through its effects on photosynthesis, mediates the effect of ocean acidification on calcification of *Acropora secale*. The interactive effect is large, with the sensitivity of calcification to decreasing Ω_{Arag} increasing by ~0.5% per cms^{-1} increase in flow. To elucidate the mechanisms behind the flow-ocean acidification interaction, I then use an experimental micro-sensor study to parameterize a basic diffusion-reaction-uptake model (Chapter 5). The model predicted tissue surface pH well and showed that low flow, through thickening of the diffusive boundary layer, increases tissue surface pH. However, these elevations in tissue surface pH have been found at relatively low flows that are rarely encountered by corals in nature, suggesting that the DBL effect is unlikely to ameliorate the decreases in coral calcification under ocean acidification.

The overarching aim of my thesis was to improve upon previous models projecting the impacts of ocean acidification on coral reefs. This is achieved both by incorporating the effects of ocean acidification (from all existing experimental studies) on every stage of the coral life cycle into projections, and also by deepening our understanding of an important interactive factor (flow) that is driving variability in sensitivity of calcification to ocean acidification. In a broader context, this thesis provides a template for quantitatively summarizing existing knowledge of how demographic rates change in response to a stressor, and a modelling framework that can be used to assess the impacts those changes on population growth and stability.

TABLE OF CONTENTS

LIST OF FIGURES

Chapter 2

Chapter 3

Chapter 4

Chapter 5

LIST OF TABLES

Chapter 3

Chapter 4

Chapter 5

1. General Introduction

Due to anthropogenic fossil fuel burning, atmospheric CO_2 has risen from pre-industrial levels of ~280 ppm to ~380ppm (Sabine et al., 2004, Feely et al., 2009). If fossil fuel consumption continues unabated, atmospheric CO_2 is projected to double (RCP 6.0 Kw^{-2}: stabilization scenario in which total radiative forcing is stabilized shortly after 2100, by the application of a range of technologies and strategies) or triple (RCP 8.0: scenario with increasing greenhouse gas emissions over time) by the end of this century (IPCC, 2013, Tans, 2009). This rise in atmospheric CO_2 leads not only to global warming, but also a phenomenon known as ocean acidification. Ocean acidification refers to the lowering of the pH of the oceans due to atmospheric carbon dioxide (CO_2) dissolving into the oceans (Doney et al., 2009).

Lowering of pH alters the distribution of dissolved inorganic carbon (DIC), which comprises 3 species (dissolved carbon dioxide (CO_2), bicarbonate (HCO_3^-) and carbonate ions (CO_3^{2-})) that are linked by the following reversible chemical reactions:

$$CO_2 + H_2O \leftrightarrow H_2CO_3 \leftrightarrow HCO_3^- + H^+ \leftrightarrow CO_3^{2-} + 2H^+$$ (Zeebe and Wolf-Gladrow, 2001)

The distribution of these chemical species is set by the two equilibrium constants that describe the acid/base reactions of inorganic carbon in seawater:

$$K_1 = \frac{[HCO_3^-][H^+]}{[CO_2]} \text{ and } K_2 = \frac{[CO_3^{2-}][H^+]}{[HCO_3^-]}$$ Eqn 1.1

where [X] is the total concentration of component X in seawater, and K_1 and K_2 are the equilibrium constants which depend on temperature, salinity and pressure (Dickson and Millero, 1987). Speciation depends strongly on pH ($pH = -\log_{10}[H^+]$). In 'standard' surface seawater pH_T of ~8.05, the distribution is 90% HCO_3^-, 10% CO_3^{2-}, <1% CO_2. Ocean

acidification leads to an increase in hydrogen ions (H^+) and HCO_3^-, and a decrease in CO_2 & CO_3^{2-}.

1.1 Ocean acidification: Implications for reef-building corals

Aragonite saturation state (Ω_{Arag}) is a measure of the thermodynamic potential for aragonite to precipitate or dissolve, and is described by the following equation:-

$$\Omega_{Arg} = \frac{[Ca^{2+}][CO_3^{2-}]}{K_{sp}} \qquad \text{Eqn 1.2}$$

where $[Ca^{2+}]$ and $[CO_3^{2-}]$ are concentrations of calcium and carbonate, respectively, and K_{sp} is the solubility constant for a particular mineral phase of $CaCO_3$ (Stumm and Morgan, 1981). K_{sp} is dependent on temperature, salinity and pressure. Due to the concentration of Ca^{2+} being conservative and determined solely by the salinity of the ocean (which generally vary by less than +/- 10%), Ω_{Arag} is determined entirely by $[CO_3^{2-}]$, temperature and salinity. A value of unity means saturation equilibrium (i.e. neither precipitation nor dissolution is thermodynamically favoured), while values greater than 1 indicate supersaturation. Present day surface seawater is supersaturated with typical values of 3.4-3.8 at temperature of 25°C and salinity of 35ppt (Gattuso et al., 1999). Ω_{Arag} is expected to decline to about 2.1 – 2.5 under RCP 6.0 (IPCC, 2013).

Aragonite ($CaCO_3$) is the specific mineral form of calcium carbonate from which coral skeleton is constructed. It is known from chemical theory that the precipitation of aragonite is increasingly facilitated as Ω_{Arag} increases above 1.0. Changes in the aspect ratio of aragonite minerals in coral skeletons grown under low Ω_{Arag} indicate reduced rates of biomineralization (Cohen and Holcomb, 2009). Because of this, some ocean acidification researchers have argued that ocean acidification will slow rates of coral calcification to the

point where rates of reef erosion exceed rates of skeletal accretion, leading to widespread loss of coral reef ecosystems as we know them (e.g. Silverman et al. 2009).

The study of the effects of ocean acidification is a relatively new field. Studies specifically designed to test the impacts of rising atmospheric CO_2 on coral and coral reef communities began in the late 1990s (e.g. Marubini & Atkinson, 1999, Gattuso et al. 1999, Langdon et al. 2000). Most of these studies have focused on the effects of ocean acidification on the calcification of adult coral colonies, but studies investigating the effects of ocean acidification on pre- and post- settlement stages are beginning to emerge (see Chua et al. 2013 for a review). While adult calcification rate has mostly been found to vary positively with Ω_{Arag}, there has been large variability in their sensitivity: ranging from a 25% increase to a 66% decrease in calcification per unit decrease in Ω_{Arag} (Pandolfi et al. 2011). Moreover, our knowledge of the impacts of ocean acidification is based overwhelmingly on short-term experimental studies of individual organisms' physiological responses. However, it is concerns about reef-scale impacts that will inform national and international policies on carbon emission targets. Thus, projection models have been employed to scale these individual physiological responses up to reef-scale responses. Unfortunately there are shortcomings in current projection models that must be addressed if we are to adequately project the long-term reef-scale impacts of ocean acidification.

1.2 Shortcomings in the way effects of ocean acidification are currently being modelled

Firstly, as the primary concern has been the slowing of calcification by ocean acidification, many models have (e.g. Silverman et al. 2009, van Hooidonk et al. 2013). While projections of this type give important insights into whether reef accretion can keep up with erosion, they only tell part of the story. Corals have complex life cycles, with pelagic larvae and sessile adults. Ocean acidification has recently been shown to reduce rates of

larval recruitment (Albright et al. 2010, Doroupolus et al. 2012, Webster et al. 2013) which could have large impacts on population level measures such as abundance, percentage cover, and long-term population growth rate, and thus flow on effects for ecosystem level calcification. Thus it is necessary to consider the effects of ocean acidification on every part of the life cycle of corals.

Secondly, models predicting the population level impacts of ocean acidification have often modelled coral cover in aggregate, using non-size structured models (e.g. Baskett et al. 2009, Anthony et al. 2011). However, corals have been shown to have size dependent fecundity (Hall & Hughes 1996) and mortality (Madin et al. 2014). Ocean acidification driven decreases in calcification will lead to either a decrease in growth rate, a decrease in skeletal density, or a combination of the two. If it's a decrease in growth, it will lead to decreased fecundity and lifetime reproductive output, and also increased mortality as coral colonies spend longer in more vulnerable smaller size classes. If it's a decrease in skeletal density, colonies (especially branching ones) will be less tolerant to wave action and storms, leading to decreased niche width and increased mortality, respectively. Thus, non-size structured models do not adequately capture the full effect of ocean acidification.

Thirdly, because there is no good consensus of how calcification declines with ocean acidification (the 4th IPCC report reported a 20 – 60% decrease in calcification by 2100, the 5th IPCC report did not even contain a consensus estimate), most models are based on the calcification-Ω_{Arag} relationship from a single experimental study. As an example, projections in Silverman et al. (2009) are based on the relationship in Silverman et al. (2007), while projections in Anthony et al. (2011) based on the relationship in Anthony et al. (2008). The only exception is Madin et al. (2012), who explored relationships from three different studies that form extremes that bracketed all other relationships (Langdon & Atkinson, 2005,

Silverman et al 2007, Anthony et al 2008). As pointed out in the previous section, there is large variability in experimental results in the sensitivity of calcification to ocean acidification, thus there is a need to quantitatively synthesize existing experimental results into an average sensitivity.

1.3 Interactions between ocean acidification and other factors

Aside from Ω_{Arag}, studies examining environmental limits of coral reefs have identified temperate and light as the other primary determinants that potentially affect reef distribution, while salinity, hydrodynamic conditions and biological variables have been classified as secondary determinants (Kleypas et al., 1999b). A number of studies have examined the interactive effects of ocean acidification and temperature, nutrients or light, and the results support the position that interactions between ocean acidification and other factors may account for a proportion of the variability between experimental results to date (Atkinson and Cuet, 2008, Pandolfi et al., 2011). Calcification has generally been found to be more sensitive to ocean acidification when corals are also experiencing elevated temperatures (Reynaud et al., 2003, Anthony et al., 2008, Edmunds et al., 2012). However, some studies have found no interaction between ocean acidification and temperature (Langdon & Atkinson, 2005), whereas others have found certain species (e.g., massive *Porites*) to be resistant to both ocean acidification and increases in temperature (Edmunds et al 2012). Effects of ocean acidification on calcification have been found to be lessened when nutrients are added to the water surrounding corals (Langdon and Atkinson, 2005, Atkinson and Cuet, 2008, Renegar and Riegl, 2005, Marubini and Atkinson, 1999, Atkinson et al., 1995). The interactive effect of light and ocean acidification is more variable. Some have found calcification to be more sensitive to ocean acidification under optimum light (compared to suboptimum light) (Comeau et al., 2013b, Marubini et al., 2001, Dufault et al., 2013) while others have found calcification to be more sensitive to ocean acidification under low light

(Suggett et al., 2012). Yet others have found no interaction between light and ocean acidification (Comeau et al., 2013a, Langdon and Atkinson, 2005).

1.4 Flow: a potential interacting factor

One potential interacting factor that has not received any attention is flow, although water-flow rates have a long recognized role in shaping reefs (Done 1983). Numerous studies have documented the positive influence of flow on the nutrient uptake rates (Atkinson and Bilger, 1992, Thomas and Atkinson, 1997, Reidenbach et al., 2006, Falter et al., 2004, Baird and Atkinson, 1997), photosynthetic production (Dennison and Barnes, 1988, Hoogenboom and Connolly, 2009, Carpenter and Willaims, 2007) and nitrogen fixation in corals and algae (Carpenter et al., 1991, Willaims and Carpenter, 1988), proving that the exchange of metabolites between reef communities and their surrounding environment is mass transfer limited (Falter et al., 2005, Falter et al., 2004). The cause of this positive relationship between flow and uptake rates is the thin layer of water, where molecular diffusion governs the passage of dissolved substances (e.g. nutrients and carbon species), which exists at the surface of aquatic organism. This water film, which is typically only 10s to 100s um thick, is known as the diffusive boundary layer (DBL) (Falter et al., 2005). The rate at which molecules diffuse across DBLs depends both on the thickness of the DBL and on the internal and external concentrations of molecules (Fick's laws: (Nobel 1983)). DBL thickness depends on water flow velocity and turbulence. Higher flow leads to thinner DBLs, and thus enables greater mass flux across the DBL. Likewise, turbulence leads to an effectively thinner DBL and greater mass flux. Under conditions of mass transfer limitation, thinning of the DBL can promote transport of metabolites and increase physiological processes.

Because ocean acidification modifies the external concentration of molecules, the effects of ocean acidification on both calcification and photosynthesis have been proposed to

be linked to the uptake of available carbon (in the form of CO_3^{2-}, HCO_3^- or CO_2) from bulk seawater (Comeau et al., 2012, Schneider and Erez, 2006) and the efflux of excess H^+ back into bulk seawater (Jokiel 2011a,b). Flow, through its influence on mass transfer would thus be expected to interact with ocean acidification. Moreover, flow has also been shown to influence particle capture success (Sebens et al., 1997), which could have flow on effects as corals have been shown to be less sensitive to ocean acidification when able to feed heterotrophically (Edmunds, 2011).

1.5 Thesis overview

If we are to truly understand the long-term ecosystem level impacts of ocean acidification on coral reefs, we will need projection models that adequately describe the effects of ocean acidification on coral populations. This chapter has identified a number of areas where research should be targeted in order to improve on existing models projecting the future abundance and distribution of reef-building corals. In the first half of the thesis, I focus on building a model that takes into account responses of calcification to ocean acidification from all available experimental studies and also incorporates the effects of ocean acidification on recruitment. In the second half, I aim to reduce the uncertainty in projections by investigating the interacting effects of flow and ocean acidification as a potential source of variation in the response of calcification to ocean acidification.

For models to take into account calcification sensitivity from all available experimental studies, a better consensus estimate is needed. As noted above, experimental studies investigating the effects of ocean acidification on calcification have produced a wide range of responses. And while there have been a number of attempts to summarize the data (Hendriks et al 2010, Kroeker et al 2010), these attempts only tell us whether there is a response, and if there is, whether it is positive or negative. As yet there have been no attempts

to produce a summary response that can be used in projection models (i.e. mean % decline in calcification per unit decline in Ω_{Arag}). Nor have there been attempts to quantify the variability in responses. In Chapter 2, I use regression-based meta-analysis to produce a quantitative summary of experimental results on the effects of ocean acidification on calcification and quantify the variability around this consensus estimate. I also tested whether methodological and biological factors that have been hypothesized to drive variation in response magnitude explain a significant proportion of the among-study variation.

There have been many studies investigating the effects of ocean acidification on calcification, but only recently have studies investigating the effects of ocean acidification on coral recruitment begun to emerge. These studies suggest that coral recruitment (when including the effects on crustose coralline algae) is very sensitive to ocean acidification. However, projection models to date have yet to take into account the effects of ocean acidification on pre- and post-settlement stages of corals. In Chapter 3, I produce a quantitative summary of experimental results on the effects of ocean acidification on recruitment. Using this estimate and the estimate of sensitivity of calcification to ocean acidification from Chapter 2, I build an integral projection model to determine the relative impacts of the effects of ocean acidification on growth and recruitment on long-term population growth rate, and to assess whether the impacts are additive or synergistic. Studies have suggested that life-history traits can predict which corals will be 'winners' and 'losers' in the face of environmental change (Loya et al. 2001, van Woesik et al. 2012), so I also investigate if life-history strategy of fast versus slow growing has any effect on the impacts of the effects of ocean acidification on long-term population growth rate.

In Chapters 4 and 5, I attempt to reduce the uncertainty in model projections by exploring interactions between ocean acidification and flow. Given that flow affects mass

transfer through its effects on the DBL, and the effects of ocean acidification on corals have been proposed to be linked to the uptake of available carbon or efflux of excess H^+ and O_2 (Mass et al., 2010), flow has been suggested as a factor that could lead to variation between predicted responses and actual findings of ocean acidification studies (Hendriks et al., 2010). However, no study at the date of commencement of our experiments had looked at the interactive effects of flow and ocean acidification on coral metabolism. In Chapter 4, I use a flume study to show that flow mediates the effect of ocean acidification on calcification of *Acropora secale*.

Low flow, which leads to increases in tissue surface pH (and thus Ω_{Arag}), has been shown to ameliorate the effects of ocean acidification in algae through a thickening of the DBL (Cornwall et al., 2014). In corals, flow has been shown to influence DBL thickness, with lower flows leading to thicker DBLs (de Beer et al., 2000, Jimenez et al., 2011), but so far no studies have investigated how flow influences tissue surface pH under either ambient or acidified conditions. In Chapter 5, I investigate whether low flows can lead to increases in tissue surface pH and thus produce the short-term flow-ocean acidification interaction exhibited in Chapter 4. I construct a model to elucidate the factors driving tissue surface pH and use microsensor experiments to parameterize and validate the model. Also, it is known from engineering literature that morphology could lead to different DBL dynamics (Patterson, 1992, Jimenez et al., 2011), so we investigate whether morphological differences in DBL dynamics lead to different increases in tissue surface pH.

1.6 Publication details

Chapter 2 of my thesis was published in *Global Change Biology* in 2013 (Chan & Connolly et al 2013). Chapter 4 is currently under review. Chapters 3 and 5 have not yet been submitted for publication.

2. Sensitivity of coral reef calcification to ocean acidification: a meta-analysis

2.1 Summary

To date, meta-analyses of effects of ocean acidification have focused on the overall strength of evidence for statistically significant responses; however, to anticipate likely consequences of ocean acidification, quantitative estimates of the magnitude of likely responses are also needed. Here, we use random-effects meta-analysis to produce a systematically integrated measure of the distribution of magnitudes of the response of coral calcification to decreasing Ω_{Arag}. We also tested whether methodological and biological factors that have been hypothesized to drive variation in response magnitude explain a significant proportion of the among-study variation. We found that the overall mean response of coral calcification is ~15% per unit decrease in Ω_{Arag} over the range $2<\Omega_{Arag}<4$. Among-study variation is large (standard deviation of 8% per unit decrease in Ω_{Arag}). Neither differences in carbonate chemistry manipulation method, study duration, irradiance level, nor study species growth rate explained a significant proportion of the among-study variation. However, studies employing buoyant weighting found significantly smaller decreases in calcification per unit Ω_{Arag} (~10%), compared to studies using the alkalinity anomaly technique (~25%). These differences may be due to the greater tendency for the former to integrate over light and dark calcification. If the existing body of experimental work is indeed representative of likely responses of corals in nature, our results imply that, under business as usual conditions, declines in coral calcification by end-of-century will be ~22%, on average, or ~15% if only studies integrating light and dark calcification are considered. These values are near the low end of published projections, but support the emerging view that variability due to local environmental conditions and species composition is likely to be substantial.

2.2 Introduction

Crucial to the capacity of coral reefs to provide various ecological and economic goods and services is corals' ability to form three dimensional skeletal structures through the process of calcification (Moberg and Folke, 1999). One ongoing environmental change that has potential negative impacts on coral calcification is ocean acidification. Ocean acidification refers to the lowering of the pH of the oceans due to rising atmospheric carbon dioxide (CO_2), which is caused by fossil fuel burning (Sabine et al., 2004). Under the Intergovernmental Panel on Climate Change's "business as usual" (IS92a) scenario, increases in atmospheric CO_2 will cause oceanic pH to decrease by 0.77 units by the year 2300 (Caldeira and Wickett, 2003), altering the current distribution of dissolved inorganic carbon (DIC) ion species in seawater, causing a reduction in carbonate (CO_3^{2-}) and the saturation state of aragonite (Ω_{Arag}):

$$\Omega_{Arg} = \frac{[Ca^{2+}][CO_3^{2-}]}{K_{sp}} \qquad \text{Eqn 2.1}$$

Where $[Ca^{2+}]$ and $[CO_3^{2-}]$ are concentrations of calcium and carbonate, respectively, and K_{sp} is the solubility constant for a particular mineral phase of $CaCO_3$ (Stumm and Morgan, 1981). Changes in Ω_{Arag} are of particular relevance for coral calcification because rates of precipitation of abiotic aragonite are positively dependent on saturation state (Burton and Walter, 1987). Coral reefs in the modern ocean are restricted to regions where oceanic Ω_{Arag} exceeds ~3.3 (Kleypas et al., 1999b) and coral calcification rate has been found to vary positively with Ω_{Arag} in experimental studies (Schneider and Erez, 2006).

Although there is broad agreement that ocean acidification will lead to decreased coral calcification, considerable uncertainty remains about the likely magnitude of the effect (i.e., the amount by which calcification will decline in response to a given decrease in Ω_{Arag}),

and about the factors that may drive geographic and inter-specific variation in the calcification response. The 4th IPCC report projected a 20-60% reduction in coral calcification with doubling of atmospheric pCO_2 (roughly 34% decline in Ω_{Arag}), and stated that by 2070, many reefs could reach critical Ω_{Arag} (IPCC, 2007). A more recent projection suggests a response towards the upper end of this range, with many reefs experiencing net dissolution by mid-century (Silverman et al., 2009). Some reviews report an average 30% decline in calcification in response to doubling of pCO_2 (Kleypas et al., 2006) while yet other reviews argue that it is still unclear to what extent ocean acidification will influence calcification and call for more research (Atkinson and Cuet, 2008). Existing reviews that have graphically compared calcification response to ocean acidification from multiple studies have all noted both an overall tendency for calcification to decline as Ω_{Arag} declines, and a high degree of variability in apparent rates of decline. Several hypotheses have been proposed to explain this variability (e.g. Langdon & Atkinson 2005; Pandolfi et al 2011; McCulloch et al. 2012). For instance, differences in carbonate chemistry manipulation method, duration of study, irradiance levels, coral energetic status, and study species growth rate have all been proposed as a possible cause of variation in results, but experimental studies explicitly investigating these hypotheses have yielded mixed results (Marubini et al., 2001, Marubini et al., 2003, Cohen and Holcomb, 2009, Schulz et al., 2009, Krief et al., 2010, Rodolfo-Metalpa et al., 2010). Thus, understanding variability in the calcification response remains an active research area (Pandolfi et al., 2011).

The number of experimental studies seeking to estimate the sensitivity of calcification to Ω_{Arag} has increased dramatically in recent years, but the magnitude of the calcification response estimated in these studies has varied enormously, from an increase of 25% to a decrease of 66%, per unit decrease in Ω_{Arag}. For this body of work to inform our

understanding of the likely response of calcification to ocean acidification, a quantitative approach to synthesizing the information from these studies is required. Meta-analysis is an analytical method for combining evidence from multiple studies, and for identifying the factors that explain variation between studies in measured experimental effects (Gurevitch and Hedges, 1999). To date, there have only been two meta-analyses published on the effects of ocean ocean acidification. Hendriks et al. (2010) examined the survival, metabolism, calcification and growth of bivalves, coccolithophores, coral, cyanobacteria, phytoplankton and sea grasses, while Kroeker et al. (2010) examined the survival, calcification, growth and photosynthesis (where applicable) of calcifying algae, coral, coccolithophores, molluscs, echinoderms, crustaceans, fish, fleshy algae and sea grasses. Both studies confirmed that, overall, ocean acidification causes a significant decrease in coral calcification. Moreover, Kroeker et al. (2010) considered the method of carbonate chemistry manipulation, and the duration of experiments, but found no evidence that either explained a significant proportion of the among-study variation in effect size (Kroeker et al., 2010). These two studies used "effect size" meta-analysis. This allows an assessment of whether ocean acidification has a positive, negative, or no significant effect on a response variable such as calcification. However, because this compares control and treatment effects without regard to the magnitude of the treatment imposed (Gurevitch and Hedges, 2001), and because the magnitude of decline in Ω_{Arag} varies dramatically among studies (e.g., from 0.8 to 2.5 in Hendricks et al. 2010), this approach cannot be used to quantitatively estimate the sensitivity of calcification to a given decline in Ω_{Arag}. The effect-size approach also complicates interpretation of tests for differences between groups of studies, since statistical power may be impaired by differences between studies in the magnitude of decline in Ω_{Arag} imposed in experimental treatments.

Here, we quantitatively synthesize the available experimental evidence to produce an overall estimate of the sensitivity of calcification to changes in Ω_{Arag}, and to determine how well among-study variation in the calcification response can be explained by biological and methodological differences between studies. Specifically, we use a random effects meta-analysis of regression slopes to produce a combined mean slope for calcification against Ω_{Arag}. We test carbonate chemistry manipulation methods, calcification measurement methods, study duration, irradiance level and species growth rate, as possible drivers of variation in responses between studies. We also assess the possibility of publication bias.

2.3 Methods

2.3.1 Data selection

Our meta-analysis included 25 published estimates of the relationship between calcification and Ω_{Arag} (Appendix A). This collection of studies was compiled by searching the biological literature for studies that reported the effects of altered seawater chemistry on coral calcification. Literature searches were conducted using the ISI Web of Science database for the relevant keywords: coral calcification AND (ocean acidification OR increased CO_2 OR carbonate chemistry OR aragonite saturation state). We also searched the literature cited of all studies identified in that search. Studies were collected for analysis until 30 June 2011.

We collected studies that reported calcification responses to decreases in Ω_{Arag} amongst populations of a single species as well as responses in multiple species assemblages. We then restricted our dataset to those studies reporting pH and total alkalinity (TA) values for the given manipulations. This was done to get a consistent measure of Ω_{Arag} because there are four different pH scales (total, free, NBS, and seawater scale) and a number of different carbonate system calculation programs (e.g. Seacarb and CO2SYS) used in the literature. Because regression-based meta-analysis assumes a linear relationship between the

explanatory and response variable, we took several steps to ensure that non-linearity in the relationship between calcification and Ω_{Arag} did not bias the estimates in our study. Firstly, we restricted our dataset by excluding studies which had a minimum Ω_{Arag} larger than 3 or a maximum Ω_{Arag} smaller than 2. This allowed us to focus on studies that encompassed a similar range of Ω_{Arag} values (Fig. 2.1), and where the calcification response was likely to be approximately linear (Anthony et al., 2011). It also focused our analysis on the range of values within the included studies most relevant to likely changes in tropical regions over the next century (a pH reduction from ~8.05 to ~7.8 and Ω_{Arag} reduction from ~3.5 to ~2). Secondly, we checked to confirm that there was no evidence of non-linearity by plotting standardized residuals (see section 2.3.2 for details on how data were standardized) against standardized Ω_{Arag}: a decelerating response would produce systematically positive residuals in the middle of the range of Ω_{Arag}, whereas approximate linearity would produce unbiased residuals. Finally, we considered only those studies examining calcification during the day (for studies using the alkalinity anomaly method) or across multiple days (for studies using the buoyant weighting method), i.e., excluding alkalinity anomaly method studies of dark calcification only, because previous studies have shown significant differences in sensitivity of day and night calcification to Ω_{Arag} (e.g., Anthony et al 2011).

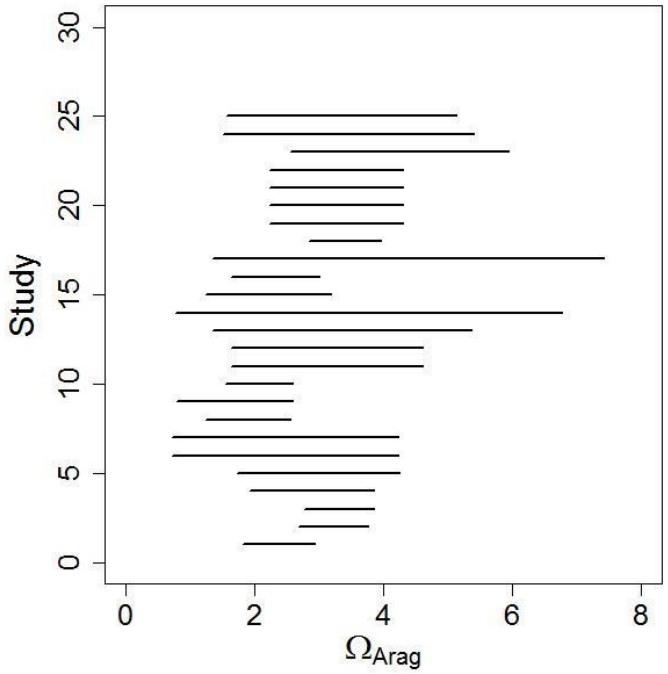

Figure 2.1 The range of Ω_{Arag} explored in each study included in the meta-analysis. Each line represents an individual paper.(sometimes encompassing multiple experiments), and extends from the minimum Ω_{Arag} to the maximum Ω_{Arag} of the study

Many papers included experimental factors in addition to Ω_{Arag} (e.g. temperature), or more than one study species. If studies tested multiple study species, these were included as separate experiments (e.g. *Acropora intermedia* and *Porites lobata* in Anthony et al (2008)). However, following previous meta-analytical approaches (e.g., Kroeker et al 2010), only the experiments with other factors set to ambient were included in the meta-analysis.

2.3.2 Data extraction and preparation

We recorded all information about the study (pH, TA, DIC, temperature and salinity), the organism (species and growth rate) as well as methodological factors (duration of

experiment, method of carbonate chemistry manipulation and method of calcification measurement). Data were extracted from the primary literature using GraphClick (v3.0) (Neuchatel, Switzerland). pH, TA, temperature and salinity were then entered into the program Seacarb (Lavigne and Gattuso, 2011) in R (R Development Core Team 2011) to calculate other carbonate chemistry parameters (Ω_{Arag} and DIC). Due to the many different ways that calcification is measured and reported in the literature, a way of standardizing the sensitivity of calcification to declining Ω_{Arag} was necessary so that results from various studies could be combined. Thus, we chose to standardize each study's calcification to be a percentage of a calcification at a selected baseline Ω_{Arag} level (hereafter termed baseline calcification). This was done because calcification is measured in many different ways in the literature (including % decline), thus standardizing the data in a more usual approach would have excluded too many studies from an already small pool. Previous studies have used a projected Ω_{Arag} and calcification that was outside of the experimental range as a baseline (e.g., pre-industrial Ω_{Arag}: Langdon & Atkinson 2005). However, this requires extrapolating the calcification-Ω_{Arag} response well beyond the range of the data, which can be biased even if nonlinearity in the relationship between calcification and Ω_{Arag} is relatively modest. Therefore, for our baseline Ω_{Arag}, we first calculated ambient Ω_{Arag} for each study (in Seacarb using study specific temperature and salinity, and pCO_2 levels of 380). TA of seawater changes conservatively and is typically around 2300, so we used this value in our calculations (Kleypas & Langdon (2006). We then took the median of the ambient Ω_{Arag} values, which was 3.517, to be our baseline. This baseline value of Ω_{Arag} is roughly the Ω_{Arag} of present-day average tropical seawater.

For each study, the slope (of calcification against Ω_{Arag}), and its associated standard error, was estimated differently depending on whether studies reported all data points or only

mean calcification and standard error at particular levels of Ω_{Arag}. For studies that reported all data points, we fit a linear regression model to the calcification versus Ω_{Arag} data, using least squares regression (the lm() function in R) (R Development Core Team 2011). Calcification was then re-scaled so that predicted calcification at baseline Ω_{Arag} was 100%, and the value of the slope and its associated standard error re-computed on this normalized scale. For studies that only reported mean calcification and standard error, we used a Monte-Carlo routine to estimate the standard error of the regression slope. Specifically, using the sample size *n* and the standard error of calcification for each treatment, we calculated the within-treatment standard deviation of calcification. We then drew *n* calcification values at random for each treatment, using the appropriate mean and standard deviation, and fit a linear regression model to the Monte-Carlo sample, and noted the estimated slope, and then recalculated the slope with predicted calcification normalized to 100% at baseline Ω_{Arag}. We repeated this procedure 1000 times to obtain a bootstrap distribution of regression slopes. The standard deviation of this distribution is an estimate of the standard error of the regression slope for that study (Efron and Tibshirani, 1993).

2.3.3 Data analysis

There are two common meta-analysis approaches, fixed effects and random effects meta-analysis. Fixed effects meta-analysis assumes that all included studies share a common effect size (i.e. the true effect is the same for all studies), with the observed effects distributed about the common effect with a variance among studies that depends only on sampling effects (Borenstein et al., 2009). In contrast, random effects meta-analysis assumes that true effect sizes exhibit random variation among studies (i.e. the "combined effect" represents the mean of a distribution of "true" study-specific effects), and variance among studies therefore consists of a combination of the variance of true effect sizes among studies, and sampling effects (which cause the measured effect in any one study to differ from its study-specific

"true" value) (Borenstein et al. 2009). Our experiments varied widely in methodology and biological factors (such as different study species and duration of study); thus, we considered random effect meta-analysis to be most appropriate for the present study. Specifically, we used the random-effects procedure for combining regression slopes from Borenstein et al (2009) (Appendix B).

To quantify the variability between studies, we calculated the I^2 statistic, which is the ratio of excess dispersion to total dispersion, using the procedure from Borenstein et al (2009) (Appendix B). To examine the variation in the sensitivity of coral calcification to Ω_{Arag}, studies were separated to test for differences between *a priori* defined sub-groups (see Appendix A for information on groupings). Specifically, we compared studies using different carbonate chemistry manipulation methods, because the two most commonly used approaches acid addition and CO_2 bubbling, decrease alkalinity at constant DIC and increase DIC at constant alkalinity respectively (Gattuso and Lavigne, 2009, Langdon and Atkinson, 2005, Rodolfo-Metalpa et al., 2010). We also compared calcification measurement method (alkalinity anomaly technique versus buoyant weighting), as most studies using the alkalinity anomaly technique measure calcification over a couple of hours (and thus measure only light calcification) while buoyant weighting studies integrate over both light and dark calcification. Studies measuring light and dark calcification separately have shown them to have different sensitivities to Ω_{Arag} (Ohde and Hossain, 2004, Leclercq et al., 2000, Anthony et al., 2011), suggesting that calcification measurement method could lead to differences in results. Finally, we tested for differences based on whether study species were fast or slow-growing, because it has been hypothesized that fast growing corals might exhibit larger decreases in calcification due to their increased demand for carbonate (Rodolfo-Metalpa et al. 2010) or an increased need to dissipate hydrogen ions (Jokiel, 2011a). Growth rate classifications were

based on literature values for the study species, or values for the most-closely related species with similar growth forms that we could find. The fast-growing category had linear extension rates > 3cm yr^{-1} and included the branching *Acropora* and *Stylophora* and the plating *Turbinaria*, while slow-growing species had estimated linear extension rates <2cm yr^{-1} and included all other genera. To test for differences amongst these *a priori* defined groups, we performed separate random effects meta-analyses for each hypothesis and compared effects between subgroups using a Z-test (Borelstein et al 2009: summarized in Appendix B).

Meta-regression is a tool used in meta-analysis to examine the impact of among-study variation in the value of continuously varying independent variables on study effect size using regression-based techniques. Meta-regressions were carried out to test for an effect of study duration and irradiance level on sensitivity of calcification to decreasing Ω_{Arag}, following the procedure for weighted regression that incorporates residual heterogeneity by including an additive between-study variance component (model 3a in Thompson & Sharp 1999; summarized in Appendix B). Because both study duration and irradiance level varied by orders of magnitude across studies they were log-transformed to obtain a more even spread in the independent variable of the regression (transformations did not affect the statistical significance of the effects). The effect of study duration was tested because it has been suggested that, due to the possibility of coral acclimation, studies conducted over weeks or months are likely to show less sensitivity of calcification to decreasing Ω_{Arag}, compared to studies lasting less than a day (Langdon and Atkinson 2005; Krief et al. 2010; Pandolfi et al. 2011). The effect of irradiance level was tested because light is known to be an environmental parameter that has a strong effect on calcification (Barnes, 1982) and previous work has found that the reduction of calcification by decreased Ω_{Arag} was greater in corals in high light than in corals in low light (Marubini et al. 2001).

2.3.4 Publication bias

Publication bias occurs whenever the strength or direction of the results of published studies differ from those of unpublished studies (Moller and Jennions 2001). Two independent methods were used to investigate whether publication bias occurs in the ocean acidification literature. The first method was visual inspection of a "funnel graph" of sample size against estimated slope (Moller and Jennions 2001). If slopes derive from a random sample of studies using similar research methods, a plot of sample size against estimated slope should reveal a funnel centered on the weighted mean slope, with larger variation in values at small sample sizes and decreasing variance with increasing sample size (Moller and Jennions, 2001, Jennions et al., 2001). We also calculated the "fail-safe number", *X*, for the dataset: this is an estimate of the number of future studies needed to change a significant effect to a non-significant one (Moller and Jennions 2001). Rosenthal (1991)(Rosenthal, 1991) suggests that, if the fail-safe number is at least five times larger than the number of studies plus 10, publication bias is unlikely to alter conclusions about statistical significance from the meta-analysis (see Appendix B for details).

2.4 Results

2.4.1 General results

We found 30 studies that quantified the calcification responses of corals to ocean acidification and of those, 25 studies met our criteria (Appendix A). Meta-analysis of these data revealed a significant negative effect on calcification, with an average 15% decline in calcification per unit decline in Ω_{Arag}, and an among study standard deviation of 8% (Fig. 2.2). This heterogeneity in the calcification responses was large, relative to measurement error ($I^2 = 85.36$), indicating that among-study variation reflected real differences in biology or methodology among studies and that a distribution of true means better reflected the data than a single fixed effect magnitude. In particular, estimated 95% confidence intervals on

study-specific effects (i.e., combined slope ± 1.96 times the among-study standard deviation) ranged from 0%-31% per unit of Ω_{Arag}. Inspection of standardized residuals versus both standardized Ω_{Arag} and absolute Ω_{Arag} suggested than any non-linearity present for the studies we included was small, relative to the residual variation. Specifically, residuals were symmetrically distributed around zero, exhibiting no evidence of linear or curvilinear trends (Fig. 2.3), indicating that linear regression slopes provide an adequate approximation for the calcification response for the studies in our analysis.

Experiments that manipulated carbonate chemistry using acid addition (varying TA at a constant DIC) and those that modified pH using CO_2 bubbling (increasing DIC at a constant TA) did not differ significantly ($Z = 1.76$, $p = 0.08$; Fig. 2.4). In contrast, studies that measured calcification using the total alkalinity method showing a 25% decline in calcification per unit decline in Ω_{Arag} which was significantly larger than the 10% decline shown in studies that measured calcification using the buoyant weighting method ($Z = 2.85$, $p = 0.004$; Fig. 2.4). The effects of Ω_{Arag} on calcification also did not differ significantly among experiments using fast versus slow growing coral taxa ($Z = 1.88$, $p = 0.06$; Fig. 2.4). Between study variability in sensitivity of calcification to Ω_{Arag} was not significantly explained by either study duration ($t = 0.146$, $p = 0.89$; Fig. 2.5a) or irradiance level ($t = -0.773$, $p = 0.45$; Fig. 2.5b)

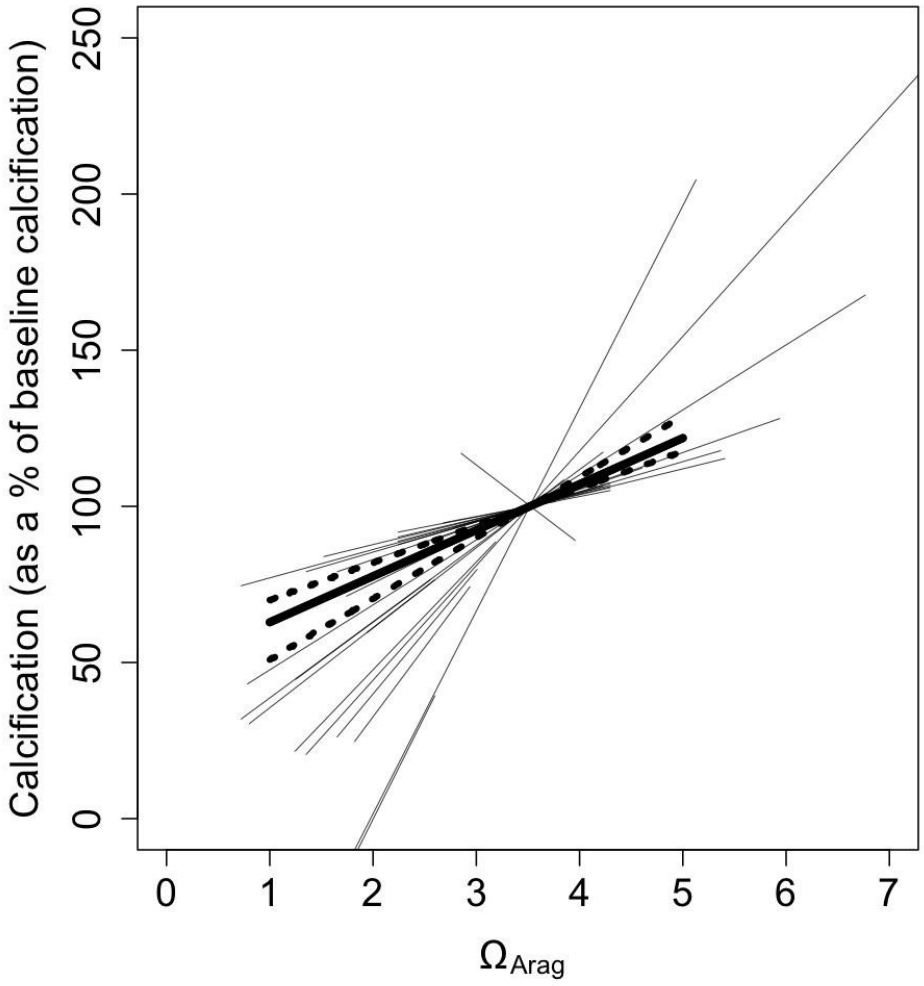

Figure 2.2 Overall effects of ocean acidification on coral calcification. Calcification is denoted as a percentage decrease from baseline calcification (calcification at Ω_{Arag} of 3.517) per unit decrease in Ω_{Arag}. Thus, all lines intersect the point (Ω_{Arag}=3.517, calcification=100%). The thin black lines show the calcification responses for individual studies. The endpoints of these lines indicate the range of Ω_{Arag} values spanned in each study. The thick black line represents the combined (mean) calcification response across all studies, and the dashed lines represent upper and lower 95% confidence intervals for this combined

response (that is, they represent the uncertainty around the mean response, not the overall among-study variability)

(a) (b)

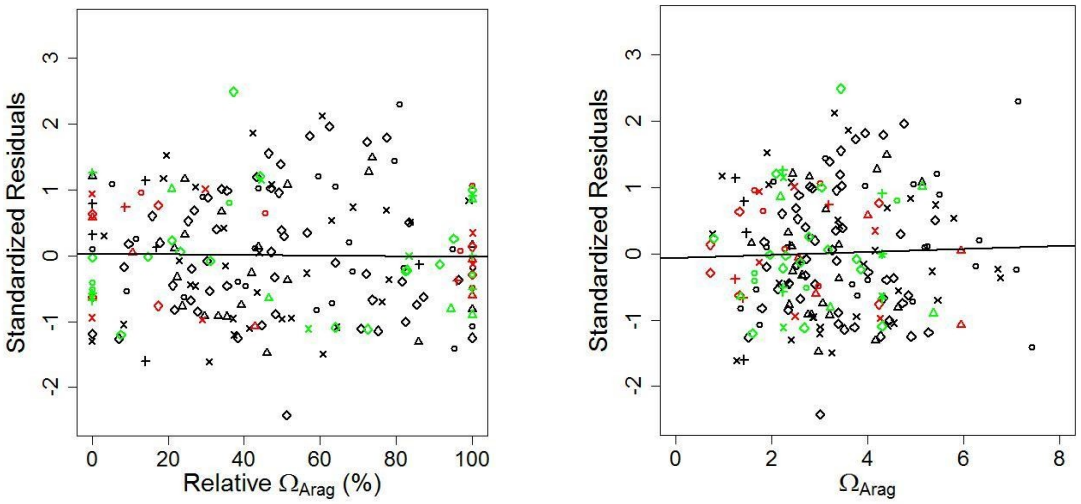

Figure 2.3 Standardized residuals, pooled across individual experiments. Residuals from each study were standardized against that study's residual standard error, and (a) Ω_{Arag} was scaled in each study so that maximum and minimum Ω_{Arag} for each study were 100 and 0 respectively (b) absolute Ω_{Arag} was plotted. Each combination of colour and symbol represents residuals from an individual study. The solid line is a regression line relating standardized residuals against standardized Ω_{Arag}. Note that the regression has a slope of approximately zero, and there is no evidence of a curvilinear trend in the residuals, as would be apparent if there were a qualitatively consistent pattern of nonlinearity in the calcification response over the range of Ω_{Arag} values considered.

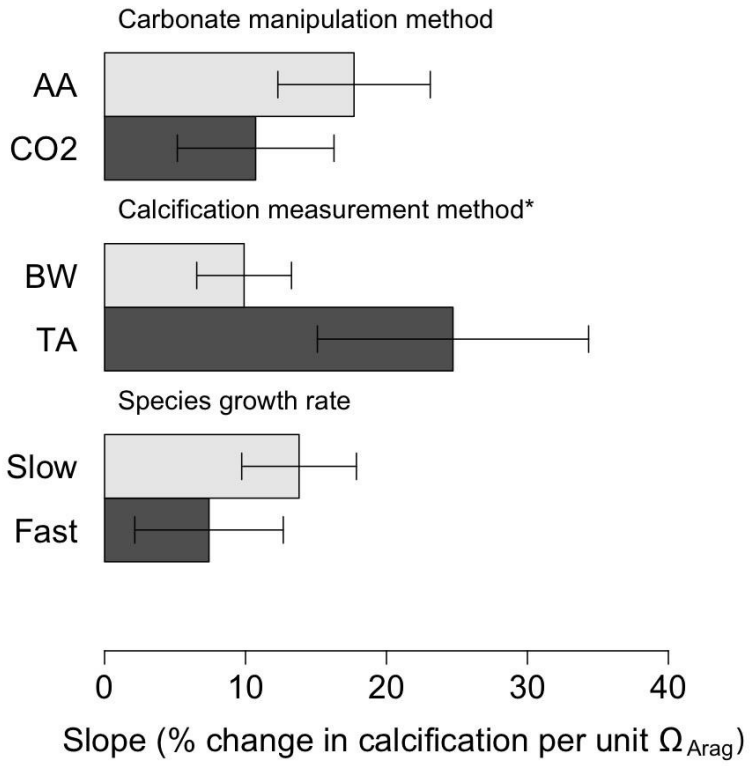

Figure 2.4 Methodological and biological variation in effects of ocean acidification on coral calcification. Bars indicate the mean decrease in calcification per unit decrease in Ω_{Arag} for each subset of studies. Whiskers indicate 95% confidence intervals on the mean response. Abbreviations are as follows: AA = acid addition studies, CO2 = CO_2 bubbling studies, BW= buoyant weighting studies, TA=Alkalinity anomaly technique studies, Slow = Studies using slow growing species (Fast) Studies using fast growing species. The slopes are significantly different only by calcification measurement method (indicated with an asterisk).

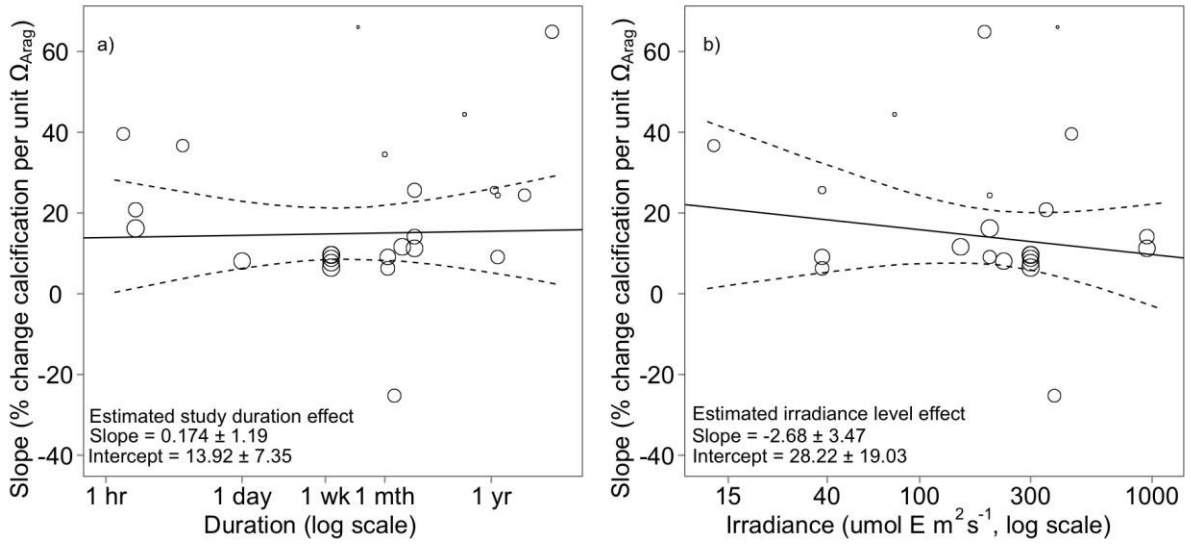

Figure 2.5 Slope (percentage change in calcification per unit Ω_{Arag}) against a) duration of experiment on the log scale, with ticks below indicating (left to right) durations of an hour, a day, a week, a month and a year b) irradiance level. The circles correspond to each study and have area proportional to the study's weighting (reciprocal of the variance of the slope estimate). The line is obtained by weighted least squares regression using a maximum likelihood estimate of the residual heterogeneity. Note that the "slope" and "intercept" values reported in the figure panel are estimates of the parameters (with standard errors) that describe how the slope of the calcification-Ω_{Arag} relationship changes as a function of a) study duration and b) irradiance.

2.4.2 Publication bias

The fail-safe number was over an order of magnitude larger than five times the number of studies plus 10 (X=2681>>135), indicating that the overall negative effect of decreasing Ω_{Arag} on calcification is very robust to any publication bias that may be present. However, inspection of the funnel plot does suggest a bias towards publication of studies that find negative effects of decreasing Ω_{Arag} (i.e., a positive slope of calcification vs Ω_{Arag}: Fig.

2.6). If slopes derive from a random sampling of studies using similar research methods, a plot of sample size against slope should reveal values distributed within a funnel (solid lines in Fig. 2.6) symmetrically around the weighted mean slope (dashed line in Fig. 2.6), with larger variation in values at small sample sizes (studies with small sample size are less precise) and a decreasing variance with increasing sample size. In our study, while there were roughly the same number of studies on both sides of the weighted mean slope, the distribution of estimated slopes was highly asymmetric: values above the weighted mean slope were broadly distributed within the funnel, whereas values below the weighted mean slope were, with only one exception, concentrated above zero (dotted line in Fig. 2.6), very close to the weighted mean slope (Fig. 2.6).

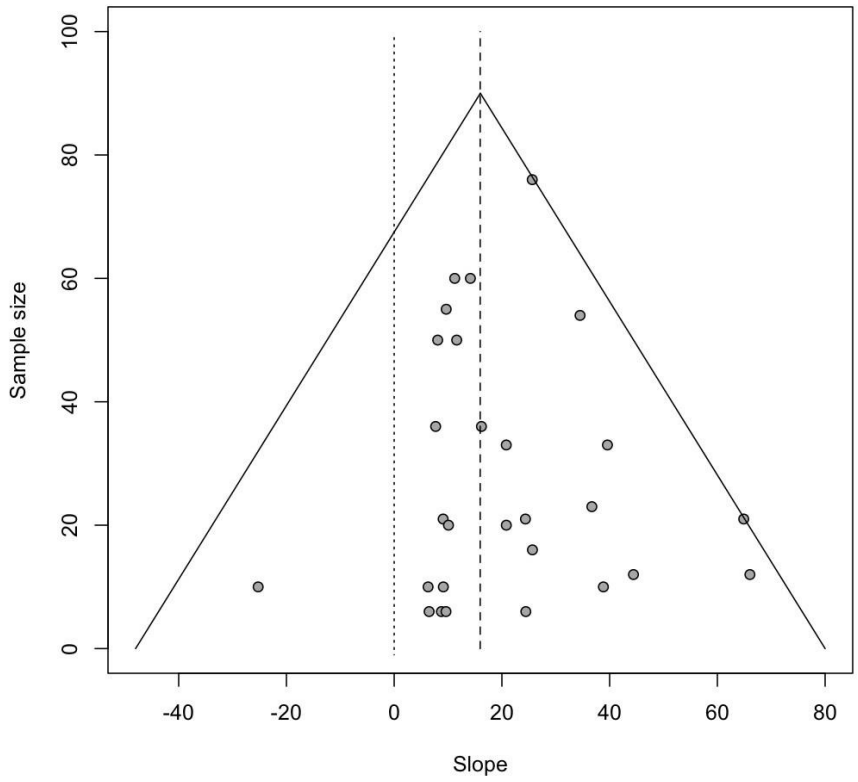

Figure 2.6 Funnel plot depicting the relationship between sample size and slope. The points are individual studies, each with their own sample size and slope. The dotted line is a slope of 0 (decreasing Ω_{Arag} has no effect on calcification). The dashed line is the observed weighted mean slope. The solid lines are an illustration of a funnel that should be formed by the points if there is no publication bias.

2.5 Discussion

Our random effects meta-analysis found that coral calcification declines by ~15% on average per unit decrease in Ω_{Arag} but with considerable among study variability. If existing experimental studies are indeed representative of the likely response to ocean acidification in nature, this finding implies that, on average, calcification will decline by ~22% by 2100,

under a "business as usual" emissions scenario. Specifically, assuming pCO_2 doubles from 400ppm to 800ppm and Ω_{Arag} decreases from 3.5 to 2, the consensus from reviews is for a 20-60% reduction in coral calcification by the end of the 21st century (IPCC, 2007, Kleypas and Langdon, 2006, Langdon and Atkinson, 2005). Our estimate is within, but towards the low end of, the range of likely responses to ocean acidification that have been proposed in earlier work. However the large between study variability indicates that, while some corals' responses are likely to fall below the range of estimates from previous work, others will be towards the middle or potentially upper end of the range. The decreases suggested by our analysis are not trivial, but they do suggest a consensus distribution of responses to ocean acidification from experimental studies that may be less severe than has been suggested by some recent reviews and models (e.g. Hoegh-Guldberg et al 2007 and Silverman et al 2009).

Our results also reveal that studies measuring calcification via the alkalinity anomaly (TA) method found significantly larger decreases in calcification than studies using buoyant weighing. This would seem to contradict recent experiments that show no difference in decreases between calcification measured by TA or by buoyant weight, when all other factors are held constant (Holcomb et al., 2010). One possible explanation for this is that buoyant weighting studies, of necessity, estimate calcification over relatively long time scales (weeks to years). Consequently, they implicitly integrate over both light and dark calcification. In contrast, TA measurements can be made over very short intervals, even when studies themselves are conducted over a long period. Typically, these measurements are made during the day and thus include only effects of ocean acidification on light calcification. There is some evidence that the decrease in dark calcification with decreasing Ω_{Arag} is less pronounced than that of light calcification (Leclercq et al. 2000; Anthony et al. 2011). If this is a common phenomenon, then the average decrease across light and dark calcification

measured in buoyant weighting studies would be less than the decrease in light calcification alone measured in TA studies. Consistent with this explanation, Holcomb et al (2010), who found no difference between the two methods, were unusual in carrying out their TA analysis over a 2 day period, thereby incorporating both light and dark calcification in both TA and buoyant weighting measurements. One other important aspect to using TA to measure calcification is that, in order to generate a significant change in TA over the (usually) short experimental period, it requires not only a higher (compared to buoyant weighting) amount of biomass relative to the amount of seawater being incubated but also a closed system (no exchange of seawater) during measurement. This results in an increased likelihood of environmental fluctuation and thus is increasingly likely to invoke more stressful environmental conditions with regards to flow and water quality, which could lead to an increased sensitivity to acidification. Our interpretation of this discrepancy between buoyant weighting and alkalinity anomaly studies warrants further testing. If correct, it would indicate that the calcification response is likely to be somewhat weaker than our headline result suggests: a decline of 10%, on average, per unit decrease in Ω_{Arag}, with 95% intervals on the among-study variation of 5.5 – 14.5%.

In contrast to calcification measurement method, we found no significant difference between mean slopes for CO_2 bubbling and acid addition methods, consistent with previous findings from effect-size meta-analysis (Kroeker et al 2010), and with reviews of methodology, which indicate that differences in speciation of the carbonate system, for moderate pCO_2 levels, is small enough so as not to lead to differences in calcification (Cohen et al. 2009; de Putron et al. 2011; Gattuso et al. 2010; Schulz et al 2009). Although fast-growing corals have been hypothesized to be more sensitive to ocean acidification than slow-growing corals (Rodolfo-Metalpa et al. 2010), we did not find significant differences between

estimated slopes for experiments on fast versus slow growing corals. Similarly, although acclimation has been hypothesized to reduce the sensitivity of calcification to decreasing Ω_{Arag} (Pandolfi et al. 2011), we found no evidence that such a phenomenon explains significant variation in calcification sensitivity among studies in our analysis. We also found that differences in irradiance level did not explain significant variation in calcification sensitivity among studies in our analysis. These findings do not mean that growth rate, acclimation, or light have no effect on the response of calcification to ocean acidification, but they do indicate that these factors do not account for a statistically significant proportion of the large among-study variability in the calcification response to changes in aragonite saturation state documented to date.

The mean sensitivity that we have produced could be an over-estimate if the published studies are a biased sample of those conducted. Publication bias has only been assessed once in previous studies, which reported a large fail-safe number but conjectured nevertheless that the published literature is probably biased towards studies that find significant effects (Kroeker et al 2010). We too determined the fail-safe number, which is the standard way of analyzing publication bias (Gurevitch and Hedges 1999), and also found that the conclusion that calcification is negatively affected by deceasing Ω_{Arag} is robust, consistent with previous work. However, the large fail-safe number does not confirm necessarily the robustness of the magnitude of that negative effect, and our funnel plot suggests that publication bias may well be present: studies to the left of the mean response are concentrated near it, rather than being spread more evenly within the left half of the funnel. This result should be interpreted with caution because skewed funnel plots may also be caused by other factors such as previous knowledge of effect sizes from pilot studies, reduced sample sizes for certain species, choice of effect measures and chance (Moller et al 2001). The large

variability in experimental techniques and lack of information about the role of prior knowledge in experimental design in published studies makes it difficult to rule out these other factors.

Our finding that calcification responses, on average, are likely to fall towards the lower end of the range reported in the 4th IPCC report (IPCC, 2007) is consistent with some recent studies that have sought to infer calcification response based on estimates of the extent to which corals increase pH at the site of calcification, relative to the surrounding seawater. Specifically, four different approaches (pH microsensors, aragonite crystal aspect ratios, live tissue imaging, and boron-isotope schematics) indicate consistently higher pH at the site of calcification compared to the surrounding seawater (Al-Horani et al. 2003; Cohen et al. 2009; Venn et al 2011; McCulloch et al 2012). This provides a potential explanation for why coral calcification changes less steeply with seawater Ω_{Arag}, on average, than one would predict based on abiogenic aragonite precipitation rates (e.g., Langdon and Atkinson 2005; Silverman et al. 2009). For instance, the calibration of McCullouch et al. (2012) implies an average decline in calcification of ~11% per unit Ω_{Arag} when Ω_{Arag} is close to the median value from the studies in our meta-analysis (obtained by normalizing the calcification rates in their Fig. 2 to calcification at Ω_{Arag}=3.5, and then numerically differentiating the curve at this value). This is similar to our overall mean slope of 15%, and virtually identical to the mean slope of 10% obtained from our meta-analysis of the buoyant weighting subset of studies. McCulloch et al. (2012) also found that the ability of corals to elevate calcification site Ω_{Arag} differed between species, suggesting that this varying ability to elevate calcification site Ω_{Arag} could be a possible explanation for the large among-study variance that we found.

Our findings indicate that, while that ocean acidification will have significant negative consequences for coral calcification by the end of this century, this decline will be, on

average, towards the low end of the range of responses that have been suggested in the literature. Nevertheless, even a relatively small (compared to previous projections) 15% decrease in coral calcification, has the potential to materially alter the accretion/erosion balance of reefs, particularly if climate change-induced increases in reef dissolution occur simultaneously (Yates and Halley, 2006, Langdon et al., 2000), and if other reef calcifiers such as crustose coralline algae and calcareous benthic macroalgae are more susceptible to ocean acidification than corals (Diaz-Pulido et al., 2012, Price et al., 2011). Moreover, there is some evidence that prevailing Ω_{Arag} levels on shallow-water reefs may be lower or higher than nearby open-ocean values, depending on whether they are net carbon sources or sinks (Kleypas et al., 2011). Thus, coral dominated reefs (which are more likely to be net CO_2 sources) may tend to have lower Ω_{Arag} levels compared to those commonly used as "ambient" in experimental studies. If there is greater sensitivity in the calcification response at lower Ω_{Arag} values (de Putron et al 2011; Ries et al 2010; Anthony et al 2011), then corals on low-Ω_{Arag} reefs may exhibit somewhat greater sensitivity to ocean acidification than is suggested by the experimental data. A recent review highlighted the need to better understand the magnitude of the calcification response, and the causes of its variability, in order to better inform projections of ocean acidification's likely impact on coral reefs (Pandolfi et al. 2011). The present study contributes to those goals, by providing a quantitative synthesis of existing experimental work on the effects of ocean acidification on coral calcification, and evaluating some of the potential drivers of the apparent variation in the calcification responses of coral.

3. Scaling up impacts of ocean acidification on individual coral growth and reproduction into effects on long-term population growth rate

3.1 Summary

Recent experimental studies have revealed significant declines in coral recruitment under ocean acidification, which could affect long-term population growth rates (hereafter λ). Yet no models predicting the effects of ocean acidification on coral populations to date have taken the effect of ocean acidification on pre- and post- settlement stages into account. In this study, we use random effects meta-analysis to quantitatively synthesize available experimental evidence into an overall estimate of the sensitivity of coral recruitment to changes in aragonite saturation state (Ω_{Arag}). We then use an integral projection model to investigate the relative impacts of the effects of ocean acidification on growth and recruitment on λ under climate scenarios based on RCP 6.0. We also investigated whether differences in life history strategy (fast versus slow growing) lead to differences in the relative impacts of the effects of ocean acidification on growth and recruitment on λ. We found that recruitment success decreased by 32.25% on average per unit decrease in Ω_{Arag} and that the effects of ocean acidification on recruitment potentially exert more influence on λ than the effects of ocean acidification on growth. However, the uncertainty around our estimate of decrease in recruitment success per unit decrease in Ω_{Arag} is very large compared to the estimate of how growth decreases under ocean acidification. We also found that λ of fast growing species are more sensitive to ocean acidification (larger percentage decrease in λ per unit decrease in Ω_{Arag}) than that of slow growing species. Our study highlights both the importance of including recruitment in future ocean acidification models and the need to improve our understanding of the variability in the response of coral recruitment to ocean acidification.

3.2 Introduction

Ocean acidification, the abnormally rapid reduction in ocean pH due to uptake of anthropogenic carbon emissions by the oceans, has been highlighted as an important threat facing coral reefs (Pandolfi et al., 2011). This is due to the fact that ocean acidification leads to a reduction in aragonite ($CaCO_3$) saturation state Ω_{Arag}, which is a measure of the accessibility of aragonite to calcifying organisms. Experimental studies have shown that corals reared under decreasing levels of Ω_{Arag} have a skeletal morphology that is consistent with a slowdown in crystal growth rate (Cohen and Holcomb, 2009). There is, therefore, growing concern that ocean acidification may slow rates of $CaCO_3$ production or calcification by reef building corals to the point where rates of reef erosion exceed rates of skeletal accretion, leading to widespread loss of coral reef ecosystems as we know them (Silverman et al., 2009).

Currently, our understanding of the future ecological effects of ocean acidification is based overwhelmingly on short-term experimental studies of individual organisms' physiological responses. Projection models have been employed to scale up these documented short-term organism-level responses into long-term reef-scale impacts (Pandolfi et al., 2011). Because the primary concern has been the slowing of calcification by ocean acidification, models have generally been used to project how much calcification would decline at various levels of atmospheric pCO_2 (Silverman et al., 2009, van Hooidonk et al., 2013). While these projections give us important insights into whether reef accretion can keep up with erosion, they only tell part of the story. Reductions in calcification could also lead to reductions in colony growth, and thus impact upon species abundance, percentage cover, and long term per-capita population growth rate (hereafter λ), with flow-on effects for ecosystem level calcification. Early models have begun to investigate ocean acidification driven reductions in coral populations by modeling reduced growth in the dynamics of coral

cover in the aggregate (Anthony et al., 2011, Baskett et al., 2009). However, these early population level models were not size structured, and thus did not take into account size-dependent demographic rates. Corals have size dependent growth, fecundity and survival (Hall and Hughes, 1996, Madin et al., 2014, Madin et al., 2012), and models of coral cover dynamics cannot capture important implications of these flow on effects of ocean acidification (e.g. ocean acidification not only reduces growth but that reduced growth shifts size structure of populations, changing fecundity and survival).

Indeed, only one study to date has attempted to improve upon early projections by incorporating size-dependent demographic rates into projections of the effects of ocean acidification on coral populations (Madin et al., 2012). In their study, Madin *et al.* (2012) evaluated the population level effects (on cover, lifetime reproductive output, and λ) of ocean acidification, thermal stress, and increased storm intensity on the ecologically dominant table coral *Acropora hyacinthus*. Their size-structured model allowed for size dependent coral growth, fecundity and mortality. However, at the time of their study, a good quantitative summary of the sensitivity of calcification to ocean acidification did not yet exist (which now does – Chan and Connolly, 2013) , so they used estimates from three different experimental studies (Langdon and Atkinson, 2005, Silverman et al., 2007, Anthony et al., 2008), that form extremes that bracket the responses of all other studies. Moreover, their study did not take into account the effect of ocean acidification on pre- and post- settlement stages. A recent meta-analysis has suggested that various life history stages are likely to respond differently to ocean acidification (Kroeker et al., 2013) and thus could contribute differently to the effects of ocean acidification on population level measures. As such, it is important to assess the impact of the effect of ocean acidification on pre- and post- settlement stages on λ of corals as new data becomes available. With respect to the pre- & post-settlement stages of corals,

recent studies have revealed no significant effects of ocean acidification on fertilization, embryonic development, larval respiration, larval survival or larval metamorphosis (Albright et al., 2010, Chua et al., 2013, Cumbo et al., 2013, Nakamura et al., 2011). However, when the settlement substratum is also exposed to the acidified treatment, recruitment is significantly reduced (Albright et al., 2010, Doropoulos et al., 2012, Webster et al., 2013). This reduction in recruitment with ocean acidification could have significant impacts on λ.

As a group, scleractinian corals encompass a wide range of life history strategies and it is unlikely that they will all respond equally to ocean acidification. Studies have suggested that life-history traits can predict which corals will be 'winners' and 'losers' in the face of environmental change (van Woesik et al., 2012, Loya et al., 2001). While there is still much debate over the perfect framework of life history strategies for this diverse group, most frameworks separate strategies by colony morphology, growth rate (fast growing versus slow growing) and reproductive strategy (brooders vs spawners) (Darling et al., 2012, Jackson and Hughes, 1985, Edinger and Risk, 2000). Fast growing, branching species that are sensitive to stress and disturbance are predicted to be 'losers' whereas slow growing massive species and fast growing small corals with brooding reproduction and high population turnover, which have the ability to persist in unfavourable environments, are predicted to be 'winners' (McClanahan et al., 2007). Moreover, since the effects of ocean acidification on coral calcification are proposed to be due mass transfer, fast growing corals may be more susceptible due to their larger need to uptake carbon/dispose of H^+ (Comeau et al., 2012, Jokiel 2011a,b). If the sensitivity of long-term population growth rate to ocean acidification does indeed vary with colony growth rate, with fast growing, branching species more susceptible, then ocean acidification could lead to a shift in reef species composition, from

branching dominated to massive dominated reefs, which would reduce habitat complexity (Molberg & Folke, 1999).

In this study we, examine how effects of ocean acidification on growth and recruitment combined to affect λ. To do this, we first use random effects meta-analysis to quantitatively synthesize available experimental evidence into an overall estimate of the sensitivity of coral recruitment to changes in Ω_{Arag}. We then use this estimate to project the effects of ocean acidification on λ using climate scenarios based on RCP 6.0 (IPCC, 2013). We determine the relative impacts of the effects of ocean acidification on growth and recruitment on λ and also whether the effects of ocean acidification on growth and recruitment acts additively or synergistically to impact λ. Next, we extend upon the previous projection by asking whether life history strategy of fast versus slow growing influences how ocean acidification affects λ, and whether it leads to differences in the relative impacts of the effects of ocean acidification on growth and recruitment on λ. Also, because many of the relevant biological parameters needed to project the effects of ocean acidification on coral reefs are known with considerable uncertainty, we characterize the uncertainty around the effects of ocean acidification on λ projections and the sensitivity of λ projections to model parameters.

3.3 Methods

3.3.1 Meta-analysis of the effects of ocean acidification on recruitment

Of all the studies of the effects of ocean acidification on coral recruitment, there have only been three studies that have included the effects of ocean acidification on the ability for crustose coralline algae (CCA) to act as a suitable substrate in their investigations (i.e. CCA preconditioned to treatment pCO_2 prior to conducting settlement assays) (Albright et al 2010, Doropoulos et al 2012, Webster et al 2013). Crustose coralline algae have been shown to be

the primary provider of settlement cues for coral recruits on coral reefs (Harrington et al., 2004, Negri et al., 2001) so these studies are most likely to represent what will happen in nature. All three studies are focused on the *Acropora* group – *A. palmata* (Albright et al 2010) and *A. millepora* (Doropoulos et al 2012, Webster et al 2013). Although we recognize that three studies are very few for a meta-analysis, we carried out a regression based, random effects meta-analysis to allow comparison with results from Chapter 2. As in Chapter 2, we calculated the mean percentage decrease in recruitment success per unit decrease in Ω_{Arag}. The meta-analysis was carried out using the metafor package (Viechtbauer, 2010) in R. Amount of heterogeneity was estimated using the Dersimonian-Laird estimator to maintain consistency with the meta-analysis in Chapter 2.

3.3.2 Integral projection model

First introduced by Easterling et at. (2000), integral projection models (IPMs) have become an increasingly popular tool for modelling organisms whose demographic rates vary continuously with size, as it allows the avoidance of coarse and arbitrary size classification that traditional matrix modelling applies. Corals are a prime example of such an organism, so IPMs were used to translate effects of ocean acidification on individual organism growth and recruitment into effects on λ. We modelled the number of individuals of size (measured as planar [projected] area) y within the total population at time $t+1$ given the number of individuals of size x at time t:

$$n(y,t+1) = \int_L^U K(y,x)\, n(x,t)\, dx \qquad \text{Eqn 3.1}$$

with the integration being over the entire set of all possible sizes (L = lower size bound, U = upper size bound). $K(y,x)$ is a nonnegative surface representing all possible transitions from size x to size y, and is analogous to the projection matrix in matrix models. $K(y,x)$ contains

the probability function for yearly growth (*g*), survival (*s*), fecundity (*f*) and recruitment success (*r*):

$$K(y,x) = g(y,x) * s(x) + r * f(y,x) \quad \text{Eqn 3.2}$$

Growth, survival rate and fecundity are all a function of size *x*. To calculate λ, we ran each model for 150 years. To avoid transient effects, we estimated λ as the exponential of the slope of the natural logarithm of population size against time for just the last 50 years. All modelling was carried out in R (R Core Development Team 2011).

3.3.3 Probability functions and parameter estimates

We parameterized the IPM with estimates for *Acropora nasuta*, a corymbose shaped, reef building species on the Great Barrier Reef (see Tab. 3.1 for a full list of demographic parameter estimates). Constant linear growth estimates were taken from studies that measured linear extension over time (all three studies measured linear extension rates for *A. nasuta* that were quite similar) (Stimson, 1985, Morgan and Kench, 2012, Babcock, 1991). This was converted into projected planar area using the equation

$$A_t = \pi(l_t * \cos(45))^2 \quad \text{Eqn 3.3}$$

where A_t is projected area at time *t* and l_t is branch length at time *t*. Branches are assumed to grow at 45° angle to the ground. Quadratic models were then used to describe the relationship between size (projected planar area) at time *t+1* (*y*) and size at time *t* (*x*). Standard deviation around size at time *t+1* was taken from unpublished data of size at time *t+1* against size at time *t* from Lizard Island, Great Barrier Reef (Dornelas et al., unpublished data). Survival estimates for *A. nasuta* were taken from a previous study describing the quadratic (due to hydrodynamic dislodgement of the largest size classes) relationship between mortality and colony size for coymbose morphologies (Madin et al. 2014). For colonies smaller than those

used in Madin et al. (2014) we set mortality to be the same as that of the smallest colony. Fecundity and size at first maturity for *A. nasuta* was taken from data of fecundity against size from Lizard Island (Hoogenboom et al., unpublished data). Due to the planktonic nature of coral larvae, estimates of recruitment success for individual organisms are almost nonexistent. Therefore, we chose values for baseline recruitment success that produced baseline size structures similar to those observed in previous studies (Roth et al., 2010).

For estimates of the effect of ocean acidification on recruitment, the results of the meta-analysis described above were used. Effect of ocean acidification on calcification was taken from Chapter 2 which calculated a mean percentage decrease of 16% in coral calcification per unit decrease in Ω_{Arag} based on 26 studies. We needed a conversion factor to convert projected decreases in calcification to projected decreases in growth. Only three studies have simultaneously measured decreases in calcification and growth under ocean acidification. Jokiel et al. (2008) estimated that decreases in linear extension were 74% that of calcification in *Montipora capitata*, De'ath et al. (2009) found that decreases in linear extension were equal to decreases in calcification in massive *Porites*, and Enoch et al. (2014) showed that ocean acidification only decreased skeletal density and not linear extension in *Acropora cervicornis*. We chose the intermediate estimate (0.74) from Jokiel et al. (2008) as our baseline, but we investigate the sensitivity of our projections to the choice of conversion factor (see sensitivity analysis below). λ was calculated at year 2050 and 2100 based on IPCC projections of atmospheric pCO_2 under RCP 6.0 (IPCC, 2013). Ω_{Arag} was calculated from values of pCO_2 (2014 –380uatm, 2050 – 500uatm, 2100 – 670uatm), TA of 2300, temperature of 25°C and salinity of 35ppt using CO2Calc (Robbins et al., 2010).

3.3.4 Implementing and evaluating the effects of ocean acidification

To implement the effect of ocean acidification on growth, we reduced constant linear growth by a percentage decrease per unit decrease in Ω_{Arag} based on the calcification meta-analysis multiplied by the calcification-to-growth conversion factor (e.g., a rate of 16%*74% or an 11.8% decline in extension rates per unit decline in Omega). To implement the effect of ocean acidification on recruitment, we reduced recruitment success (r) by the percentage decrease per unit decrease in Ω_{Arag} found in the recruitment meta-analysis. To tease apart the various effects of ocean acidification on λ, we ran three different models: One where ocean acidification only reduced growth, one where ocean acidification only reduced recruitment, and one where ocean acidification reduced both growth and recruitment. To determine if the effects of ocean acidification on growth and recruitment were additive or synergistic in nature, we compared the reduction in λ from the model with effect of ocean acidification on both growth and reproduction against the sum of the reductions from the models with effect of ocean acidification on either growth and reproduction.

3.3.5 Life history strategy and sensitivity analysis

To determine whether life history strategy of fast growing versus slow growing influenced how ocean acidification affected λ, we slowed growth rate while keeping λ constant (at year 2014, under ambient conditions) by either increasing recruitment success or decreasing mortality (models referred to as 'slow growing (increased recruitment)' and 'slow growing (decreased mortality)', respectively hereafter). There were only minor quantitative differences between results from slow growing (increased recruitment) and slow growing (decreased mortality) models, so only results from the slow growing (increased recruitment) model are presented in the main text with results from the slow growing (decreased mortality) model presented in Appendix C. We evaluated the effect of ocean acidification on λ at 0.5x constant linear growth rate (hereafter 0.5x) and 0.1x constant linear growth rate (hereafter

0.1x) of *A. nasuta*. Given that most slow growing species are of massive morphology, which do not share corymbose colonies' increased mechanical vulnerability (to hydrodynamic dislodgement) at their largest size classes (Madin et al. 2014), we evaluated a model where survival stayed constant once it reached its highest point (hereafter massive survival) (Fig. 3.3b). Due to their slow growth rates, massive species also tend to have smaller size at first maturity, so we also evaluated a model that used size of first maturity estimate for *Goniastrea retiformis* taken from Hall & Hughes (1996). 0.5x models produced results (effects of ocean acidification on λ) that were on the continuum between 1x and 0.1x models, and there was little difference in the results between models with different survival curves and sizes at first maturity. Thus we only present results of the 0.1x, massive survival and *G. retiformis* size at first maturity model as our archetypal slow growing species. The distributions of the archetypal slow growing species is quite right skewed (compared to natural populations) because it is a single species model and thus the size distribution is not shaped by competition as would occur in nature. We also ran models of slow growing species where λ was allowed to vary (leading to slow growing species having lower λ than fast growing species), but had to remain over 1 at 2014, and found that the results produced by those models were not qualitatively different to the constant λ models.

To test the sensitivity of model projections to parameters of growth and recruitment, we ran the model using growth and recruitment parameters that were ±10% of their baseline values. Sensitivity to the conversion factor for reductions in calcification to reductions in growth was tested by running the model using conversion factors of 0.5 and 1 respectively. To examine how the different uncertainties in the calcification and recruitment meta-analyses affected the confidence of projections of reduction in λ, we plotted upper and lower confidence intervals around projections using ±1.96*SE of the mean effect size.

Table 3.1. Statistical models and parameter estimates describing the demography of a fast growing (*Acropora nasuta*) and an archetypal slow growing (based on *Goniastrea retiformis*) species. y is size (projected area) at time $t+1$, x is size at time t, σ is standard deviation, m is morality, f is fecundity.

Demographic process	***Fast growing***	***Slow growing***
Growth	$y = 1.568+0.16x+0.119x^2$ $\sigma = 0.12$	$y = 0.299+0.81x+0.032x^2$ $\sigma = 0.12$

Mortality	For (x<1)
	$m = 0.903$
	For (1<x)
	Logit(m) = $0.659+1.645x+03271x^2$
		For (x<1)
		$m = 0.903$
		For (1<x<2.6)
		Logit(m) = $0.659+1.645x+03271x^2$
		For (2.6<x)
		$m = 0.138$

Fecundity	$f = 0.48+1.93x$	$f = 0.48+1.93x$
Recruitment success	1.94×10^{-6}	8×10^{-5} (increasing recruitment success)
Size at first maturity (cm^2)	158	8

(a) (b)

Figure 3.1 Images of the model species. Fast growing *A. nasuta* (a) and slow growing *G. retiformis* (b). © Charlie Veron

(a) (b)

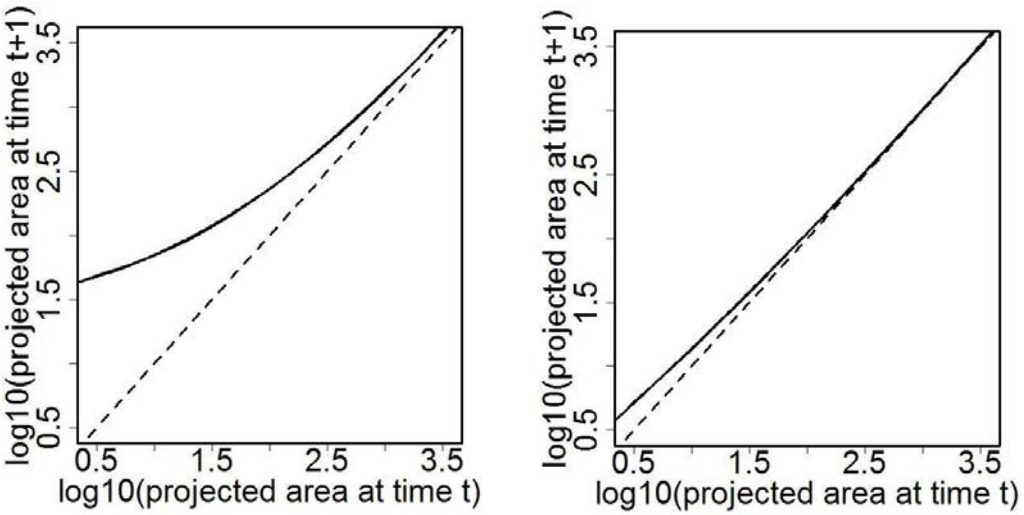

Figure 3.2 Projected colony area (cm^2) at year $t+1$ plotted against area at year t for fast (a) and slow (0.1x constant linear growth of fast growing species) (b) growing species. Dashed line indicates unity line.

(a) (b)

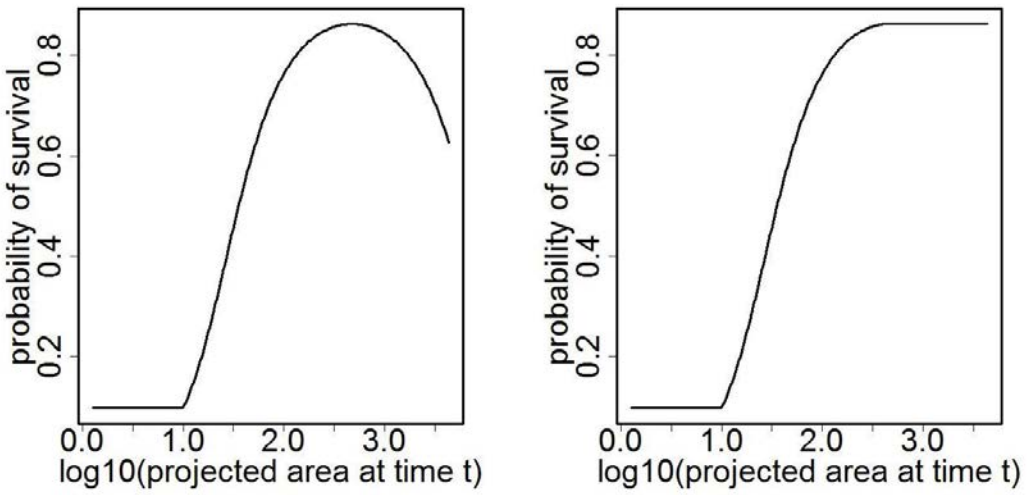

Figure 3.3 Survival plotted against projected colony area at year *t* for fast (a) and slow (increased recruitment) (b) growing species.

(a)

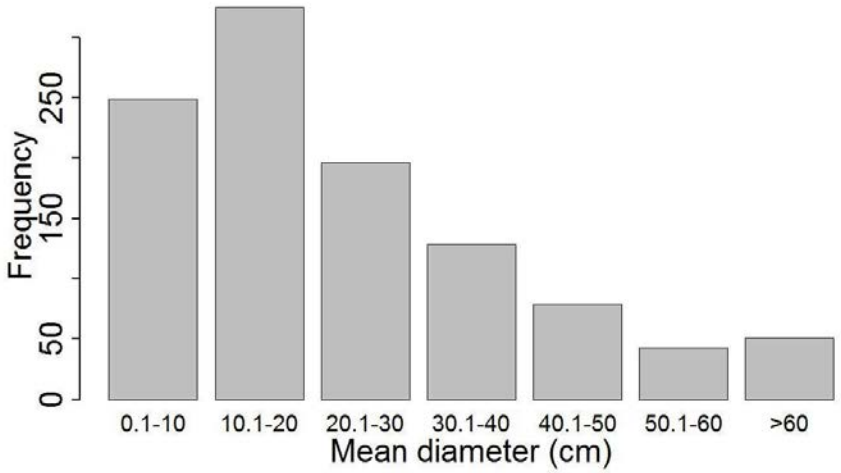

(b)

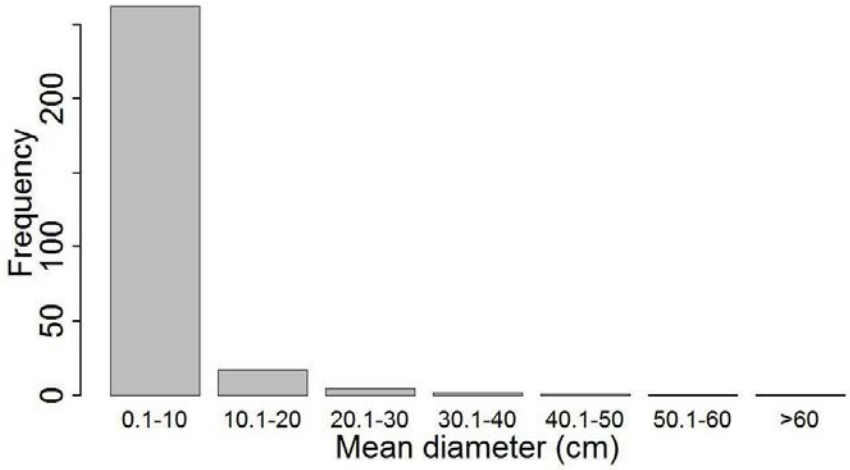

Figure 3.4 Colony size structure at year 2014 for fast (a) and slow (increased recruitment) (b) growing species.

3.4 Results

Meta-analysis of the three studies of effects of ocean acidification on recruitment produced a mean decrease in recruitment success of 32.25% per unit decrease in Ω_{Arag}.

Among study variation in the sensitivity of recruitment to ocean acidification is large with a standard deviation of 12% per unit decrease in Ω_{Arag}.

Regardless of whether species are fast or slow growing, effects of ocean acidification on recruitment exert more influence on λ than effects of ocean acidification on growth (dashed lines are always steeper than solid lines in Fig. 3.5). However, sensitivity of λ to ocean acidification depends on life history strategy – the λ of fast growing species is more affected by ocean acidification than that of slow growing species (lines in Fig. 3.5a are always steeper than similar typed lines in Fig. 3.5b). In spite of this, the proportional contribution of effects of ocean acidification on growth and recruitment to declines in λ were similar between fast growing species and slow growing species. In models where ocean acidification affected both growth and recruitment, 33% of the decrease in λ could be attributed to the effect of ocean acidification on growth, and 67% to the effect of ocean acidification on recruitment (Fig. 3.5).

Due to the small number of studies on the effect of ocean acidification on coral recruitment, the confidence intervals around projected decreases in λ rate are much larger when considering uncertainty around effect of ocean acidification on recruitment than effect on growth (red shaded area is much larger than grey shaded area in Fig. 3.5). In general, fast growing species are more sensitive to perturbations of growth and recruitment rate, relative to slow growing species (dashed lines are further away from the solid line in Fig. 3.6a than in Fig. 3.6b). Moreover, fast growing species are more sensitive to perturbations in growth rate than perturbations in recruitment rate (black dashed lines are further away from the solid

(a) (b)

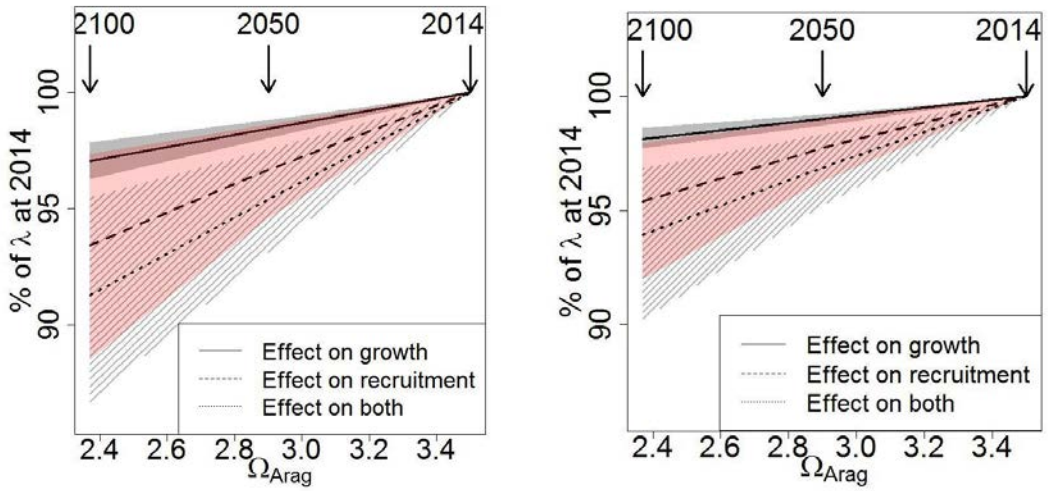

Figure 3.5 Model projections of the effects of ocean acidification under RCP 6.0 on the λ of (a) a fast growing species and (b) a slow growing species (increased recruitment success). The solid line represents the mean and the grey shade the confidence interval bounds (±1.96*SE) of projections with effect of ocean acidification on growth only, the dashed line represents the mean and the red shade the confidence interval bounds for projections with effect of ocean acidification on recruitment only, and the dot dashed line represents the mean and the line shade the confidence interval bounds for projections with effect of ocean acidification on both growth and recruitment.

line than red dashed lines in Fig. 3.6a), whereas slow growing species are equally sensitive to both (Fig. 3.6b). With respect to the conversion factor (from reduction in calcification to reduction in growth), varying it between 0.5 and 1 led to only a small difference (1% at most) in reductions in long-term population growth rate (Fig. 3.7). Lastly, the influence of ocean acidification on growth and recruitment are approximately additive in their effect on λ (points fall close to the dotted (unity) line in Fig. 3.8).

(a) (b)

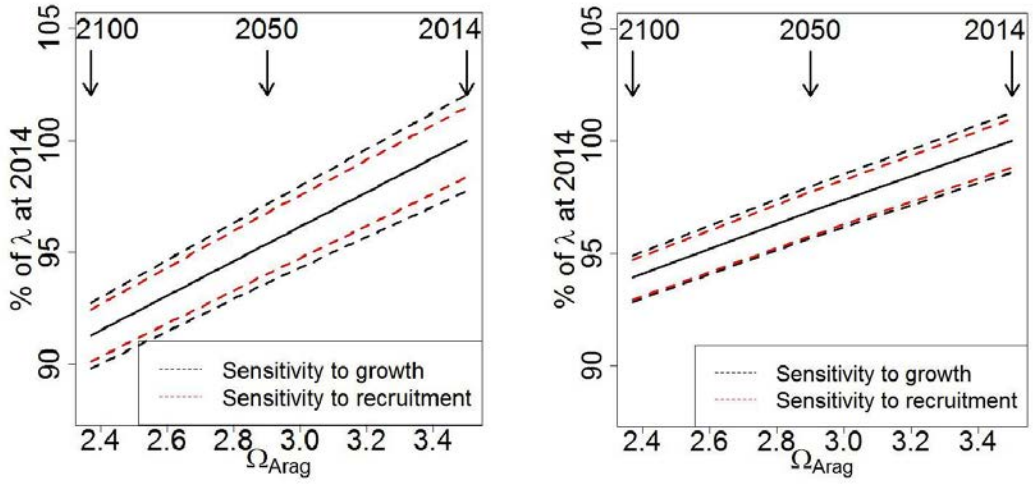

Figure 3.6 Sensitivity of λ of a fast growing species (a) and a slow growing species (b) to ±10% changes in growth and recruitment/fecundity

(a) (b)

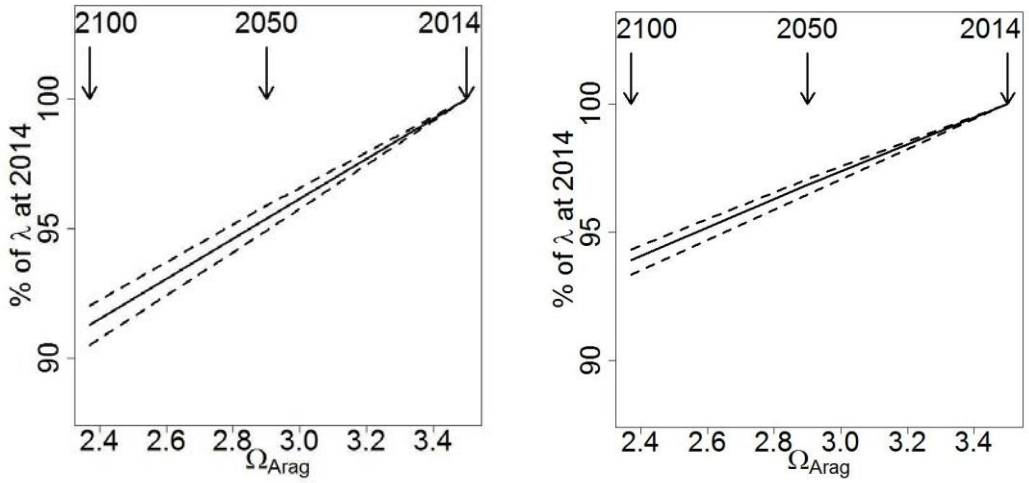

Figure 3.7 Sensitivity of λ of a fast growing (a) and a slow growing (b) species (increased recruitment success) to conversion factor for calcification to growth. Dashed lines are with conversion factor of 0.5 and 1

(a) (b)

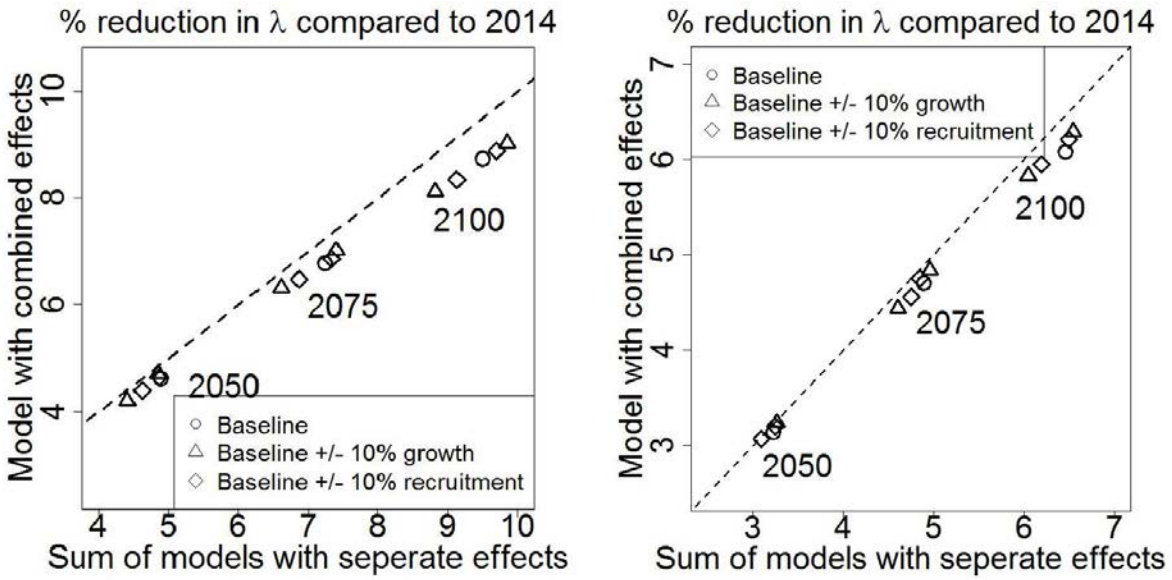

Figure 3.8 Comparison of λ produced by model with effect of ocean acidification on both growth and reproduction against the sum of the results from models with effect of ocean acidification on either growth or reproduction for a fast growing species (a) and a slow growing species (increased recruitment success) (b). If effect of ocean acidification on growth and reproduction was additive, points would fall on the dotted (unity) line.

3.5 Discussion

In this chapter, we compared the relative impacts on λ of the effects of ocean acidification on individual colony growth and recruitment, and investigated whether life history strategy of fast versus slow growth influenced how ocean acidification affected λ. Our results show that the impact of ocean acidification, via growth and recruitment, on λ are approximately additive and that regardless of life history strategy (fast or slow growing) the effects of ocean acidification on recruitment exert more influence on λ than effects of ocean acidification on growth. Because the effects of ocean acidification on growth and recruitment

are additive, we were able to compare their sensitivities directly. We found that recruitment is three times as sensitive to ocean acidification (32.25% decrease per unit decrease in Ω_{Arag}) as growth is (11.68% decrease per unit decrease in Ω_{Arag}, based on estimates of ocean acidification effects on calcification from Chapter 2 and the conversion factor from Jokiel et al. (2008)). In their latest meta-analysis of the effects ocean acidification on marine organisms, Kroeker et al. (2013) found that differences in sensitivity to ocean acidification among life history stages varied between groups (e.g. while ocean acidification significantly decreased growth and survival of mollusk larvae and juveniles, but not adults, it had consistent effects on crustacean juveniles and adults). This led them to suggest the identification of potential life history bottlenecks for each taxonomic group – i.e. whether a particular life history stage's susceptibility to ocean acidification could have a disproportionality large effect on λ. Our results suggest that while λ for coral populations is less sensitive to changes in recruitment (relative to changes in growth), recruitment could still be the population bottleneck for corals as it appears to be much more sensitive to ocean acidification (relative to growth). This highlights the importance of including recruitment (and the effect of ocean acidification on it) in future models that look to project the effects of ocean acidification on coral population trajectories (unlike what has been done in van Hooidonk et al. 2013 and Silverman et al. 2009).

Despite assuming a similar percentage decrease in growth and recruitment per unit Ω_{Arag} between fast and slow growing species, we find that that λ of fast growing species is more sensitive to ocean acidification (larger percentage decrease in λ per unit decrease in Ω_{Arag}) than that of slow growing species. Underpinning this is the fact that λ of fast growing species are more sensitive to changes in growth and recruitment rate in general, than that of slow growing species. Previous studies have suggested that slow growing species could be

'winners' and fast growing species 'losers' in the face of warming oceans (Marshall and Baird, 2000, Loya et al., 2001). Our finding that λ of fast growing species is more sensitive to ocean acidification than that of slow growing species, coupled with recent findings from a short term laboratory study that calcification of fast calcifiers is more sensitive to ocean acidification than slow calcifiers (Comeau et al., 2014b), suggests that this trend also holds for ocean acidification. Thus, ocean acidification could contribute to climate driven shifts in species composition on reefs – from faster growing branching dominated to slower growing massive dominated. This means that habitat complexity of reefs would be severely reduced, which would reduce their ability to supply ecosystem services (Moberg and Folke, 1999).

Unfortunately, while our study shows how vital it is that recruitment's response to ocean acidification be included in projection models, our understanding of how ocean acidification impacts coral recruitment is very limited compared to our understanding of the sensitivity of calcification to ocean acidification. Given that only three experimental studies have investigated realistic scenarios (i.e. including effects on CCA) of how recruitment is likely to decrease with ocean acidification (Albright et al 2010, Doropoulos et al 2012, Webster et al 2013), the uncertainty around our estimate of the recruitment-Ω_{Arag} relationship is very large compared to the growth-Ω_{Arag} relationship. Moreover while the calcification meta-analysis included responses from 18 different species across 10 different families, all three studies in the recruitment meta-analysis focused on the Acropora genus, so the among–study variation estimated is intra–genus variation and likely to be much smaller than inter–family variation. More experimental studies investigating the effects of ocean acidification on recruitment success of different coral species are needed to improve our understanding of the variability in the response of coral recruitment to ocean acidification and to lessen uncertainty in projections.

The other parameter that was not known with much certainty was the extent to which reductions in calcification translate into reductions in growth versus reductions in skeletal density. Experimental results so far suggest species specific decreases in growth (ranging from 0 to 100% of the reduction in calcification). Models so far have used conversion factors of 0.75-1 with no increases in mortality due to weaker skeletons (except for Madin et al. 2012). In our study, the uncertainty in the conversion factor makes very little difference to estimates of λ (less than 1% difference). Our model does not take into account the effects of weaker skeletons on mortality rates. It has been shown that such effects lead to smaller declines in λ than when decreased growth rates do (Madin et al. 2012). Assuming no weakening of the substrate, Madin et al. (2012) found that reduction in skeletal density led to reduction in λ of ~0.01-0.02 (roughly 2%) up to atmospheric pCO_2 of 600 uatm (the threshold point for species that are mechanically vulnerable to hydrodynamic forces). This suggests that our estimates are towards the pessimistic end of the spectrum.

The only other size-structured projection of coral populations under ocean acidification to date showed that λ of a fast growing tabular coral is only likely to decline below unity (indicating that populations are shrinking) towards atmospheric pCO_2 of 600 uatm (which will be reached by 2100 by the RCP 6.0 scenario) (Madin et al. 2012). Our results that the effects of ocean acidification on growth and recruitment are additive, and that the sensitivity of recruitment to ocean acidification is at the very least equal to the sensitivity of growth to ocean acidification suggest that λ is likely to decline below unity at lower levels of atmospheric pCO_2, making ocean acidification a very real threat to coral population existence. More research into the effects of ocean acidification on recruitment success is needed (to reduce the uncertainty around projections), if we are to accurately predict the large-scale, long-term effects of ocean acidification

4 Flow mediates the effects of ocean acidification on reef coral calcification and photosynthesis

4.1 Summary

Reef-building corals, which perform critical ecosystem functions such as reef growth and carbon cycling, are vulnerable to ocean acidification. Growing evidence indicates that corals' responses to ocean acidification are highly variable, but little is known about what drives this variability. Here, we investigated how flow, which influences both photosynthesis and calcification, changes the effects of ocean acidification on the coral *Acropora secale*. We found that calcification under high flow is more sensitive to ocean acidification (i.e., to lowered aragonite saturation state, Ω_{Arag}) than under low flow. For photosynthesis, due to high residual variance, the estimated flow and flow x ocean acidification effects, while potentially large in magnitude, were not statistically significant. Unexpectedly, the calcification/photosynthesis (g_n/p_n) ratio exhibits a considerably stronger relationship with Ω_{Arag} than either of these processes alone. These results suggest that the effects of ocean acidification vary substantially with flow speed, with flow having a stronger interactive effect on calcification than on photosynthesis. Differences in flow may account for some of the variability in calcification responses to ocean acidification documented in previous work, highlighting the potential for effects of ocean acidification to vary substantially along gradients of flow in coral reefs. Moreover, because many laboratory experiments on ocean acidification in corals have been conducted in low-flow conditions, the effects of ocean acidification on calcification in nature may be stronger than those experiments imply.

4.2 Introduction

Photosynthesis and calcification are fundamental processes that enable tropical scleractinian corals to form extensive three-dimensional reef structures that underpin high concentrations of biodiversity and supply critical ecosystem goods and services (Moberg and Folke, 1999, Allemand et al., 2004). However, coral photosynthesis and calcification are sensitive to changes in ocean chemistry that are associated with ongoing carbon emissions (e.g. Hoeke et al 2010). Specifically, ocean acidification, the reduction in pH of the oceans due to uptake of increased amounts of atmospheric CO_2, leads to an increase in the concentration of dissolved inorganic carbon (DIC) of seawater, which is a carbon source of coral symbiont photosynthesis (Furla et al., 2000). Also, ocean acidification leads to a decrease in the concentration of carbonate ions (CO_3^{2-}) and thus a reduction in the ocean's aragonite saturation state (Ω_{Arag}), which has been shown to correlate positively with coral calcification (Gattuso et al., 1999, Cohen and Holcomb, 2009, Schneider and Erez, 2006). To date, research into the effects of ocean acidification on corals has mainly focused on calcification, and while the consensus is that net calcification rate (calcification minus dissolution) varies positively with Ω_{Arag} (Anthony et al., 2011, Schneider and Erez, 2006, Langdon and Atkinson, 2005), results have been highly variable (Chan and Connolly, 2013). Sensitivities ranged from +25% to -66% calcification per unit decline of Ω_{Arag} and the cause of this variability is still poorly understood (Chan and Connolly 2013). Effects of ocean acidification on photosynthesis in corals are even less conclusive, with studies showing results varying from significant increases (Langdon and Atkinson, 2005, Marubini et al., 2008) to significant reductions in photosynthesis with ocean acidification (Reynaud et al., 2003, Anthony et al., 2008).

The effects of ocean acidification on both calcification and photosynthesis have been proposed to be linked to the uptake of available carbon (in the form of CO_3^{2-}, HCO_3^- or CO_2)

from bulk seawater (Schneider and Erez, 2006, Comeau et al., 2012) or the efflux of excess H^+ back into bulk seawater (Jokiel, 2011a, Jokiel, 2011b). Thus, any factors influencing the rate of mass transfer would be expected to modulate effects of ocean acidification (Mass et al., 2010). Mass transfer is partly a function of the thickness of the diffusive boundary layer (DBL) surrounding aquatic organisms, through which dissolved substances (e.g. nutrients and carbon species) enter and leave by diffusion (Shashar et al., 1996, de Beer et al., 2000, Jimenez et al., 2011). The rate at which molecules diffuse across DBLs also depends on the internal and external concentrations of molecules (Fick's laws: (Nobel, 1983). In turn, DBL thickness depends on water flow velocity over the surface of the organism: for a given organism shape and size, the DBL is thinner when flow is faster (Denny, 1988, Nobel, 1983). Previous studies have shown rates of nutrient uptake (Atkinson and Bilger, 1992, Thomas and Atkinson, 1997), photosynthetic production (Dennison and Barnes, 1988, Hoogenboom and Connolly, 2009) and nitrogen fixation in corals and algae to increase with greater water motion, proving that the exchange of metabolites between reef communities and their surrounding environment is mass transfer limited (Falter et al., 2005, Falter et al., 2004). Thus, flow velocity has been hypothesized to influence the effects of ocean acidification on marine organisms (Hendriks et al., 2010). Daily average flow rates among reef habitats vary within the range of 5 – 40 cms^{-1} (Fulton and Bellwood, 2005, Dennison and Barnes, 1988). Previous work has found no effect of flow on the effects of ocean acidification in the upper part of this range (20 – 40 cms^{-1}) (Langdon and Atkinson, 2005). However, because DBL thickness asymptotically approaches zero as flow increases, effects of flow on coral carbon metabolism have been found to be more pronounced at lower flows (Lesser et al., 1994, Hoogenboom and Connolly, 2009, Mass et al., 2010). It is not known how flow and ocean acidification interact in this lower range.

Here, we investigate how coral calcification and photosynthesis are influenced by combinations of ocean acidification and water-flow rates, focusing on a range of flows over which the DBL has been shown to affect metabolic rates (Mass et al., 2010, Hoogenboom and Connolly, 2009). Previous studies have shown that, under low flow, pH at the surface of a photosynthesizing organism is much higher than in bulk seawater, due to the dampening effect provided by the thicker boundary layer (Kühl et al., 1995, Hurd et al., 2011). Thus, we hypothesize that this dampening will reduce the impact of ocean acidification at low flows compared to high flows. Specifically, we test two hypotheses: 1) low flow will weaken the (negative) effect of ocean acidification on calcification, and (2) low flow will weaken the (positive) effect of ocean acidification on photosynthesis.

4.3 Methods

4.3.1 Experimental study

The study was carried out over 3 weeks from mid September to early October 2011. Colonies of *Acropora secale* were collected by scuba diving from a depth of 5 – 10m at Davies Reef (18.83S, 147.64E) on the Great Barrier Reef, Australia. Colonies were then relocated to the aquarium facilities at Reef HQ (the National Reef Education Centre for the Great Barrier Reef Marine Park Authority - www.reefhq.com.au) in Townsville and allowed to acclimate in rooftop holding tanks (continuous flow of seawater) for 4 weeks before laboratory experiments began. Holding tanks were shaded by shade cloth and had an average irradiance of 290 μmol photons $m^{-2}s^{-1}$. During experiments, four to five colonies (7 – 12cm in diameter) were placed in each of two 0.15m wide by 0.15m deep by 1m long recirculating flow tanks (Fig. 4.1). The flow tanks conformed to the design of Vogel and LaBarbera (1978) and are described as 'producing fully turbulent flow with boundary layers with a clearly definable logarithmic layer, similar to measurements in the field taken under steady flow conditions' (Jonsson et al., 2006). The use of the alkalinity anomaly technique to measure

calcification requires high ratio of coral surface area to water volume, and it's implausible to have many individual coral colonies all lined up perpendicular to the direction of the flow, thus corals were lined up parallel to direction of flow and arranged by height, from shortest to tallest to minimize obstruction of flow to corals at the back by corals in front. The same corals were used for all treatment levels, with corals remaining in the flumes in the same configuration for the duration of the experiment. Four-hour long experimental runs (one run per day) were carried out at five different pH levels and three different flow velocities (with the same pH and flow velocity used in both flumes simultaneously), with no two consecutive days having the same flow (see Tab. 4.1 for details). Also, down (non experiment) time flow was always set to be different to the treatment flow immediately following that particular down time. There was no pre-incubation of corals to a given treatment. All measurements were made in the light (no dark period during incubation). Temperature was measured with Aquatronica temperature sensors and conductivity was measured with an Aquatronica saltwater high conductivity electrode (www.aquatronica.com). Salinity was calculated from values of temperature and density using Unisense seawater tables (www.unisense.com/files/PDF/Diverse/Seawater%20&%20Gases%20table.pdf). Light was provided by Aqua Medic Ocean Light Pluses (www.aqua-medic.com) at ~200 μmol photons $m^{-2}s^{-1}$ on a 10h on 14h off photoperiod. Photosynthesis saturation occurs in corals in the range of 200-300 μmol photons $m^{-2}s^{-}1$ (Goiran et al., 1996, Trench, 1987). As the objective of the study was to compare the effect of acidification at various flows, we did not require the corals to be photosynthesizing at maximum rate and, hence, we picked a light level that was around about the sub-saturation irradiance (i.e. where photosynthesis is 50-75% of maximum rate of photosynthesis but light levels aren't high enough to cause any photoinhibition). Corals were also allowed to acclimate to experimental light conditions for 3 days. Seawater used in experimentation was taken directly from the inshore water outside Reef HQ. Flow in

each tank was manipulated by varying the voltage to the propeller until measured (via particle tracking) flow velocity was equal to target flow. Neutrally buoyant brine shrimp (*Artemia*) eggs were used as markers and were visually tracked between two points on the flume. Flow velocity was measured with corals present. An Aquatronica control unit connected to a Dupla CO_2 manipulation system (www.dupla.com.au) was used to establish the initial desired treatment pH by dosing CO_2 into a 250 L seawater reservoir. Flumes were filled from the reservoir at the start of each run and then pH was allowed to drift during incubation. As the initial total alkalinity (A_T) was simply that of the incoming natural seawater, the highest Ω_{Arag} levels used in our experiments were that of the unmanipulated seawater from outside Reef HQ. These Ω_{Arag} levels were within the range of Ω_{Arag} found over the span of a day on Davies reef during winter (3.0-3.8) (Albright et al., 2013). A layer of bubble wrap was floated on the surface of flumes to reduce gas exchange with air. Empty flume runs were conducted as controls at each flow and pH treatment combination, with background pH changes (increases of 0.25, 0.25 and 0.35 for 5, 12 and 20 cms^{-1} respectively) used to correct all data. Water samples were collected (in triplicate) before and after each experimental run and were analyzed the same day for pH (Dupla pH probe in experimental flumes at Reef HQ) and A_T. Potentiometric determination of the pH was performed on the NBS hydrogen ion concentration scale (pH_{NBS}). The precision of the analysis based on triplicate measurements using the two different pH probes (Dupla pH probe at Reef HQ and Metrohm 888 Titrando Titrator at James Cook University) was better than ±0.02 units. A_T was determined by automatic potentiometric titration to pH values well below the second end point (~3.3) (Metrohm 888 Titrando Titrator Metrohm AG, Switzerland), and the Gran function plot method, to within 1% of certified reference material (Prof. A. Dickson, Scripps Institute of Oceanography). The precision of the analysis based on triplicate measurements was typically ±4 umol kg^{-1}. Calculation of Ω_{Arag} and all other carbonate system parameters were carried out

using CO2Calc (Robbins et al., 2010) using the constants K1 and K2 from Mehrbach et al. (1973) refit by Dickson & Millero (1987) , and Dickson for $KHSO_4$.

(a) (b)

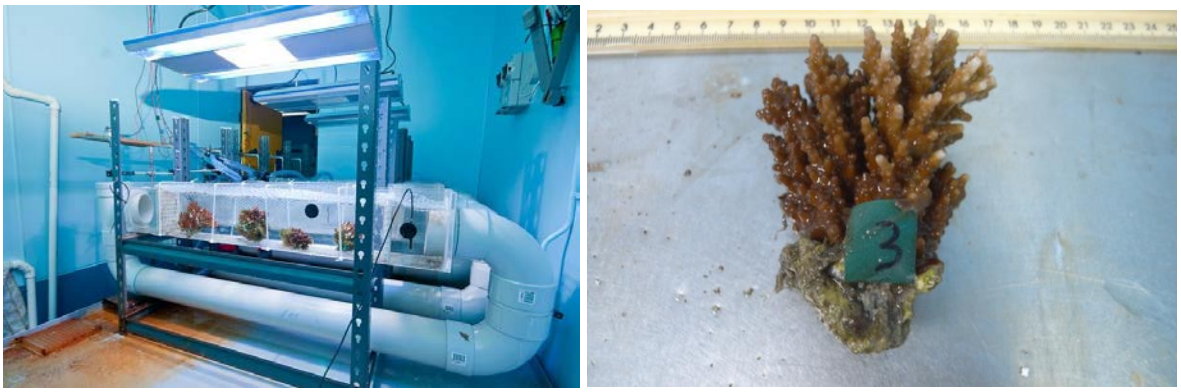

Figure 4.1 Images of the experimental setup. a) The flume b) Example of an *A. secale* colony used

Table 4.1 Carbonate chemistry for each experimental treatment. Flow is in cms^{-1}, temperature is in °C, salinity is ppt, atmospheric pCO_2 is in µatm, pH is on the NBS hydrogen ion concentration scale, and total alkalinity (A_T), bicarbonate (HCO_3^{2-}), carbonate (CO_3^{2-}), CO_2, and dissolved inorganic carbon (DIC) are all in umol kg^{-1}. Aragonite saturation state (Ω_{Arag}) is unit less.

Order	Flow	Temp	Sal	pCO_2	pH_{NBS}	A_T	HCO_3^{2-}	CO_3^{2-}	CO_2	DIC	Ω_{Arag}
1	5	24.3-25.3	38	576	8.04-8.08	2397-2489	1973	192	16	2181	2.97
1	5	24.3-25.3	37.7	508	8.08-8.13	2409-2460	1929	206	14	2149	3.21
9	5	25.7-26.3	37.4	948	7.76-7.97	2297-2419	2040	129	26	2195	2.03
9	5	25.7-26.3	37.9	988	7.77-7.95	2379-2486	2106	134	27	2266	2.08
6	5	24.4-25.1	38.2	1515	7.62-7.78	2468-2540	2269	97	42	2408	1.50
6	5	24.4-25.1	38.4	1547	7.62-7.77	2502-2551	2291	97	43	2431	1.50
3	5	24.2-25.2	37	2943	7.28-7.54	2341-2395	2251	48	83	2382	0.74
3	5	24.2-25.2	37.3	2793	7.33-7.55	2407-2433	2292	52	79	2423	0.82
12	5	25-25.9	37.8	3859	7.15-7.48	2450-2473	2360	42	106	2508	0.65

12	5	25-25.9	38.1	3887	7.18-7.45	2473-2492	2380	43	107	2529	0.66
2	12	24.3-25.2	37.5	453	8.09-8.19	2341-2440	1863	215	13	2090	3.34
2	12	24.3-25.2	37.7	465	8.09-8.18	2390-2461	1894	217	13	2124	3.37
10	12	25.6-25.9	37.6	1161	7.72-7.87	2374-2459	2136	115	32	2283	1.80
10	12	25.6-25.9	38	1187	7.73-7.85	2413-2476	2161	116	32	2310	1.81
5	12	24.4-25.4	37.3	1295	7.65-7.84	2341-2424	2140	99	36	2275	1.55
5	12	24.4-25.4	37.7	1334	7.64-7.84	2395-2466	2183	101	37	2322	1.57
7	12	24.6-25.5	38.4	2788	7.3-7.61	2471-2549	2369	58	77	2505	0.90
7	12	24.6-25.5	38.5	2845	7.3-7.6	2515-2549	2391	58	79	2528	0.90
14	12	24.9-26	38.1	4436	7.07-7.45	2484-2484	2393	38	122	2553	0.59
14	12	24.9-26	38.3	4592	7.07-7.43	2506-2519	2422	37	126	2586	0.58
15	20	24.7-25.5	38.1	734	7.89-8.05	2380-2513	2079	166	21	2265	2.59
15	20	24.7-25.5	38.2	736	7.9-8.06	2418-2547	2045	164	20	2230	2.54
13	20	24.8-25.5	38.2	1252	7.7-7.84	2415-2512	2193	111	35	2339	1.72
13	20	24.8-25.5	38.3	1273	7.71-7.82	2435-2514	2205	111	35	2351	1.71
4	20	24.5-25.3	37.8	1700	7.49-7.8	2395-2484	2236	83	48	2367	1.30
4	20	24.5-25.3	38.1	1689	7.5-7.8	2416-2501	2250	86	47	2383	1.33
8	20	24.3-25.7	38.3	2964	7.22-7.63	2464-2499	2351	54	82	2487	0.83
8	20	24.3-25.7	38.1	2847	7.24-7.65	2470-2524	2364	56	79	2499	0.87
11	20	24.5-25.8	38.2	2989	7.32-7.53	2480-2515	2366	54	83	2503	0.84
11	20	24.5-25.8	38.4	3169	7.31-7.5	2514-2537	2398	53	88	2538	0.81

4.3.2 Data analysis

Net calcification (g_n) was calculated from the change in A_T with the following equation:

$$g_n = -\frac{1}{2}\Delta A_T \times \frac{(V_{flume}-V_{colonies})\times 1.026}{\Delta t \times SA} \quad \text{Eqn 4.1}$$

where ΔA_T (umol kg^{-1}) is the difference in A_T between samples taken before and after each flume run, V_{flume} (cm^3) is the volume of the flumes used for the incubation, $V_{colonies}$ (cm^3) is the displacement volume of the corals , 1.026 (g cm^{-3}) is the seawater density, Δt (h) is the duration of the incubation and SA (cm^2) is the surface area of the calcifying coral (Smith and Kinsey, 1978). Net photosynthesis (p_n) was calculated from the change in DIC and A_T using the following equation:

$$p_n = (\Delta DIC - -\frac{1}{2}\Delta A_T) \times \frac{(V_{flume}-V_{colonies})\times 1.026}{\Delta t \times SA} \quad \text{Eqn 4.2}$$

where Δ DIC (umol kg^{-1}) is the difference in DIC between samples taken before and after each flume run (Chauvin et al., 2011, Nakamura and Nakamori, 2009, Smith, 1978). DIC was calculated from measured A_T and pH values using program CO2Calc, as previous studies have showed that the average percent error between predicted (from pH and A_T) and measured values of DIC is 2% (Ries et al., 2010).

4.3.3 Calculation of surface area and volume

To estimate surface area, each coral was divided into branches and a hemisphere below the branches. Branches were assumed to be cylinders of variable radius, so surface area was estimated by numerically integrating up each branch with equation $\int_0^{hmax} 2\pi r(h)\, dh$ where h is branch height and r is branch radius at height h. Hemispheres were assumed to have surface area $2\pi R^2$, where R is the radius of the hemisphere. Total surface area was thus $N * \int_0^{hmax} 2\pi r(h)\, dh + 2\pi R^2 - N * 2\pi r(0)^2$ where N is the number

of branches. The first term (with the integral) is the surface area of each branch. The second term is the surface area of the basal hemisphere. The final term subtracts the parts of the basal hemisphere that where the branches are attached (which would therefore not be covered by tissue). Volume of colonies was calculated as $\int_0^{hmax} \pi r(h)^2 \, dh$ (volume of a cylinder) plus $\frac{2}{3}\pi r^3$ (volume of a hemisphere). All measurements were performed using the software ImageJ (National Institute of Health, USA) with pixel counts standardized to ruler length.

4.3.4 Fitting of models to data

All statistical analyses were performed using the software R (R Development Core Team 2011). Linear model analysis was used to investigate how net calcification responds to flow and Ω_{Arag}, and how net photosynthesis responds to flow and DIC concentration. For photosynthesis, we used DIC, rather than Ω_{Arag}, because DIC is a more direct measure of substrate availability for photosynthesis. While photosynthesis is commonly believed to utilize only CO_2 from the surrounding seawater, Al-Moghrabi et al. (1996) showed that 100% of DIC dependent O_2 evolution is sensitive to DIDS (an anion exchange protein inhibitor), suggesting that HCO_3^- uptake is responsible for the total DIC supply of zooxanthellae photosynthesis. These two carbon species make up the bulk of DIC. To better elucidate the mechanisms through which ocean acidification and flow affect net carbon fluxes, we also examined how the ratio of calcification to photosynthesis changed with ocean acidification and flow. To do this, we normalized net calcification to net photosynthesis, g_n/p_n, and used linear models to analyze how this composite response variable responded to Ω_{Arag} (as in Chauvin et al. 2011). Preliminary analysis suggested a non-linear response of net calcification to Ω_{Arag} (as has been found by Ries et al (2010) and Anthony et al (2011)), but log-transformation of Ω_{Arag} linearized the relationship between net calcification and Ω_{Arag}. This

allowed exploration of the interaction between ocean acidification and flow using standard linear model analysis.

Because the study involved repeated experimental runs conducted on the same corals, we checked for temporal auto-correlation in the data. We also tested for tank effects in our analysis. All models were fitted using the gls() (generalized least squares) function from the nlme package (Pinheiro et al., 2012). We used model selection to test for temporal autocorrelation by the Likelihood ratio test using Restricted Maximum Likelihood estimation (Zuur et al., 2009). Specifically, we fit models including the compound asymmetry and auto-regressive moving average (ARMA) models implemented by gls(), and then we compared the best-fitting of these models with a model assuming no temporal autocorrelation. Models were then checked for normality and homogeneity of variance using standard visual diagnostics. We next used model selection to test for tank effects by likelihood ratio test using Maximum Likelihood estimation (Zuur et al., 2009). Where model selection indicated that the relevant effect did not significantly improve model fit, we excluded the variable from the final model.

In addition, we carried out a leverage analysis (using Cook's distance) to ensure that results of the linear model analysis were not sensitive to outliers. This involves measuring the effect on the model fit by deleting each observation and examining the response. Our observations were well below the recommended threshold Cook's Distance of <1 as a rule of thumb for robust results (Zuur et al., 2009). Nevertheless, we re-ran our analyses without the point with the largest Cook's distance value (0.46). As expected, we found no qualitative difference in the results: all statistically significant effects remained so after re-analysis; likewise, non-significant results remained non-significant.

4.4 Results

For calcification, model selection identified an ARMA(2,0) temporal autocorrelation structure, and an interaction between flow and ocean acidification, but no tank effect (Appendix D, Tab. 4.2). The negative effect of ocean acidification on coral calcification increased with flow velocity. Specifically, higher flows were associated with higher calcification at high Ω_{Arag} but also greater sensitivity to decreasing Ω_{Arag}, compared to lower flows (Fig. 4.2a, Tab. 4.2).

a) b)

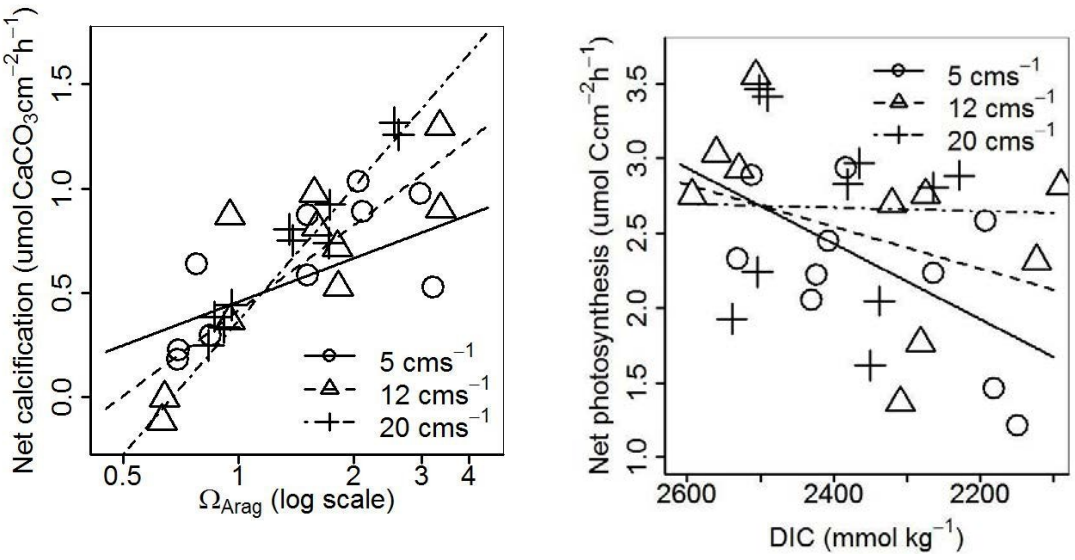

Figure 4.2 a) Calcification (ΔA_T, g_n) as a function of aragonite saturation state (Ω_{Arag}) and for *A. secale*, illustrating the nature of the interaction between flow and ocean acidification. Each point (N=30) is an individual experimental run. b) Photosynthesis (alkalinity corrected ΔDIC, p_n) as a function of dissolved inorganic carbon (DIC) for *A. secale*, illustrating the nature of the interaction between flow and ocean acidification. Each point (N=30) is an individual experimental run. Note that under ocean acidification, DIC increases from 2100 to 2600. The different symbols used for the points represent different flow velocities (circles – 5 cms^{-1}, triangles – 12 cms^{-1}, and crosses – 20 cms^{-1}). See table 4.2 for function parameters.

Table 4.2 Fitted parameters for linear models relating calcification to flow velocity and log(Ω_{Arag}), relating photosynthesis to flow velocity and DIC, and relating the ratio of calcification to net photosynthesis to log(Ω_{Arag}).

	estimate	**standard error**	**p-value**
calcification (µmol $CaCO_3$ cm^{-2} h^{-1})			
intercept	0.487	0.123	**0.0005**
log Ω_{Arag}	0.094	0.107	0.3912
flow (cms^{-1})	-0.006	0.004	0.1924
flow (cms^{-1}) x log Ω_{Arag}	0.041	0.009	**0.0001**
photosynthesis (µmol C cm^{-2} h^{-1})			
intercept	-5.647	4.3	0.2006
DIC (umol kg^{-1})	0.003	0.002	0.0785
flow (cms^{-1})	0.4014	0.348	0.2590
flow (cms^{-1}) x DIC	-0.0002	0.0001	0.2822
Calcification/photosynthesis			
intercept	0.213	0.018	**0.0000**
log Ω_{Arag}	0.290	0.023	**0.0000**
tank	-0.05	0.024	**0.0435**

For photosynthesis, model selection indicated neither temporal autocorrelation nor tank effects (Appendix D). For flow and ocean acidification, parameter estimates suggested a potentially large interaction, with increased DIC having a smaller effect under high flow than low flow, contrary to our second hypothesis. However, due to high residual variance, the estimated flow and flow x DIC effects, while large in magnitude, were not statistically significant (Fig. 4.2b, Tab. 4.2).

For g_n/p_n , model selection yielded no temporal autocorrelation structure but a significant main effect of tank (Appendix D). Analysis also showed that decreasing Ω_{Arag} reduces g_n/p_n, but that there was no effect of flow on this relationship (Fig. 4.3, Tab. 4.2). In other words, the effects of flow on calcification are canceled out by the effects of flow on photosynthesis. Coupled responses of calcification and photosynthesis are further suggested by the unexplained (residual) variability in the calcification and photosynthesis analyses: residuals from the calcification analysis are strongly positively correlated with the residuals from the photosynthesis analysis (Fig. 4.4). Consistent with this, the residual standard error (0.055) of the g_n/p_n analysis was an order of magnitude lower than that of the calcification (0.426) and photosynthesis (0.531) analyses. Tank did not interact significantly with flow or Ω_{Arag}, which meant that the tanks had different intercepts but the effect of Ω_{Arag} was consistent across tanks (Fig. 4.3, Tab. 4.2).

a) b)

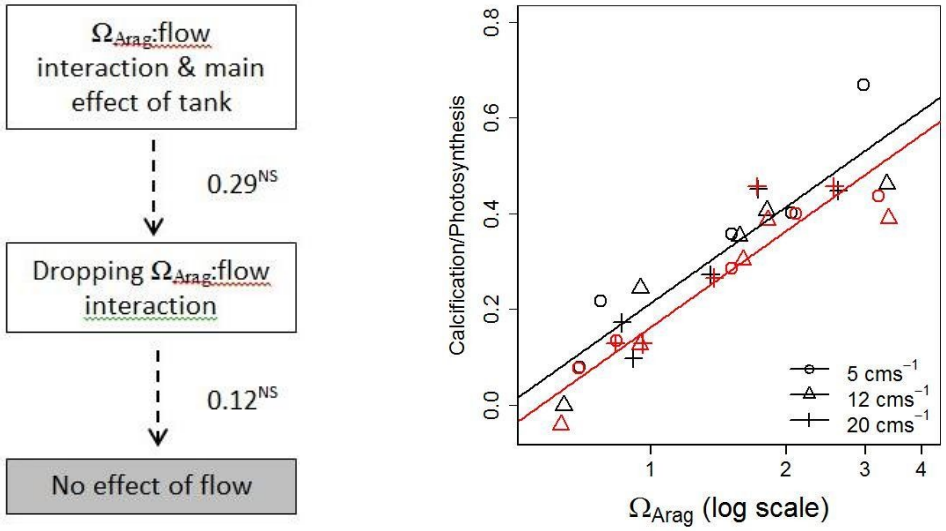

Figure 4.3 (a) Flow diagram of model selection for the ratio of net calcification to photosynthesis (g_n/p_n) based on Likelihood Ratio statistics (using ML estimation). Values on arrows represent the Likelihood ratio when comparing the two alternative models connected by the arrow, with the arrow indicating the direction of preference i.e. points to the favoured model. Dashed lines indicate that the more complex model is not significantly better (at **α**=0.05), in which case the simpler model is preferred (b) g_n/p_n of *A. secale* as a function of aragonite saturation state (Ω_{Arag}). See table 4.2 for function parameters. Each point (N=30) is an individual experimental run. The different symbols used for the points represent different flow velocities (as shown in legend). The line was plotted using the best-fit parameter estimates from Tab. 4.2. Black symbols and lines represent tank 1 and red symbols and lines represent tank 2.

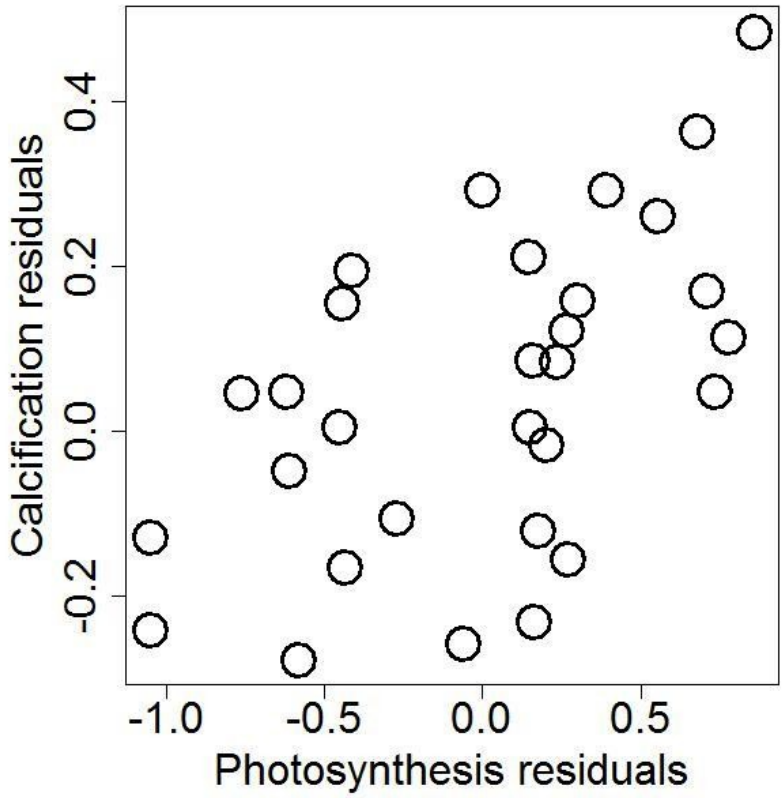

Figure 4.4 Residuals from the calcification model versus residuals from the photosynthesis model. Each point is an individual run.

4.5 Discussion

This study shows that high flow increases the sensitivity of calcification to ocean acidification (measured as decreasing Ω_{Arag}), which is consistent with our first hypothesis: that low flow will weaken the (negative) effect of ocean acidification on calcification. This also is consistent with experimental work on other marine organisms showing that low flow leads to a thicker boundary layer and thus higher pH at the surface of a photosynthesizing organism (Hurd et al., 2011, Kühl et al., 1995). It is contrary to suggestions that the dampening effect may not happen in corals due to the spatial segregation in calcifying and photosynthesizing zones (Jokiel 2011b). A likely explanation for the reduced sensitivity with

lower flow is that thicker DBLs lead to increased O_2 saturation at the coral tissue surface (Hoogenboom and Connolly, 2009). Increased O_2 saturation has been shown to increase calcification rates (Wijgerde et al., 2012) and, in combination with glucose or glycerol, has been shown be the driver of 'light enhanced' calcification (Holcomb et al., 2014). More recently, hyperoxia has even been shown to reduce the sensitivity of calcification to changes in pH (Wijgerde et al., 2014).

A recent meta-analysis summarizing the sensitivity of coral calcification to ocean acidification found that calcification decreases by ~25%, on average, per unit decrease in Ω_{Arag}, when calcification is measured by total alkalinity (TA), as in our study (Chan and Connolly, 2013). However, 40% of studies in that analysis had sensitivities less than 20%, which is of a similar magnitude to the sensitivity of our low flow treatment. This could be due to the fact that many experimental studies are conducted under laboratory conditions likely to be associated with very low flow (e.g., coral nubbins in small containers with circulation induced purely by the flow-through of seawater). Indeed, two studies in the meta-analysis which used wave generators to reproduce flow regimes more characteristic of natural reef conditions (20 – 50 cms^{-1}) produced results at the uppermost end of the sensitivity distribution (40% and 65% change in calcification per unit of Ω_{Arag}, respectively Langdon et al., 2000, Langdon and Atkinson, 2005). Our results suggest that differences in flow may account for some of the variability in responses to ocean acidification documented in previous work, and highlights the potential for effects of ocean acidification to vary substantially along gradients of flow in coral reefs. Our results also suggest that the response found by experimental studies carried out under low flow conditions could be underestimating the effects of ocean acidification in the field, particularly at sites exposed to ocean currents and wave action.

Our finding that flow has a stronger effect on calcification than it does on photosynthesis is consistent with current understanding of the spatial distribution of calcification and photosynthesis in corals generally (see Jokiel 2011a for a review), and with the dynamics of flow around branching corals in particular (Chang et al., 2009, Reidenbach et al., 2006). Previous work on flow through densely packed branching corals indicates that friction between moving water and colony branches leads to reduced flows through the colony, with most of the water diverted around the coral (Chamberlain and Graus, 1977, Reidenbach et al., 2006). In branching corals, branch tips, which are exposed to the full effects of changing flow, have high calcification rates and low photosynthesis rates, whereas branch sides, which are mostly sheltered within the colony, have higher concentrations of zooxanthellae (Jokiel 2011a). Thus, changing flow could be expected to have a larger effect on calcification than it would on photosynthesis. This reduction of flows adjacent to zones of photosynthesis is likely to be less pronounced in encrusting or mound corals, suggesting that different colony morphologies might exhibit differing effects of flow and ocean acidification on coral production.

The ratio of calcification to photosynthesis decreased with Ω_{Arag} but not with flow. At $\Omega_{Arag} \approx 3$, we found a g_n/p_n ratio of approximately 0.5, which is consistent with findings for patches of *Acropora* spp. on reef flats of Ishigaki Island, Japan (Nakamura and Nakamori, 2009). A striking and unexpected finding of our study was that g_n/p_n was independent of flow, despite the existence of a strong flow- Ω_{Arag} interaction, at least for calcification. A direct linkage between the responses of the two variables is indicated by the strong positive correlations between the residuals of the calcification and photosynthesis analyses (Fig. 4.4). That is, experimental runs with unusually high calcification, given the flow and ocean acidification levels, also tended to have unusually high photosynthesis, and runs with

unusually low calcification tended to have low photosynthesis. Consequently, the g_n/p_n model explained more variability (had a lower residual standard error) than the calcification and photosynthesis models individually. The smaller residual variation of the g_n/p_n model suggests that photosynthesis and calcification are coupled (i.e. a reduction in one will cause a reduction in the other). Such a coupling, most probably with changes in photosynthesis driving changes in calcification (but see McConnaughey & Whelan, 1997 for a counter hypothesis), could be due to photosynthesis providing energy for calcification (Colombo-Pallotta et al., 2010), increasing O_2 saturation in the tissue (Wijgerde et al., 2012), or increasing the pH of the polyp coelenteron (Al-Horani et al., 2003, McCulloch et al., 2012, Venn et al., 2011).

The extent to which metabolic responses of corals to flow, such as those measured here, may be influenced by acclimation is relatively poorly understood. A previous study found that, after 14 days of acclimation to a new flow, there was an ~25% difference in net and gross photosynthesis (normalized to surface area) between flows of 1.3cms^{-1} and 11cms^{-1} (Lesser et al., 1994). This is similar in magnitude to the difference that we found over a similar range (5 to 12 cms^{-1}), suggesting that our results are likely robust to acclimation on physiological time scales. However, Lesser et al. (1994) did find that colonies of the coral *Pocillopora damicornis* had different morphologies when growing in low versus high flow environments in nature, in such a way that they had the same Reynolds numbers and metabolic rates across flow regimes. Likewise, a two-year long in-situ experimental study on *Pocillopora verrucosa* found that enhanced flow lead to more compact morphology, denser skeletons, higher chlorophyll and protein concentrations, a higher density of zooxanthellae and higher reproductive output (Mass et al., 2011). This suggests that corals with the capacity to alter their growth form substantially in response to flow environments may be able to

partially alter their metabolic responses to flow, relative to what may be measured in experimental settings.

Experimental studies that combine multiple variables that affect calcification in marine organisms recently have been highlighted as a research priority (Kleypas and Langdon, 2006, Pandolfi et al., 2011). Flow is a critically important environmental driver of coral ecosystem functioning, via its influence on mass transfer (Atkinson and Bilger, 1992), and reef community structure (Done, 1983). The present study demonstrates a significant interaction between flow and ocean acidification in the calcification response of the coral *Acropora secale*. Coral calcification in high flow environments is more sensitive to decreasing Ω_{Arag} than in low flow environments, and higher flow shifts from promoting calcification to inhibiting it as Ω_{Arag} changes from over-saturated to under-saturated. Increased O_2 saturation at the coral tissue surface, due to lower flow and thus thicker DBLs, potentially accounts for the reduction in sensitivity of calcification rates to ocean acidification under lower flows. Our results suggest that variation in corals' responses to ocean acidification could be flow-mediated, but that the ratio of calcification to net photosynthesis ratios is likely to respond much more consistently to ocean acidification among different flow environments. Our findings also suggest that experimental studies are likely to underestimate the effects of ocean acidification on coral calcification in nature, when they are conducted under water flow conditions that are low, relative to what typically occurs on coral reefs.

5. Interaction of flow and colony morphology in determination of coral tissue surface pH

5.1 Summary

Considerable uncertainty remains about the impact of ocean acidification on coral calcification. Boundary layer effects have been suggested as one factor leading to differences between early models predicting ocean acidification to be a major threat to marine biodiversity and actual sensitivity of organisms to ocean acidification found in experimental studies. The build-up of a diffusive boundary layer (DBL) surrounding aquatic organisms, wherein solute transport is controlled by diffusion, can lead to steep concentration gradients of metabolic gases and ions. Such boundary layer effects can lead to pronounced differences between the bulk seawater pH, and the actual pH experienced by the organism. Tissue surface pH is modulated by both mass transfer and metabolic activity, which are in turn dependent on DBL thickness and thus flow and morphology. In the present study, we experimentally parameterized and evaluated a basic diffusion-reaction-uptake model to elucidate the factors that underpin the flow/morphology interaction. Specifically, we investigated whether the effect of flow on DBL dynamics differed between a branching and a massive species, and whether morphology-driven differences in DBL characteristics lead to differences in tissue surface pH. We also ask whether the model predicts differences in tissue surface pH under ambient versus acidified condition. Consistent with model predictions, we observed increases in the elevation of tissue surface pH at lower flows, and thus thicker DBLs. Moreover, under ocean acidification, elevations in tissue surface pH can reach a point at which tissue surface pH under acidified conditions is equal to tissue surface under non-acidified conditions. We also show that the degree of elevation of tissue surface pH differs by morphology, with massive corals able to elevate tissue surface pH to higher levels than branching corals. However, these elevations in tissue surface pH have been found at relatively low flows that

are rarely encountered by corals in nature, suggesting that the DBL effect is unlikely to ameliorate the decreases in coral calcification under ocean acidification.

5.2 Introduction

Besides harbouring a substantial proportion of the ocean's biodiversity, corals reefs are estimated to have a net global economic value of $29.8 billion each year. Such reefs form when scleractinic corals (and a number of other calcifying reef organisms) can produce calcium carbonate ($CaCO_3$) skeletons faster than the sea can erode them (Cohen and Holcomb, 2009, Cesar et al., 2003). These processes are inherently linked to the inorganic carbon chemistry of the oceans and atmosphere. Over the last half century, anthropogenic CO_2 emissions have caused atmospheric CO_2 to rise steadily from ~320 ppm to ~390ppm (IPCC, 2013). About 33% of this enhanced atmospheric CO_2 dissolves into the oceans, causing a shift in the seawater carbonate system that results in a decrease in both oceanic pH and the abundance of carbonate ions that corals use to build their skeletons. These effects of enhanced dissolution of CO_2 into the oceans are commonly termed ocean acidification, which has been identified as a global threat for coral reefs, predicted to slow coral calcification to a point where the rate of reef erosion exceeds the rate of skeletal accretion (Silverman et al., 2009, van Hooidonk et al., 2013). However, considerable controversy remains about the actual impact of ocean acidification on coral calcification (Pandolfi et al., 2011, Chan and Connolly, 2013).

The build-up of a diffusive boundary layer (DBL) surrounding aquatic organisms, wherein solute transport is controlled by diffusion (Jørgensen and Revsbech, 1985, Boudreau and Jørgensen, 2001), can lead to steep concentration gradients of metabolic gases and ions (Boudreaux and Jørgensen 2001). Such boundary layer effects can lead to pronounced differences between the bulk seawater pH, and the actual pH experienced by the organism,

which is modulated by both mass transfer and metabolic activity (Kühl et al., 1995). Microsensor measurements across the DBL thus show elevated pH at the tissue surface of corals during daylight and lower pH in darkness as compared to the bulk seawater (de Beer et al., 2000, Al-Horani et al., 2003, Kühl et al., 1995). Hence, the actual tissue surface pH of corals does not necessarily correspond to that predicted to occur in the bulk water phase by the end of the century, which tends to be what current predictions are based upon (Hendricks et al. 2010). The lack of consideration of so-called boundary layer effects has thus been suggested as one factor leading to differences between early models predicting ocean acidification to be a major threat to marine biodiversity (Kleypas et al., 1999a) and actual sensitivity of organisms to ocean acidification found in experimental studies (Hendriks et al., 2010, Ries et al., 2009).

Tissue surface pH of coralline alga and foraminifera has been shown to be dependent on the metabolic rate of the organism (i.e. photosynthesis, respiration and calcification) and the thickness of the DBL (Wolf-Gladrow et al., 1999, Cornwall et al., 2014). In turn, DBL thickness is largely a function of fluid velocity and surface roughness (Denny, 1988, Jumars and Nowell, 1984). Although flow regime has a central role in determining coral surface pH, experimental studies on the effects of ocean acidification on coral calcification are just only beginning to recognise the interactive effects of ocean acidification and flow (Comeau et al., 2014a). As such, previous studies have been carried out over a large range of flow velocities, ranging from 1 cm s^{-1} (Ohde and Hossain, 2004) to 40 cm s^{-1} (Langdon et al., 2000), making a direct comparison of ocean acidification related effects difficult. Moreover, experiments have been carried out on a large variety of study species, and the effect of flow on respiration and photosynthesis has been shown to differ by genus (Hoogenboom and Connolly, 2009). Thus, flow velocity driven differences in tissue surface pH could possibly explain some of

the large variation in the response of corals to ocean acidification among experimental studies carried out so far.

Coral morphology is another factor that could interact with flow velocity to further drive pH variation among coral studies. For instance, the DBL thickness of branching and massive corals can be very different, despite similar regimes of ambient flow (Jimenez et al., 2011). Such differences in DBL thickness might explain why branching *Porites* have been found to be more negatively affected by ocean acidification than massive *Porites* (Edmunds et al 2012). While branching colonies are often more abundant than massive colonies on tropical Indo-Pacific reefs, there are some regions (e. g. in the Caribbean) where massive colonies dominate (Bates et al., 2010). If the sensitivity of coral calcification to ocean acidification varies with colony morphology and flow exposure, then varying responses to ocean acidification between reefs could arise from differences in the most prevalent morphology of the primary reef builder. Such differences could also lead to a shift in reef species composition under climate change, from branching dominated to massive dominated reefs, which would reduce habitat complexity.

The overarching aim of this study was to better understand the drivers that determine tissue surface pH of corals. Specifically, we compared whether flow effects on tissue surface pH differed between massive and branching colonies, and under ambient and acidified conditions in the water column. To elucidate the factors determining tissue surface pH, we constructed and parameterized (from microsensor measurements) a basic diffusion-reaction-uptake model, and evaluated how well the model predicted tissue surface pH across a range of flows for branching versus massive colonies, or between ambient versus acidified conditions. We also evaluated the likely generality of morphological differences in DBL

dynamics by analysing the Reynold/Sherwood number relationship for different branching and massive species.

5.3 Methods

5.3.1 The model

We tested whether a simple diffusion-reaction-uptake model of the DBL, previously developed to describe the inorganic carbon chemistry in the DBL of foraminifera (Wolf-Gladrow et al 1999), could replicate tissue surface pH measured over corals with microsensors. The model calculates concentration profiles of chemical species in the carbonate system from the coral surface to bulk seawater as a function of distance from the coral surface (x), where x ranges from 0 at the coral surface to x_{bsw} at bulk seawater. The model calculates the concentrations depending on diffusion, chemical conversion and the fluxes generated by metabolic rates.

The following chemical reactions are taken into account (from Zeebe and Wolf-gladrow 2001) :

$$CO_2 + H_2O \underset{k_{-1}}{\overset{k_{+1}}{\rightleftarrows}} HCO_3^- + H^+ \qquad \text{Eqn 5.1}$$

$$CO_2 + OH^- \underset{k_{-4}}{\overset{k_{+4}}{\rightleftarrows}} HCO_3^- \qquad \text{Eqn 5.2}$$

$$CO_3^{2-} + H^+ \underset{k_{-5}^{H^+}}{\overset{k_{+5}^{H^+}}{\rightleftarrows}} HCO_3^- \qquad \text{Eqn 5.3}$$

$$HCO_3^- + OH^- \underset{k_{-5}^{OH^-}}{\overset{k_{+5}^{OH^-}}{\rightleftarrows}} CO_3^{2-} + H_2O \qquad \text{Eqn 5.4}$$

$$H_2O \underset{k_{-6}}{\overset{k_{+6}}{\rightleftarrows}} H^+ + OH^- \qquad \text{Eqn 5.5}$$

$$B(OH)_3 + OH^- \underset{k_{-7}}{\overset{k_{+7}}{\rightleftarrows}} B(OH)_4^- \qquad \text{Eqn 5.6}$$

$$B(OH)_3 + CO_3^{2-} + H_2O \underset{k_{-8}}{\overset{k_{+8}}{\rightleftarrows}} B(OH)_4^- + HCO_3^- \qquad \text{Eqn 5.7}$$

where k_{+i} and k_{-i} are the rate (kinetic) constants.

The basic equations of the model are of the following form

$$\frac{\partial c}{\partial t} = \text{Diffusion} + \text{Reaction} \qquad \text{Eqn 5.8}$$

where $c(x,t)$ is the concentration of a particular chemical species at distance x from the coral surface, at time t. Specific sources and sinks are added for metabolic fluxes as boundary conditions at the coral surface.

Concentration profiles are calculated as a function of the distance from the tissue surface. The time needed to establish a steady state can be estimated by the diffusional time scale $\tau = l^2/D$. where $l \approx 100–2000$ µm is the boundary layer thickness, and $D \approx 2 \times 10^{-9}$ m^2 s^{-1} is the diffusion coefficient for CO_2. Given these values, τ = 5–2000s. The time scale for the slowest reaction, i.e. conversion from HCO_3^- to CO_2 is in the order of 100s (Wolf-Gladrow et al., 1999). Because the time scale for diffusion and reaction are small compared to typical time scales of photosynthesis, respiration and calcification in the natural environment (hours to days), a steady state of the fluxes will be assumed (as in Wolf-Gladrow et al 1999). Thus

$$0 = \frac{\partial c}{\partial t} = \text{Diffusion} + \text{Reaction} \qquad \text{Eqn 5.9}$$

The complete equations of the model are (Zeebe and Wolf-gladrow 2001):-

$$0 = D_{CO_2}\frac{\partial^2[CO_2]}{\partial x^2} + (k \quad][HCO^-] - (k \quad + k \quad)[CO_2] \qquad \text{Eqn 5.10}$$

$$[H^+] \qquad -1 \qquad [OH^-] \qquad 3 \qquad +1 \qquad +4$$

$$0 = D_{HCO_3^-}\frac{\partial^2[HCO_3^-]}{\partial x^2} + (k_{+1} + k_{+4}[OH^- \quad])[CO_2] - (k_{-1}[H^+ \quad] + k_{-4})[HCO_3^-] + (k_{+5}[H^+] +$$

$$k_{-5} \qquad 3 \qquad -5 \qquad +5 \qquad 3 \qquad +8 \qquad 3 \qquad 3$$

$$k_{+8}[B(OH)_4^-][HCO_3^-] \qquad \text{Eqn 5.11}$$

$$0 = D_{CO_3^{2-}}\frac{\partial^2[CO_3^{2-}]}{\partial x^2} + (k_{-5} \quad + k_{+5} \quad [OH^- \quad])[HCO_3^-] - (k_{+5}[H^+ \quad] + k_{-5} \quad)[CO_3^{2-}] -$$

$$k_{+8}[B(OH)_3][CO_3^{2-}] + k_{+8}[B(OH)_4^-][HCO_3^-] \qquad \text{Eqn 5.12}$$

$$0 = D_{H^+}\frac{\partial^2[H^+]}{\partial x^2} + k_{+1}[CO_2] - k_{-1}[H^+ \quad][HCO_3^-] + k_{+5}[HCO_3^-] - k_{+5}[H^+ \quad][CO_3^{2-}] + k_{+6} -$$

$$k_{-6}[H^+][OH^-] \qquad \text{Eqn 5.13}$$

$$0 = D_{OH^-}\frac{\partial^2[OH^-]}{\partial x^2} + k_{+4}[HCO_3^-] - k_{+4}[OH^- \quad][CO_2] - k_{+5} \quad [OH^- \quad][HCO_3^-] + k_{-5} \quad [CO_3^{2-}] +$$

$$k_{+6} - k_{-6}[H^+][OH^-] + k_{+7}[B(OH)_4^-] - k_{-7} \quad [B(OH)_4^-][OH^-] \qquad \text{Eqn 5.14}$$

$$0 = D_{B(OH)_3}\frac{\partial^2[B(OH)_3]}{\partial x^2} + k_{+7}[B(OH)_4^-] - k_{+7}[B(OH)_3][OH^- \quad] - k_{+8}[B(OH)_3][CO_3^{2-}] +$$

$$k_{+8}[B(OH)_4^-][HCO_3^-] \qquad \text{Eqn 5.15}$$

$$0 = D_{B(OH)_4^-} \frac{\partial^2 [B(OH)_4^-]}{\partial x^2} - k_{-7}[B(OH)_4^-] + k_{+7}[B(OH)_3][OH^-] + k_{+8}[B(OH)_3][CO^{2-}] - k_{-8}[B(OH)_4^-][HCO_3^-]$$

Eqn 5.16

The model was used with two boundary conditions:-

1) The concentration of chemical species at the upper boundary of the DBL are set as bulk seawater conditions (either ambient or acidified)
2) The flux of each chemical species through the tissue surface boundary is equal to the net metabolic rate that consumes or releases that species

In the model, the values of the rate parameters are fixed constants (Zeebe and Wolf-Gladrow, 2001). The model also has 4 variable input parameters – DBL thickness, net photosynthesis, net calcification and bulk seawater chemistry. To test the model, we measured DBL thickness, net photosynthesis and bulk seawater chemistry experimentally (details in following sections). Net calcification was assumed to be a percentage of net photosynthesis as has been found in the literature (Schneider et al., 2009). The ratio of net calcification to net photosynthesis (g_n/p_n) has been found to remain constant across varying flows (Chapter 4), so we fit calcification to be a fixed percentage of net photosynthesis, independent of flow. However, we found that g_n/p_n does decrease with ocean acidification (Chapter 4), and previous work has suggested that different morphologies have different spatial patterns of zooxanthallae distribution and skeletal growth (Jokiel et al 2011). Consequently, g_n/p_n was estimated separately for different colony morphologies and bulk seawater conditions. With regards to DBL thickness, we used DBL thickness calculated from O_2 profiles as a previous study has found no significant differences between DBL thickness when calculated with O_2 or pH profiles (Cornwall et al., 2013).

Corals acquire HCO_3^- mainly from bulk seawater rather than from internal sources (Goiran et al., 1996, Schrameyer et al., 2014). To keep electric charge neutral, the uptake of HCO_3^- is compensated for by the uptake of an equal amount of H^+. Thus the equations used to represent photosynthesis and calcification were:

Photosynthesis: $HCO_3^- + H^+ \rightarrow CH_2O + O_2$

Calcification: $Ca^{2+} + HCO_3^- \rightarrow CaCO_3 + H^+$ (Allemand et al., 2004)

Thus the flux of HCO_3^- into the tissue is equal to net photosynthesis plus calcification while the flux of H^+ into the tissue equals net photosynthesis minus calcification.

5.3.2 Parameter estimation and model validation

To parameterize the model, we required estimates of DBL thickness and net photosynthesis at a number of flow velocities. To evaluate the model, we required estimates of tissue surface pH. We measured these all using massive *Favites sp.* and branching *Pocillopora damicornis* colonies (~3cm diameter). Experiments were conducted at the University of Technology, Sydney (UTS). Corals originated from the local coral holding facility at UTS (see Wangpraseurt et al. 2014 for details). Experiments were run in a custom-made black acrylic flow chamber (0.07 x 0.07 x 0.20m). Microprofiles of O_2 and pH within the DBL were measured under 4 flow velocities (0.1, 1, 2 and 5 cm s^{-1}). Flow in each tank was manipulated by varying the output on a pump until measured (via particle tracking) flow velocity was equal to target flow. Neutrally buoyant brine shrimp (*Artemia*) eggs were used as markers and were visually tracked between two points on the flume. The O_2 concentration and pH at the tissue surface was also recorded simultaneously as flow velocity was varied in light and darkness. Measurements were carried out at a temperature of 25.8°C and a salinity of 33.4, which are the prevailing conditions in the coral holding tanks. Microsensor measurements were performed at the branch tips for branching species and on the coenosarc, i.e., the tissue connecting two polyps, for massive species as these regions of the coral have been shown to have the highest calcification rate for each morphology respectively (de Beer et al 2000, Jokiel 2011).

a) b)

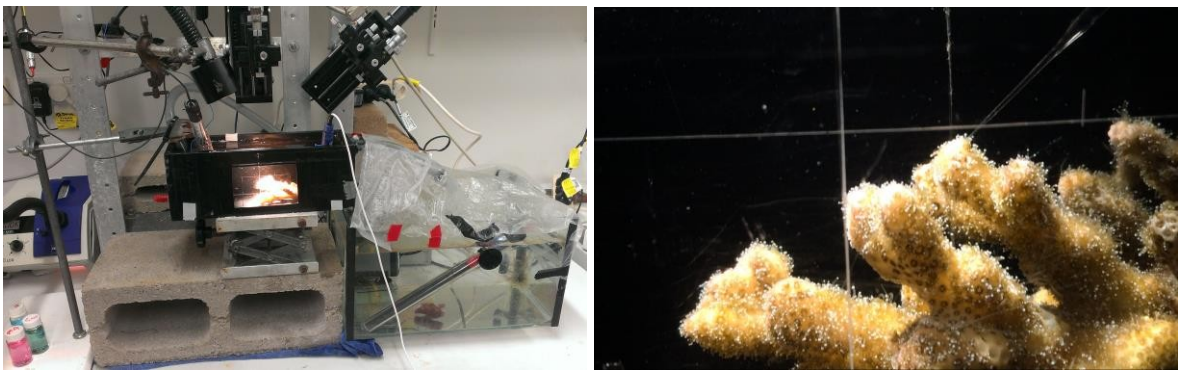

Figure 5.1 Images of the experimental setup. a) The flume b) Example of a colony used

To evaluate how well the model captured DBL dynamics under ocean acidification, we carried out additional measurements on the same *Favites* sp. colonies. Colonies were placed in acidified seawater (pH_{SWS} = 7.8 (±0.08 SD; n=10), which represents predicted conditions at 2100 under RCP 6.0, and TA = 2011 µmol kg^{-1} (IPCC, 2013)) and O_2 and pH profiles within the DBL were measured under the same flow velocities as used for the experiments with normal seawater (see above). Acidified seawater was obtained by sparging CO2 gas into tanks controlled via a pH controlling system (Tunze Aquarientechnik GmbH, Penzberg, DE), connected to a CO_2 gas cylinder, allowing for fine automated control of pH for the duration of the experiment (within ±0.01 pH units). pH electrodes of the pH controlling system (Tunze Aquarientechnik GmbH, Penzberg, DE) were calibrated every week using pH 5.0 and 7.0 standard buffers (Fluka, Sigma-Aldrich, CH). Bulk seawater pH of the flume was monitored continuously and water replaced constantly to limit pH increase (due to equilibrium with air) to 0.05 units.

5.3.3 Microsensor measurements

Microscale O_2 concentration measurements were done with Clark-type O_2 microsensors connected to a PA-meter (PA2000, Unisense, Denmark). The microsensors had

a tip diameter of 25 µm, a 90% response time of <0.5 s and a stirring sensitivity of ~1% (OX25, Unisense, Denmark). Sensors were linearly calibrated from signal readings in air saturated water and anoxic water (flushed with N_2). The percent air saturation in seawater at experimental temperature and salinity was transformed to O_2 concentration (µmol O_2 L^{-1}) using gas tables (Unisense, Denmark).

Microscale pH was measured with pH glass microelectrodes with an outer tip size of 40-60 µm (Unisense A/S, Aarhus, Denmark). The microelectrodes were connected to a high impedance mV meter (Unisense A/S, Aarhus, Denmark) that measured the pH-dependent microelectrode potential against a standard calomel reference electrode immersed in the same medium as the microelectrode and calibrated. The pH microelectrodes were calibrated in standard pH buffers (pH 4, 7, and 10).

Visible light was provided by a tungsten-halogen lamp of constant colour temperature (Schott KL2500). The incident downwelling photon irradiance (PAR, 400-700 nm) was measured with a calibrated spherical quantum sensor (US-SQS/L, Heinz Walz GmbH) connected to a light meter (Li-250A, Li-COR). All measurements were carried out at a downwelling irradiance of 800µmol photons m^{-2} s^{-1} to maintain consistency with a pilot study done on Heron Island, GBR.

For profiling, the microsensors were mounted on PC-controlled motorized micromanipulators for automatic profiling (Pyro-Science GmbH, Germany). The micromanipulators were fixed on a heavy-duty vibration-free metal stand. Positioning of the microsensors was facilitated by the manufacturer's software (Profix, Pyro-Science GmbH, Germany).

Measurements were done with the O_2 microelectrode mounted vertically, while the pH microelectrode was mounted at a 45° angle and the light at a 25° angle relative to vertical.

Microsensor measurements were done in vertical steps of 50 to 100µm. Determination of the tissue surface position was done by observation of the microsensor tip under a dissection microscope while slowly approaching the surface. In the following, all depths are given relative to the coral tissue surface (depth = 0 µm), where negative depths indicate distance above the tissue surface.

5.3.4 DBL thickness calculation

The effective DBL thickness was calculated from the intercept between the linear extrapolation of the O_2 concentration profile at the coral surface and the bulk seawater concentration (Jørgensen and Revsbech, 1985). The slope of the O_2 concentration versus distance data was fitted using the linear model function (lm) in R (R Core Team 2014).

5.3.5 Net photosynthesis calculation

The diffusive fluxes of O_2, $J(x)$ were calculated from steady state O_2 concentration profiles by Fick's first law of diffusion:

$$J(x) = -D_S \frac{\delta C(x)}{\delta x} \qquad \text{Eqn 5.18}$$

where is $\delta C / \delta x$ the slope of the O_2 profile at depth x, and D_s is the apparent diffusion coefficient of O_2. In seawater $D_s = D_O$, the molecular diffusion coefficient of O_2 in water. D_O, corrected for temperature ($2.1707 \times 10^{-5} cm^2 s^{-1}$), was taken from tabulated values provided by Unisense (Ramsing & Gunderson).

5.3.6 Calculating of ratio of calcification to photosynthesis

The model and data from one flow (5 cms^{-1}) was used to fit the ratio of net calcification to net photosynthesis. Ratio of net calcification to net photosynthesis was independently fitted for each morphology and acidified condition. We then tested model predictions against the other 3 flows (0.1, 1 and 2 cms^{-1}).

5.3.7 Morphological difference in DBL dynamics

To better understand the role of morphological difference in DBL dynamics, we examined the relationship between the Reynolds (Re) and Sherwood (Sh) numbers in our *Favites* and *P. damicornis* experiment, and, to test the generality of the morphological differences we found, we also analysed data from a pilot study on Heron Island, which investigated the DBL dynamics of (massive) *Goniastrea aspera* and (branching) *Stylophora pistillata*.

Re:Sh analysis is commonly used in mass transfer studies as it facilitates comparison to the large body of engineering theory on mass transfer to various regularly shaped, smooth structures such as cylinders and spheres (Patterson, 1992, Helmuth et al., 1997). Re is the ratio of inertial to viscous forces of the fluid, and hence characterizes flow past the coral colony (Schlichting and Gersten, 2000):

$$\mathrm{Re} = \frac{uW}{v} \qquad \text{Eqn 5.19}$$

where u is the free stream flow velocity, W is the characteristic organism size (e.g. length in direction of flow), and v is the kinematic viscosity of the fluid. Sh is the ratio of the measure of total flux of a solute to the tissue surface assisted by fluid motion to the average flux that would occur if molecular diffusion through the diffusive boundary layer under stagnant conditions was the sole mechanism for mass transport (Patterson 1992):

$$\mathrm{Sh} = \frac{h_m W}{D} \qquad \text{Eqn 5.20}$$

where D is the diffusion coefficient, and h_m is the mass transfer coefficient, which was determined empirically from the ratio of mass flux (in our case net photosynthesis) per unit area to the gas (in this case O_2) concentration difference between bulk seawater and tissue surface:

$$M = h_m(C_{sw} - C_0) \quad \text{Eqn 5.21}$$

where M is the gas flux due to photosynthesis, C_{sw} is the gas concentration in bulk seawater, and C_0 is the gas concentration at the coral surface. Net photosynthesis was determined as outlined above, and values of C_{sw} and C_0 were taken from microsensor measurements.

The relationship between Re and Sh has been well characterized experimentally as following a power law relationship

$$Sh = aRe^b \quad \text{Eqn 5.22}$$

where a and b are empirically determined coefficients that depend upon organism shape and surface roughness (Incropera and DeWitt, 1996). The exponent b is the most important coefficient in determining the degree to which flow augments mass transfer relative to diffusion, and its numerical value gives an indication of whether transport is occurring through a laminar (b = 0.5) or turbulent (b > 0.6) boundary layer (Patterson et al., 1991).

5.3.7 Statistical analysis

To determine whether there was statistical support for calibrating the model differently for different colony morphologies or bulk seawater conditions, ANCOVA was used to test whether species interacted with flow in determining DBL thickness, photosynthesis and tissue surface pH, and to test whether species/bulk seawater pH interacted with flow in determining tissue surface pH. ANCOVA was also used to test whether species interacted with Re to affect Sh (mass transfer). ANCOVAs were carried out using the aov() function in R.

5.4 Results

5.4.1 Parameter estimation

DBL thickness had a negative power law relationship with flow for both *Favites* and *P. damicornis*, i.e., it was thick at low flow and thinned out as flow increased (Fig. 5.2a). The largest change in DBL thickness occurred between 0 and 2 cm s^{-1} (Fig. 5.2a). Flow and species interacted significantly to affect net photosynthesis, with net photosynthesis increasing more with increasing flow for *Favites* than for *P. damicornis* (Fig. 5.2b, Tab. 5.1).

(a) (b)

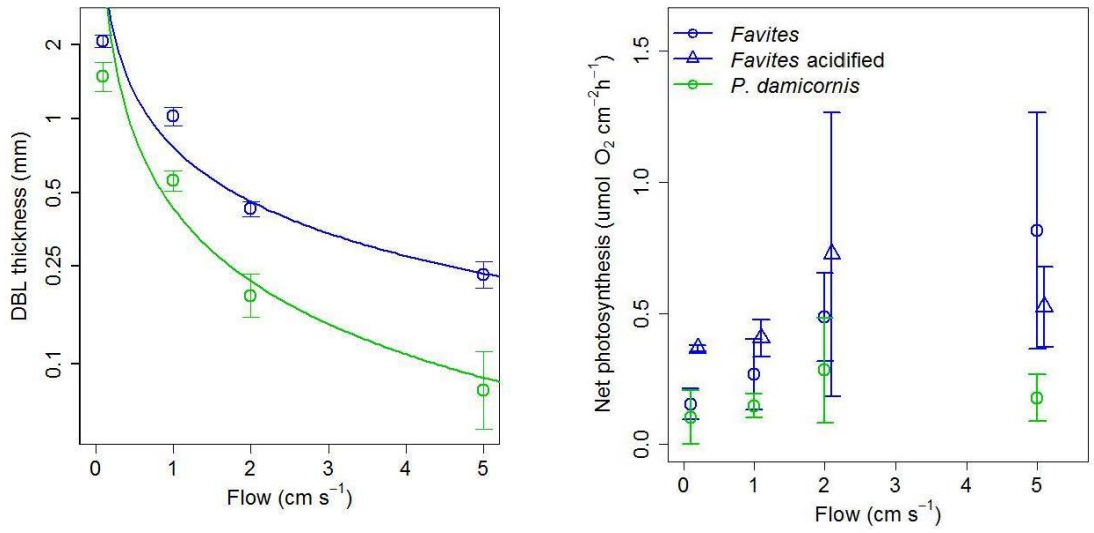

Figure 5.2 (a) DBL thickness (µm) versus flow (cm s^{-1}) for *Favites* (blue circles) and *P. damicornis* (green circles). Symbols and error bars represent the mean ±1.96*SE (n=4-6). Lines represent the relationship between DBL thickness and flow from fitted power functions ($DBL_{Favites} = 767\ flow^{-0.738}$, $DBL_{P.\ damicornis} = 432\ flow^{-0.99}$). (b) Net photosynthesis at various flows (cm s^{-1}) for *Favites* (blue circles), *Favites* under acidified conditions (blue triangles), and *P. damicornis* (green circles). Symbols with error bars represent the mean ±1.96*SE (n=4-6).

Table 5.1 ANCOVA summary for effects of flow and species on photosynthesis of *Favites* and *P. damicornis*

Factor	F	df	p
Flow	36.38	1	**<0.001**
Species	42.22	1	**<0.001**
Flow x species	15.27	1	**<0.001**

5.4.2 Microsensor measurement of tissue surface pH

Flow significantly affected tissue surface pH with lower flows leading to increased elevation in tissue surface pH (Fig. 5.3a, Tab. 5.2). Species also had a significant effect on surface pH (Tab. 5.2), with *Favites* having a larger increase in tissue surface pH (0.2-0.6 pH units) than *P. damicornis* (0-0.2 pH units) (Tab. 5.2). There was no interaction between flow and species in determining tissue surface pH. For *Favites*, the highest deviations from bulk seawater pH occurred under flows of 1 and 2 cm s^{-1}, but even at a flow of 0.1 and 5 cm s^{-1} tissue surface pH was still significantly elevated (Fig. 5.3a). For *P. damicornis*, tissue surface pH was highest at close to stagnant conditions. Enhanced flow velocities reduced tissue surface pH up until a velocity of ~5 cm s^{-1}. Tissue surface pH did not differ from the bulk seawater pH at flow velocities >5 cm s^{-1} (Fig. 5.3a).

There was a significant effect of bulk seawater pH on elevation of tissue surface pH (Tab.5.3). Tissue surface pH of *Favites* had larger elevation under acidified conditions (bulk seawater pH of 7.8) than under ambient pH conditions (bulk seawater pH of 8.2), at flows of 1 and 2 cm s^{-1} (Fig. 5.3a). At a flow velocity of 2 cm s^{-1}, there was no difference in tissue surface pH (~8.28) under ambient and acidified conditions.

5.4.3 Model predictions

Net calcification was estimated to be 65%, 55% and 80% of net photosynthesis in *Favites, Favites* under acidified conditions, and *Pocilloporia*, respectively. Using these calcification rates, the diffusion-reaction-uptake model predicted tissue surface pH quite well for both *Favites* and *P. damicornis*, under ambient and acidified conditions, at all flow velocities except for 0.1cm s^{-1} (Fig. 5.3a & b). At a flow velocity of 0.1cm s^{-1}, the model over-predicted tissue surface pH for *Favites* but under predicted it for *P. damicornis* (Fig. 5.3a).

Overall, the R^2 for a linear regression of observed versus predicted values was 0.9229 (Fig. 5.3b); moreover, the slope (1) and intercept (0) of the unity line (where observed value equal predicted value) was within the 95% confidence ellipse of the linear regression (Fig. 5.3c). Thus, the model shows both high precision and low bias as a predictor of tissue surface pH.

(a)

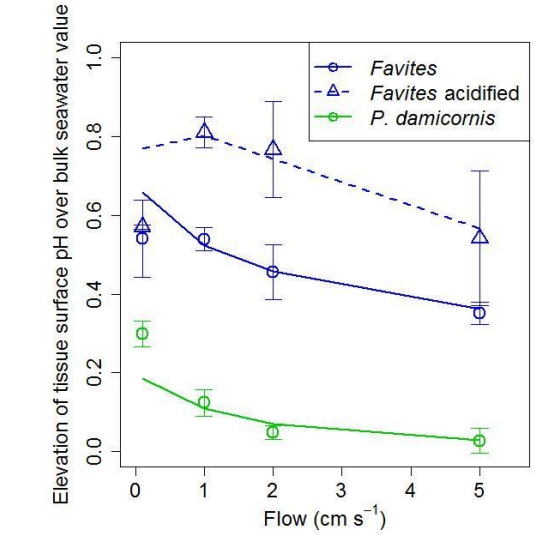

(b)

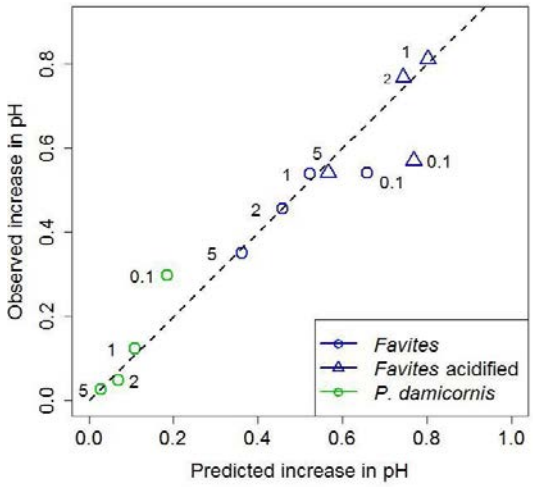

(c)

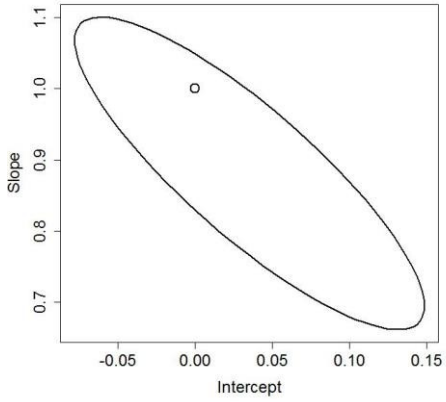

Figure 5.3 (a) Elevation of tissue surface pH relative to bulk seawater at various flows (cm s^{-1}) for *Favites* (blue circles), *Favites* under acidified conditions (blue triangles) and *P. damicornis* (green circles). Symbols with error bars represent the mean ±1.96*SE (n=4-6). Lines represent model predictions. Bulk seawater had a pH_{SWS} of 8.2 (±0.04 SD; n=10)) and TA = 2325 µmol kg^{-} for ambient conditions and a pH_{SWS} of 7.8 (±0.08 SD; n=10) and TA = 2011 µmol kg^{-1} for acidified conditions. (b) Alternative visualization of the model performance for the data and predictions shown in the first panel. Observed (measured with microsensor) are plotted versus predicted (from model) values of elevation of tissue surface pH relative to bulk seawater at various flows (cm s^{-1}) for *Favites* (blue), *Favites* under acidified conditions (blue triangles) and *P. damicornis* (green). Black numbers next to points are the flow velocities. Black dashed line represents the unity line where predicted values equal observed values. (c) 95% confidence ellipse of slope and intercept parameters for the linear regression of observed increase in pH versus model predition. The dot represents the unity line (i.e., observed = predicted). which is within the confidence ellipse.

Table 5.2 ANCOVA summary for effects of flow and species on tissue surface pH of *Favites* and *P. damicornis*

Factor	F	df	p
Flow	52.48	1	**<0.001**
Species	231.64	1	**<0.001**

Table 5.3 ANCOVA summary for effects of flow and bulk seawater pH on tissue surface pH of *Favites*

Factor	F	df	p
Flow	12.32	1	**0.002**
Bulk seawater pH	25.37	1	**<0.001**

5.4.4 Correlation between net photosynthesis and tissue surface pH

O_2 concentration (here after [O_2]) and pH at the tissue surface responded immediately to experimental changes in light and flow conditions (Fig. 3). Changes in [O_2] and pH were positively correlated across flow velocities and illumination conditions (light or darkness), with illumination leading to elevation in both [O_2] and pH (in relation to bulk seawater) and darkness leading to reductions (Fig. 5.4). The magnitude of elevation/reduction was flow dependent with larger elevation/reduction under lower flows and smaller elevation/reduction at higher flows (Fig. 5.4).

a) b)

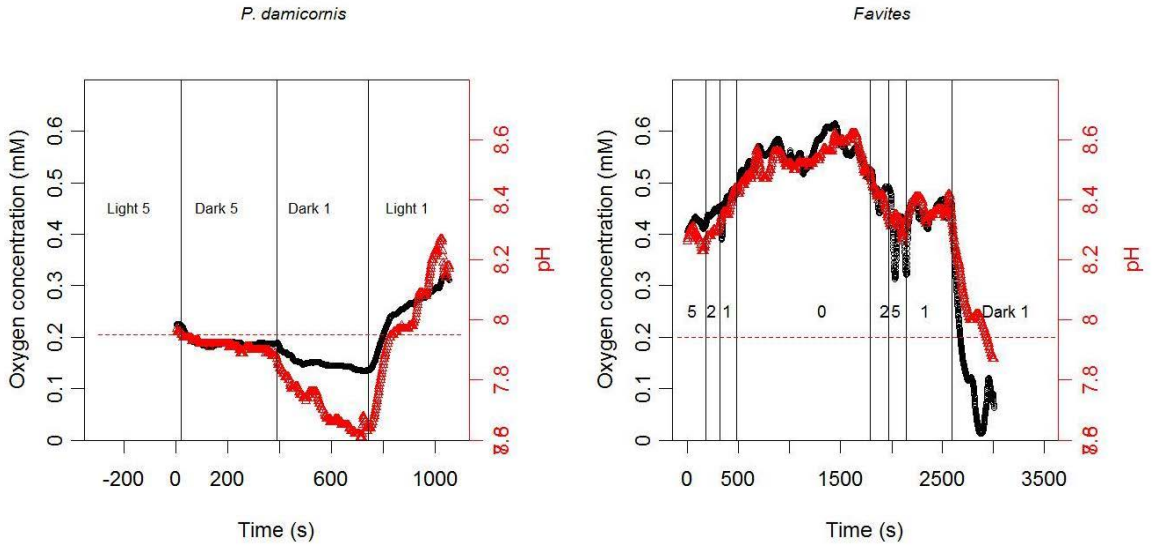

Figure 5.4 Continuous measurement of tissue surface O_2 concentration (black line) and pH (red line) for a) *P. damicornis* and b) *Favites* under varying light/dark and flow conditions. Conditions in b) are in light (800 µmol photons m^{-2} s^{-1}) unless stated otherwise. Numbers in figure represent flow velocity. Red dashed line represents pH in bulk seawater.

5.4.5 Morphological difference in DBL dynamics

We found power law relationships between Sherwood and Reynolds numbers for all coral species (Fig. 5.5). There was a significant interaction between Reynolds number and species, indicating that the slopes of the Sh:Re relationship were significantly different between species (Tab. 5.5). The exponent *b* was higher for the branching species (*Stylophora*, b = 0.785 and *P. damicornis*, b = 0.551) compared to the massive species (*Goniastrea* b = 0.419and *Favites* b = 0.507).

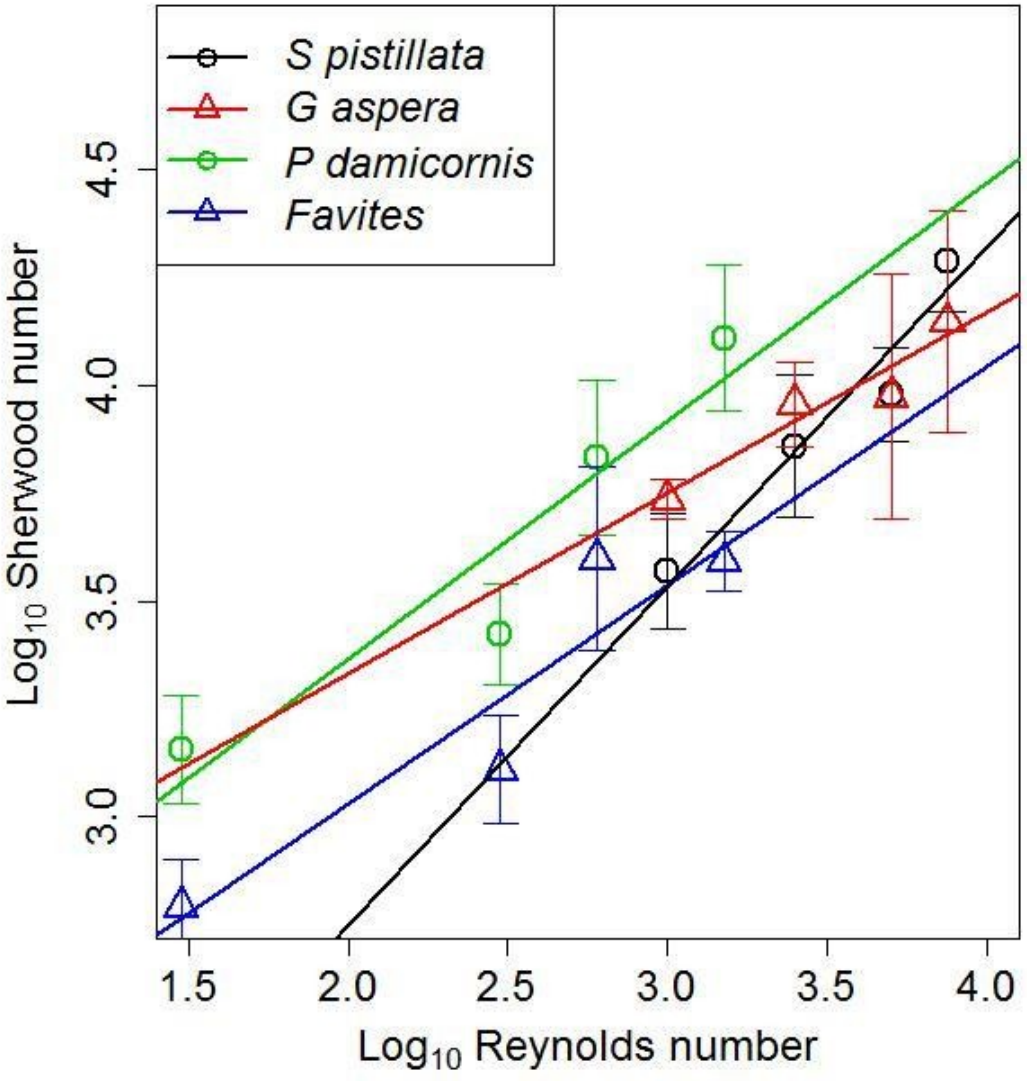

Figure 5.5 Sherwood (Sh) versus Reynolds (Re) relationship for branching (*P. damicornis* and *Stylophora,* circles) and massive morphologies (*Favites* and *Goniastrea*, triangles). Symbols and error bars represents the mean ± 1.96*SE (n=6). Lines represent the relationship between $Log_{10}(Sh)$ and $Log_{10}(Re)$ from fitted linear models of the form $Log_{10}Sh = b * Log_{10}Re + a$ ($Log_{10}Sh_{P.\ damicornis} = 0.55\ Log_{10}Re + 2.26$, $Log_{10}Sh_{Favites} = 0.51\ Log_{10}Re + 2.02$, $Log_{10}Sh_{Stylophora} = 0.79\ Log_{10}Re + 1.18$, $Log_{10}Sh_{Goniastrea} = 0.42\ Log_{10}Re + 2.49$).

Table 5.4 ANCOVA summary for effects of log_{10} Reynolds number and species on log_{10} Sherwood number of *P. damicornis, Stylophora*, *Favites* and *Goniastrea*

Factor	**F**	**df**	**p**
$Log_{10}Re$	197.30	1	**<0.001**
Species	6.916	1	**0.011**
$Log_{10}Re$ x species	4.328	1	**0.041**

5.5 Discussion

5.5.1 Determinants of tissue surface pH

A diffusion-reaction-uptake model developed for foraminifera was able to predict quite well the tissue surface pH of *Favites* and *Porites*, under ambient and acidified conditions across a range of flows. This suggests that tissue surface pH is driven by diffusion-reaction-uptake kinetics alone and that the two model input parameters (DBL thickness and the difference in coral metabolic rates) are the key factors determining pH at the tissue surface. Thicker DBLs and larger difference in coral metabolic rates lead to larger elevation of tissue surface pH. In line with previous work, we found that photosynthesis increased with flow, with the increase dependent on species (Hoogenboom and Connolly, 2009, Lesser et al., 1994). Moreover, microsensor profiles showed that the dynamics of tissue surface O_2 concentration and pH are tightly linked across a range of flows, demonstrating correlation between photosynthesis and elevation of tissue surface pH. Also, consistent with previous studies (e.g., Chapter 4 & Chauvin et al. 2011), the model fits suggest that the ratio of calcification to photosynthesis (g_n/p_n) is independent of flow. As flow and thus photosynthesis decrease, the constant ratio means that the difference in between

photosynthesis and calcification rate decreases and so does the elevation of tissue surface pH. However, we find that elevation in tissue surface pH is largest at low flow, thus we are able to conclude that DBL thickness is the major mechanism through which flow influences tissue surface pH. Under ocean acidification, we found that net photosynthesis did not increase with ocean acidification, which is consistent with previous work (Marubini et al., 2008, Reynaud et al., 2003, Houlbreque et al., 2012, Agostini et al., 2013, Anthony et al., 2008, Schneider and Erez, 2006). Thus the increase in tissue surface pH under ocean acidification is most likely due to a reduction in g_n/p_n.

The diffusion-reaction-uptake model's predicted tissue surface pH differed most from the dataset at flows of 0.1cm s^{-1} (close to stagnant), over-predicting it for *Favites* and under-predicting it for *P. damicornis*. A recent study has shown that, under conditions of zero flow, corals have the ability to use cilia beating to vigorously stir the water at the coral surface, leading to decreased DBLs and increased mass transfer (Shapiro et al., 2014). Under stagnant conditions, this biologically driven mass transport, rather than molecular diffusion, was shown to control the exchange of nutrients and O_2 between the coral surface and the environment (Shapiro et al., 2014). This may explain our finding of comparatively weak performance of the model under near-stagnant conditions. However, for higher flow velocities, we found that tissue surface pH was very well predicted by a model of molecular diffusion-driven dynamics, suggesting that diffusion is the prime transport mechanism for corals under low and moderate flow velocities.

5.5.2 Morphological differences in elevation of tissue surface pH

Based on the model, a thicker DBL, and larger difference in coral metabolic rates lead to a greater elevation of tissue surface pH as compared to a thinner DBL, and lower net photosynthesis to calcification ratio. In branching corals, measurements were taken at branch

tips, which have been shown to have high levels of skeletal growth (calcification) but very few photosynthetic zooxanthellae (and thus low areal rates of photosynthesis) (Jokiel, 2011b). The higher g_n/p_n leads to a small increase in tissue surface pH. For massive species, measurements were taken on the coenosarc, which has both high calcification and photosynthesis rates (de Beer et al. 2000). The lower g_n/p_n leads to a smaller increase in tissue surface pH. This is consistent with model fits where net calcification was estimated to be 80% and 65% of net photosynthesis in the branching versus massive colonies respectively. These fitted ratios are similar to those found by Schneider et al (2009) (~75% for branching *Acropora eurystoma* and 67% for massive *Favia favus*). Thus the spatial patters of zooxanthellae distribution and skeletal growth may partly explain why massive corals have higher tissue surface pH than branching corals in this study.

DBL thickness is affected by the type of flow over the colony surface, i. e. whether the flow is hydraulically smooth, rough or transitional (Jumars and Nowell 1984, Denny 1988). Under similar free stream flow, laminar DBLs are much thicker than turbulent DBLs (Incropera & DeWitt 1996). Thus at flows low enough for DBLs to form, species that have laminar DBLs will have larger elevations of surface tissue pH than species that have turbulent DBLs. Based on the exponents of the Sh:Re relationship, our results suggest that the massive colonies exhibited laminar DBLs (b of ~0.4-5) while branching colonies exhibited transitional to turbulent DBLs (b of ~0.55-0.8) (Patterson et al. 1991, Bilger & Atkinson, 1992, Incropera & DeWitt 1996)(Bilger and Atkinson, 1992). Most studies that have estimated a and b for corals based on direct measurements, assumed that the O_2 concentration at the tissue surface (i.e. C_0) was air saturated (100%), except for Hoogenboom & Connolly (2009) where C_0 was measured directly using oxygen micro-optodes. Since C_0 can vary between 107% - 400% of saturation during the day (Shashar et al., 1993, Kühl et al., 1995,

Wangpraseurt et al., 2012), we only compare our results to that of Hoogenboom & Connolly (2009). Using a length scale to calculate Re similar to the one we used, they found a turbulent boundary layer (*b*=0.9) for a branching species (*Acropora nasuta*). This is consistent with our results for *Stylophora* (*b*=0.79) and *P. damicornis* (*b*=0.55). However, they reported a turbulent boundary layer (*b* of 0.7) for a massive species (*Leptoria*), which was higher than what we found for *Favites* (*b*=0.51) and *Goniastrea* (*b*=0.42) (Hoogenboom & Connolly 2009). Our study used 3-7 cm wide colonies, while Hoogenboom & Connolly (2009) used 15-20 cm wide colonies. Thus the discrepancy between the laminar/turbulent nature of the DBL of massive species could be due to the different size of colonies used in the experiments, because Re (an indicator of the laminar/turbulent nature of the fluid) is depends on colony size. More studies are needed understand how colony rugosity and size influence whether DBLs are laminar or turbulent, especially for branching colonies, which have more geometrically complex forms.

5.5.3 Effects of ocean acidification on tissue surface pH

Oceanic pH is predicted to decline by 0.3-0.4 pH units by the end of this century (Caldeira and Wickett, 2003). For benthic macroalgae, it is known that a thickening of the DBL, via reduced flow velocity, causes an elevation of tissue surface pH which reduces the negative effects of ocean acidification (Cornwall et al., 2014, Cornwall et al., 2013). This is well within the range of tissue surface pH elevations measured for massive species (0.2-0.6), but higher than that of branching species (0-0.2; Fig. 5.2a). We found that at flow velocities of 2 cm s^{-1}, tissue surface pH of *Favites* was elevated to similar values under ambient and acidified treatments (pH difference of 0.5). This finding is consistent with that of Agostini et al. (2013), that tissue surface pH values of *Galaxea fascicularis* were not significantly different at atmospheric CO_2 of 400 and 700 ppm under a flow of 5 cm s^{-1}. However, all these elevations in tissue surface pH have been found a relatively low flows that are rarely

encountered by corals in nature (Falter et al., 2007), suggesting that the DBL effect is unlikely to ameliorate the decreases in coral calcification under ocean acidification, as it does in macroalgae.

5.5.4 Shortcomings of the study and directions for future research

Firstly, the experimental calibration part of the study involves the use of microsensors, so it necessitates the use of low energy flows due to the fragile nature of the microsensors. Moreover, the microsensors are relatively large compared to the thickness of the DBL, so their presence could disrupt the micro flow field around it. Both these factors mean that DBLs measured will probably be thicker than corals actually experience in nature. Consistent with this, a previous study that measured DBL thickness using Gypsum dissolution on reefs found DBLs thickness to be slightly less than the DBL thickness we measured for *P. damicornis* and much less than the DBL thickness we measured for *Favites* (Falter et al., 2005). Secondly, due to the small size of the available flume, corals used in this study were quite small (3-5cm) compared to what is growing on a real reef. As Re depends on colony size, it is likely that our results about massive species having laminar boundary layers will not hold for larger corals. Future studies should investigate the DBL thickness over a larger range of coral sizes. Lastly, the study only examined the effects of unidirectional flow, however oscillatory flow resulting from the propagation and transformation of surface gravity waves can dominate the flow environments of many shallow reef communities. Compared to unidirectional flow of the same velocity, oscillatory flow has been shown to increase the penetration of flow into branching corals, reduce boundary layer thickness, and increase mass transfer to and from the coral (Falter et al., 2005, Reidenbach et al., 2006), thus it is vital that future studies extend the analysis into conditions of oscillatory flow.

5.5.5 Implications

Our study shows that tissue surface pH is well predicted by diffusion-reaction-uptake kinetics, and is driven by boundary layer thickness and the ratio of net calcification to net photosynthesis. Our findings raise the possibility that, due to thicker DBLs and a lower net calcification to net photosynthesis ratio in regions of calcification, massive species may have higher elevation (in light) and larger depression (in darkness) of tissue surface pH than branching species, especially under ocean acidification. However, these elevation in tissue surface pH only occur at fairly low flows which are unlikely to be the norm in nature. As such, it is unlikely that the buffering effect of the DBL will ameliorate the effects of ocean acidification on corals, as has been found in benthic macroalgae.

6. General discussion

6.1 Summary of results and implications

Understanding the long-term ecosystem level impacts of ocean acidification in marine environments is critical to informing national and international policies on carbon emission targets. However, key to this is the ability of projection models to scale up short-term individual organism physiological responses to long-term ecosystem level impacts. In the first half of the thesis, I have improved upon existing models projecting the effects of ocean acidification by incorporating the effects of ocean acidification on growth and recruitment, using quantitative summaries from all existing experimental studies, into projections. While the effects of ocean acidification on growth were found to be less sensitive than originally thought (Chapter 2), effects of ocean acidification on recruitment could substantially increase the risk of population collapse (Chapter 3). This highlights the need for more study to deepen our understanding of the effects of ocean acidification on recruitment, and for future projection models to adequately account for the effects of ocean acidification on recruitment. Moreover, I found that long-term population growth rate of fast growing species is more sensitive to ocean acidification than that of slow growing species. Coupled with the fact that fast growth species are also more sensitive to warming oceans (van Woesik et al., 2012, Loya et al., 2001), it provides further support for the hypothesis that, under climate change, there will be a greater relative proportion of massive corals on reefs compared to what there is now (Glynn, 1996). A recent paper calling for ecological theory to be applied more widely in ocean acidification research stressed the need for ocean acidification research to evaluate rigorously whether observed shifts in demography and life history parameters do in fact alter population growth or stability (Gaylord et al., 2015). My work provides both a means of quantitatively summarizing our knowledge of how demographic rates change under ocean

acidification, and a modelling framework that can be used to assess the impacts those changes on population growth and stability.

It had been suggested that interactions between ocean acidification and other factors may account for a proportion of the variability between experimental results to date (Atkinson & Cuet 2008, Pandolfi et al 2011). Interactive effects of ocean acidification and temperature, light and nutrients have all been examined, but at the time of inception of this thesis, no study had investigated the interactive effects of flow and ocean acidification. In the second half of thesis, I have shown that flow mediates the effect of ocean acidification on calcification of *Acropora secale*, with low flows leading to lower sensitivity of calcification to ocean acidification (Chapter 4). The interactive effect is large, with the sensitivity of calcification to decreasing Ω_{Arag} increasing by ~0.5% per cms^{-1} increase in flow. A recent study investigating the interactive effects of flow and ocean acidification on coral communities also found a flow-ocean acidification interaction but only in darkness, in light there was only a significant effect of flow (Comeau et al., 2014a). These results suggest that more studies are needed to deepen our understanding of how flow and ocean acidification will interact to affect reef corals. In an attempt to elucidate the mechanisms behind the flow-ocean acidification interaction, I also present the first evidence of flow driven increases in tissue surface pH and that this increase can lead to similar tissue surface pH under ambient and acidified conditions in massive corals (Chapter 5). However, these elevations in tissue surface pH have been found at relatively low flows that are rarely encountered by corals in nature, suggesting that the DBL effect is unlikely to ameliorate the decreases in coral calcification under ocean acidification, as it has been found to in macroalgae.

6.2 Broader implications of this work

Broader implication of this work fall into two categories: broader conservation implications and broader scientific implications. With regard to broader conservation implications, ocean acidification is often viewed as the 'other CO_2 problem' (Doney et al., 2009) that is less of a concern for coral reefs than global warming. In Chapter 2, I show that the effects of ocean acidification, on all stages of the life cycle, could potentially lead to declining coral populations on RCP 6.0 (doubling of pre-industrial atmospheric CO_2 by 2100). While more research is required to reduce the uncertainty about our estimate of the sensitivity of coral recruitment to ocean acidification, it would be prudent for policy makers to set emissions targets to keep us below emission levels for RCP 6.0.

With regard to broader scientific implications, there is currently a debate in the literature as to whether there is causal relationship between Ω_{Arag} and calcification (Marubini et al., 2008, Andersson and Gledhill, 2013). Underpinning this is our inadequate understanding of the mechanism of coral calcification (Gattuso et al. 1999). As recently as 2008, it was still the common belief that calcification was unquestionably influenced by Ω_{Arag} (Atkinson & Cuet, 2008). However, it was still unknown why external concentrations of carbonate should have such a strong effect on calcification (Atkinson & Cuet, 2008) as calcification either utilized HCO_3^- derived from host tissue respiration (Furla et al., 2000, Allemand et al., 2004) or CO_2 taken up from the surrounding water (via diffusion) (Cohen and McConnaughey, 2003). Current understanding is that DIC is transported to the site of calcification in the form of HCO_3^- and CO_2 and converted to CO_3^{2-} under the calicoblastic layer by the elevation of pH (McCulloch et al., 2012, Venn et al., 2011). However, it is still not well understood how the elemental composition and physical chemistry of the external environment interacts with biological control under different saturation state conditions (Cohen et al., 2006). Regardless of whether there is a causal relationship between Ω_{Arag} and

calcification, Chapters 2 and 4 add to the body of evidence that calcification and Ω_{Arag} are highly correlated and that Ω_{Arag} is a good indicator of calcification.

Ocean acidification is not the only threat facing coral reefs; they also have to contend with sea surface warming and disease outbreaks on a global scale and pollution, and eutrophication and overfishing on a more local scale. The techniques used in this thesis (regression based meta-analysis combined with size structured integral projection models [IPMs]) could also be applied in the impact assessment of these other threats to long-term reef growth. Previous attempts to summarize the response of corals to a stressor have either been effect size meta-analyses (Kroeker et al., 2013, Harvey et al., 2013) or purely qualitative summaries (Loya and Rinkevich, 1980, Jackson et al., 2001, Wilkinson, 1999, Weil et al., 2006). Neither summary is of a form (e.g. mean % change in demographic rate per unit change in a particular stressor) that is needed for projection models to be able to scale up individual organism demographic rate responses to long-term reef scale impacts. I show in this thesis how regression based meta-analysis allows us to summarize all available data in such a way that it is useful in projecting the impacts of a threat. Nevertheless, is important to highlight that the quality of a meta-analysis is dependent on the quality of the experimental design from which the data came from, so judgment should be employed when selecting studies to include. For example, in Chapter 2, I omitted studies that used unrealistically low ranges of Ω_{Arag}.

With respect to the use of the size-structured IPM, mine is the third example of the utility of IPMs in modelling the impact of threats on coral populations. Bruno et al (2011) first used IPMs to model the effects of aspergillosis (disease) on sea fans, with Madin et al (2012) next using IPMs to model the effects of warming and ocean acidification on tabular corals. Other population-level studies have utilized non-size structured models (e.g. warming:

Baskett et al 2009, warming and ocean acidification: Anthony et al 2011, Hoeke et al 2011; overfishing: Gurney et al 2013) or stage structured matrix models (e.g. Riegl et al 2012). Using warming as an example, moderate elevations in temperature will increase metabolic rates and thus growth but extreme elevations increase the frequency and severity of bleaching events with negative consequences for coral survival and growth (Hoegh-Guldberg, 1999, Jones et al., 1998). However, given the size dependence of coral survival and fecundity, both the increase and decrease in growth will have flow on implications for survival and reproductive output. These flow-on effects, which have important implications for long-term population growth rate, will not be captured by non-size structured models.

6.3 Robustness of results and direction for future studies

6.3.1 Adaptation and acclimation

Like most other studies projecting the effects of ocean acidification, all the projections in this study are based on the assumption that the response to ocean acidification will remain constant over time. Thus they may be biased if corals are able to adapt (i.e. genetic evolution) to ocean acidification. Indeed it has been shown from modelling of warming, which incorporated evolution of thermal tolerance under varying emissions scenarios, that a wide range of outcomes is possible (from a complete collapse of cover by the middle of the century to maintenance of comparable levels of cover to 2100 and beyond) with the outcome dependent on the extent of thermal adaptation (Baskett et al 2009). Quite appropriately then, review papers have concluded that determining the generality of how marine organisms will evolve to cope with ocean acidification is central to accurately predicting future outcomes in an elevated-CO_2 world (Pandolfi et al 2011, Gaylord et al 2014).

The majority of ocean acidification research has focused on the physiological effects of simulated future conditions on modern populations, while the capacity for genetic adaptation has received relatively little attention (but see review by Kelly & Hofmann 2013). This is likely due to the fact that evolution is complicated in corals, as symbiosis (the inter-dependency of coral and zooxanthellae) can affect rates of evolution. Generation times of corals are orders of magnitude greater than those of zooxanthellae, so zooxanthellae are likely to show faster evolutionary responses than their host. Indeed, while the possibility of symbiont mediated changes in ocean acidification resistance in corals has not yet been tested directly, recent work has shown dramatic differences among symbiont types in the responses of free-living cells to elevated CO_2 (Branding et al., 2011), suggesting that symbionts may help corals adapt to ocean acidification. Moreover, the modular nature of corals means that somatic line mutations could provide additional sources of variation that selection could act upon within a single generation (Pandolfi et al 2011). Incorporating well-calibrated adaptation sub-models into IPMs remains an important challenge for future work.

Another way that corals could possibly modify their response to ocean acidification through time is via acclimatization (i.e. phenotypic plasticity). I investigated the possibility of this in Chapter 2 by testing for a significant relationship between study duration and sensitivity. The lack of a significant relationship suggests that acclimation does not reduce sensitivity of calcification to ocean acidification. However, an individual study on *Lophelia pertusa* has shown that 1 weeks exposure led to a 25% decline in growth but after 6 months exposure, growth was back to normal (Form and Riebesell, 2012).

6.3.2 Single species model

My IPM is a single species model, which means projections about the impacts of ocean acidification on λ do not take into account the effect of ocean acidification on species

interactions. Work in the area of warming demonstrates that most temperature associated cases of severe population decline originate not from direct physiological responses to heat but rather from modified species interactions (Cahill et al., 2013). This may well be true in the case of ocean acidification, which acts to increase resources (CO_2) for primary producers and induce energetic costs for consumers (Gaylord et al 2014). For example, increased aquatic CO_2 leads to increases in the growth rate and competitive ability of macroalgae, which is frequently found in competition for space with corals (Harley et al., 2014, Koch et al., 2013, Diaz-Pulido et al., 2009). Alternatively, ocean acidification might elevate the energetic needs of a corallivore, which may increase its consumption rate, leading to increased coral mortality. As such, an important extension to the work presented in this thesis would be the addition of species interactions.

6.3.3 Mechanism behind the flow-ocean acidification interaction

By examining the effect of flow and ocean acidification on tissue surface pH, I have only just begun to try and unravel the mechanisms behind the flow-ocean acidification interaction. While I have shown that thicker DBLs can lead to higher tissue surface pH in massive species, and to a lesser extent in branching species, it is pH under the calicoblastic layer (hereafter pH_i), and not tissue surface pH, that determines calcification rate. Unfortunately, our understanding of how the elemental composition and physical chemistry of the external environment interacts with biological control to determine pH_i is limited (Cohen et al., 2006). Corals have been shown to elevate pH_i (Al-Horani et al 2003, Venn et al 2011, McCulloch et al 2012), with the ability to increase elevation of pH_i under acidified conditions recently found to be species-specific (McCulloch et al 2012). While all corals studied so far elevated pH_i by 0.3-0.5 pH units under ambient conditions, *Stylophora pistillata* and *Porites* spp. have been shown to be able to increase the elevation of pHi by up to an additional 0.5 pH units under ocean acidification, while *Acropora* spp. and *Porites*

cylindrica were found to only be able to maintain the 03-0.5 pH unit elevation (Al-Horani et al 2003, Venn et al 2011, McCulloch et al 2012). The only study so far to have measured pH_i under various flows has suggested that it has no measurable influence on pH_i (Mass et al., 2011). However, Mass et al. (2011) only investigated *P. damicornis,* which has been shown to be exceptionally resilient to ocean acidification (Huang et al., 2014, Schoepf et al., 2013, Comeau et al., 2013c), possibly due to an abnormally strong pH regulatory mechanism (Mass et al., 2011). Moreover they made these measurements under some pretty unrealistic flow conditions, so the generality of the outcome is yet to be proven. Thus, expanding our understanding of how pH under the calicoblastic layer varies with flow and ocean acidification is a logical next step in elucidating the mechanism behind the flow-ocean acidification interaction

6.4 Conclusions

The work in this thesis has improved upon previous models projecting the impacts of ocean acidification on coral reefs by incorporating the effects of ocean acidification on every stage of the coral life cycle. Not only does it allows us to integrate the collective knowledge of individual organism's physiological responses into population level effects but it also allows us to pinpoint key areas to direct future research (recruitment response to ocean acidification). Moreover, it highlights flow as an important interactive factor that needs to be taken into consideration in future ocean acidification research. Lastly, as future research deepens our understanding of how corals will adapt to ocean acidification and how ocean acidification will affect species interactions, this work presents a template to easily incorporate the new knowledge into climate change projections.

REFERENCES

AGOSTINI, S., FUJIMURA, H., HIGUCHI, T., YUYAMA, I., CASARETO, B. E., SUZUKI, Y. & NAKANO, Y. 2013. The effects of thermal and high-CO_2 stresses on the metabolism and surrounding microenvironment of the coral *Galaxea fascicularis*. *Comptes Rendus Biologies,* 336**,** 384-391.

AL-HORANI, F. A., AL-MOGHRABI, S. M. & DE BEER, D. 2003. The mechanism of calcification anad its relation to photosynthesis and respiration in the scleractinian coral *Galaxea fascicularis*. *Marine Biology,* 142**,** 419-426.

ALBRIGHT, R., LANGDON, C. & ANTHONY, K. R. N. 2013. Dynamics of seawater carbonate chemistry, production, and calcification of a coral reef flat, central Great Barrier Reef. *Biogeosciences,* 10**,** 6747-6758.

ALBRIGHT, R., MASON, B., MILLER, M. & LANGDON, C. 2010. Ocean acidification compromises recruitment success of the threatened Caribbean coral Acropora palmata. *PNAS,* 107**,** 20400-20404.

ALLEMAND, D., FERRIER-PAGES, C., FURLA, P., HOULBREQUE, F., PUVEREL, S., REYNAUD, S., TAMBUTTE, E., TAMBUTTE, S. & ZOCCOLA, D. 2004. Biomineralisation in reef-building corals: from molecular mechanisms to environmental control. *Comptes Rendus Palevol,* 3**,** 453-467.

ANDERSSON, A. J. & GLEDHILL, D. 2013. Ocean Acidification and Coral Reefs: Effect on Breakdown, Dissolution, and Net Ecosystem Calcification. *Annu. Rev. Mar. Sci.,* 5**,** 321-348.

ANTHONY, K. R. N., KLEYPAS, J. A. & GATTUSO, J. P. 2011. Coral reefs modify their seawater carbon chemistry - implications for impacts of ocean acidification. *Global Change Biology,* 17**,** 3655-3666.

ANTHONY, K. R. N., KLINE, D. I., DIAZ-PULIDO, G. & HOEGH-GULDBERG, O. 2008. Ocean acidification causes bleaching and productivity loss in coral reef builders. *PNAS,* 105**,** 17442-17446.

ATKINSON, M. & BILGER, R. W. 1992. Effect of water velocity on phosphate uptake in coral reef-flat communities. *Limnol. Oceanogr.,* 37**,** 273-279.

ATKINSON, M., CARLSON, B. & CROW, G. L. 1995. Coral growth in high-nutrient, low-pH seawater: a case study of corals cultured at the Waikiki Aquarium, Honolulu, Hawaii. *Coral Reefs,* 14**,** 215-223.

ATKINSON, M. & CUET, P. 2008. Possible effects of ocean acidification on coral reef biogeochemistry: topics for research. *Mar. Ecol. Prog. Ser.,* 373**,** 249-256.

BABCOCK, R. C. 1991. Comparative demography of three species of scleractinian corals using age- and seize-dependent classifications. *Ecol. Mono.,* 61**,** 225-244.

BAIRD, M. E. & ATKINSON, M. 1997. Measurement and prediction of mass transfer to exprimental coral reef communities. *Limnol. Oceanogr.,* 42**,** 1685-1693.

BARNES, D. J. 1982. Light response curve for calcification in the staghorn coral *Acropora acuminata*. *Comp. Biochem. Physiol. A,* 73**,** 41-45.

BASKETT, M. L., GAINES, S. D. & NISBET, R. M. 2009. Symbiont diversity may help coral reefs survive moderate climate change. *Ecological Applications,* 19**,** 3-17.

BATES, N. R., AMAT, A. & ANDERSSON, A. J. 2010. Feedbacks and responses of coral calcification on the Bermuda reef system to seasonal changes in biological processes and ocean acidification. *Biogeosciences,* 7**,** 2509-2530.

BILGER, R. W. & ATKINSON, M. 1992. Anomalous mass transfer of phosphate on coral reef flats. *Limnology and Oceanography,* 37**,** 261-272.

BORENSTEIN, M., HEDGES, L. V., HIGGINS, J. P. T. & ROTHSTEIN, H. R. 2009. *Introduction to Meta-Analysis,* Hoboken, NJ, USA, John Wiley & Sons.

BOUDREAU, B. P. & JØRGENSEN, B. B. 2001. *The Benthic Boundary Layer,* New York, Oxford University Press.

BRANDING, P., WARNER, M. E., DAVEY, P., SMITH, D. J., ACHTERBERG, E. P. & SUGGETT, D. J. 2011. Differential effects of ocean acidification on growth and photosynthesis among phylotypes of *Symbiodimium* (Dinophyceae). *Limnol. Oceanogr.,* 56**,** 927-938.

BRUNO, J. F., ELLNER, S. P., VU, I., KIM, K. & HARVEST, C. D. 2011. Impacts of aspergillosis on sea fan coral demography: modelling a moving target. *Ecological Monographs,* 81**,** 123-139.

BURTON, E. A. & WALTER, L. M. 1987. Relative precipitation rates of aragonite and Mg calcite from seawater: Temperature or carbonate ion control? *Geology,* 15**,** 111-114.

CAHILL, A. E., AIELLO-LAMMENS, M. E., FISHER-REID, M. C., HUA, X., KARANEWSKY, C. J., RYU, H. Y., SBEGLIA, G. C., SPAGNOLO, F., WALDRON, J. B., WARSI, O. & WIENS, J. J. 2013. How does climate change cause extinction? *Proc. R. Soc. Lond. B,* 280**,** 20121890.

CALDEIRA, K. & WICKETT, M. E. 2003. Anthropogenic carbon and ocean pH. *Nature,* 425**,** 365.

CARPENTER, R. C., HACKNEY, J. M. & ADEY, W. H. 1991. Measurements of primary productivity and nitrogenase activity of coral reef algae in a chamger incorporating oscillatory flow. *Limnol. Oceanogr.,* 36**,** 40-49.

CARPENTER, R. C. & WILLAIMS, S. L. 2007. Mass transfer limitation of photosynthesis of coral reef algal turfs. *Mar. Biol.,* 151**,** 435-450.

CESAR, H., BURKE, L. & PET-SOEDE, L. 2003. The Economics of Worldwide Coral Reef Degradation. Arnhem, The Netherlands: Cesar Environmental Economics Consulting.

CHAMBERLAIN, J. A. & GRAUS, R. R. 1977. Water flow and hydromechanical adaptations of branched reef corals. *Bulletin of Marine Science,* 25**,** 112-125.

CHAN, N. C. S. & CONNOLLY, S. R. 2013. Sensitivity of coral calcification to ocean acidificaiton: a meta-analysis. *Global Change Biology,* 19**,** 282-290.

CHANG, S., ELKINS, C., ALLEY, M., EATON, J. & MONISMITH, S. G. 2009. Flow inside a coral colony measured using magnetic resonance velocimetry. *Limnol. Oceanogr.,* 54**,** 1819-1827.

CHAUVIN, A., DENIS, V. & CUET, P. 2011. Is the response of coral calcification to seawater acidification related to nutrient loading? *Coral Reefs,* 30**,** 911-923.

CHUA, C. M., LEGGAT, W., MOYA, A. & BAIRD, A. H. 2013. Near-future reductions in pH will have no consistent ecological effects on the early life-history stages of reef corals. *Marine Ecology Progress Series,* 486**,** 143-151.

COHEN, A. L., GAETANI, G. A., LUNDALV, T., CORLISS, B. H. & GEORGE, R. Y. 2006. Compositional variability in a cold-water scleractinian, *Lophelia pertusa*: New insights into "vital effects". *Geochemistry Geophysics Geosystems,* 7**,** DOI: 10.1029/2006GC001354.

COHEN, A. L. & HOLCOMB, M. 2009. Why corals care about ocean acidification: Uncovering the mechanism. *Oceanography,* 22**,** 118-127.

COHEN, A. L. & MCCONNAUGHEY, T. A. 2003. Geochemical perspectives on coral mineralization. *Biomineralization,* 54**,** 151-187.

COLOMBO-PALLOTTA, M. F., RODRIGUEZ-ROMAN, A. & IGLESIAS-PRIETO, R. 2010. Calcification in bleached and unbleached *Montastraea faveolata*: evaluating the role of oxygen and glycerol. *Coral Reefs,* 29**,** 899-907.

COMEAU, S., CARPENTER, R. C. & EDMONDS, P. J. 2012. Coral reef calcifiers buffer their response to ocean acidification using both bicarbonate and carbonate. *Proceedings of the royal society B,* 280**,** 20122374.

COMEAU, S., CARPENTER, R. C. & EDMUNDS, P. J. 2013a. Effects of feeding and light intensity on the response of the coral *Porites rus* to ocean acidification. *Mar. Biol.,* 160**,** 1127-1134.

COMEAU, S., CARPENTER, R. C. & EDMUNDS, P. J. 2013b. Effects of irradiance on the response of the coral *Acropora pulchra* and the calcifying alga *Hydrolithon reinboldii* to temperature elevation and ocean acidification. *Journal of Experimental Marine Biology and Ecology,* 453**,** 28-35.

COMEAU, S., EDMUNDS, P. J., LANTZ, C. A. & CARPENTER, R. C. 2014a. Water flow modulates the response of coral reef communities to ocean acidification. *Scientific Reports,* 4**,** DOI: 10.1038/srep06681.

COMEAU, S., EDMUNDS, P. J., SPINDEL, N. B. & CARPENTER, R. C. 2013c. The responses of eight coral reef calcifiers to increasing partial pressure of CO_2 do not exhibit a tipping point. *Limnol. Oceanogr.,* 58**,** 388-398.

COMEAU, S., EDMUNDS, P. J., SPINDEL, N. B. & CARPENTER, R. C. 2014b. Fast coral reef calcifiers are more sensitive to ocean acidification in short term laboratory incubations. *Limnol. Oceanogr.,* 59**,** 1081-1091.

CORNWALL, C. E., BOYD, P. W., MCGRAW, C. M., HEPBURN, C. D., PILDTICH, C. A., MORRIS, J. N., SMITH, A. M. & HURD, C. L. 2014. Diffusion boundary layers ameliorate the negative effects of ocean acidification on the temperate coralline macroalga Arthrocardia corymbosa. *Plos One,* 9**,** e97235.

CORNWALL, C. E., HEPBURN, C. D., PILDTICH, C. A. & HURD, C. L. 2013. Concentration boundary layers around complex assemblages of macroalgae: Implications for the effects of ocean acidification on understorey coralline algae. *Limnol. Oceanogr.,* 58**,** 121-130.

CUMBO, V. R., FAN, T. Y. & EDMUNDS, P. J. 2013. Effects of exposure duration on the response of Pocillopora damicornis larvae to elevated temperature and high pCO_2. *J. Exp. Mar. Biol. Ecol.,* 439**,** 100-107.

DARLING, E. S., ALVAREZ-FILIP, L., OLIVER, T. A., MCCLANAHAN, T. R. & COTE, I. M. 2012. Corals present a good model to investigate if this occurs within a taxonomic group. *Ecology Letters,* 15**,** 1378-1386.

DE BEER, D., KÜHL, M., STAMBLER, N. & VAKI, L. 2000. A microsensor study of light enhanced Ca^{2+} uptake and photosynthesis in the reef-building hermatypic coral *Favia* sp. *Marine Ecology Progress Series,* 194**,** 75-85.

DENNISON, W. C. & BARNES, D. J. 1988. Effect of water motion on coral photosynthesis and calcification. *Journal of Experimental Marine Biology and Ecology,* 115**,** 67-77.

DENNY, M. W. 1988. *Biology and the mechanics of the wave-swept environment,* Princeton, New Jersey, USA, Princeton University Press.

DIAZ-PULIDO, G., ANTHONY, K. R. N., KLINE, D. I., DOVE, S. & HOEGH-GULDBERG, O. 2012. Interactions between ocean acidificatioon and warming on the mortality and dissolution of coralline algae. *J. Phycol.,* 48**,** 32-39.

DIAZ-PULIDO, G., MCCOOK, L. J., DOVE, S., BERKELMANS, R., ROFF, G., KLINE, D. I., WEEKS, S., EVANS, R. D., WILLIAMSON, D. H. & HOEGH-GULDBERG, O. 2009. Doom and boom on a resilient reef: Climate change, algal overgrowth and coral recovery. *Plos One*, DOI: 10.1371/journal.pone.0005239.

DICKSON, A. G. & MILLERO, F. J. 1987. A comparison of the equilibrium constants for the dissociation of carbonic acid in seawater media. *Deep Sea Res.,* 34, 1733-1743.

DONE, T. J. 1983. Coral zonation: its nature and significance. *In:* BARNES, D. J. (ed.) *Perspectives on coral reefs.* Manukau, New Zealand: Brian Clousten.

DONEY, S. C., FABRY, V. J., FEELY, R. A. & KELYPAS, J. A. 2009. Ocean Acidification: The Other CO_2 Problem. *Annu. Rev. Mar. Sci.,* 1, 169-192.

DOROPOULOS, C., WARD, S., DIAZ-PULIDO, G., HOEGH-GULDBERG, O. & MUMBY, P. J. 2012. Ocean acidifcation reduces coral recruitment by disrupting intimate larval-algal settlement interactions. *Ecology Letters,* 15, 338-346.

DUFAULT, A. M., NINOKAWA, A., BRAMANTI, L., CUMBO, V. R., FAN, T. Y. & EDMUNDS, P. J. 2013. The role of light in mediating the effects of ocean acidification on coral calcification. *The Journal of Experimental Biology,* 216, 1570-1577.

EASTERLING, M. R., ELLNER, S. P. & DIXON, P. M. 2000. Size specific sensitivity: applying a new structured population model. *Ecology,* 81, 694-708.

EDINGER, E. N. & RISK, M. J. 2000. Reef classification by coral morphology predicts coral reef conservation value. *Biol. Conserv.,* 92, 1-13.

EDMUNDS, P. J. 2011. Zooplanktivory ameliorates the effects of ocean acidification on the reef coral *Porites* spp. *Limnol. Oceanogr.,* 56, 2402-2410.

EDMUNDS, P. J., BROWN, D. & MORIARTY, V. 2012. Interactive effects of ocean acidification and temperature on two scleractinian corals from Moorea, French Polynesia. *Global Change Biology,* 18, 2173-2183.

EFRON, B. & TIBSHIRANI, R. J. 1993. *An introduction to the bootstrap,* New York, Chapman & Hall.

ENOCHS, I. C., MANZELLO, D. P., CARLTON, R., SCHOPMEYER, S., VAN HOOIDONK, R. V. & LIRMAN, D. 2014. Effects of light and elevated pCO_2 on the growth and photochemical efficiency of *Acropora cervicornis*. *Coral Reefs,* 33, 477-485.

FALTER, J. L., ATKINSON, M. & COIMBRA, C. F. M. 2005. Effects of surface roughness and oscillatory flow on dissolution of plaster forms: evidence for nutrient mass transfer to coral reef communities. *Limnol. Oceanogr.,* 50, 246-254.

FALTER, J. L., ATKINSON, M., LOWE, R. J., MONISMITH, S. G. & KOSEFF, J. R. 2007. Effects of nonlocal turbulence on the mass transfer of dissolved species to reef corals. *Limnol. Oceanogr.,* 52, 274-285.

FALTER, J. L., ATKINSON, M. & MERRIFIELD, M. A. 2004. Mass-transfer limitation of nutriet uptake by a wave-dominated reef flat community. *Limnol. Oceanogr.,* 49, 1820-1831.

FEELY, R. A., DONEY, S. C. & COOLEY, S. R. 2009. Ocean acidification: Present conditions and future changes in a high-CO_2 World. *Oceanography,* 22, 36-47.

FORM, A. U. & RIEBESELL, U. 2012. Acclimation to ocean acidification during long-term CO_2 exposure in the cold-water coral *Lophelia pertusa*. *Global Change Biology,* 18, 843-853.

FULTON, C. J. & BELLWOOD, D. R. 2005. Wave-induced water motion and the functional implications for coral reef fish assemblages. *Limnology and Oceanography,* 2005, 255-264.

FURLA, P., GALGANI, I., DURAND, I. & ALLEMAND, D. 2000. Sources and mechanisms of inorganic carbon transport for coral calcification and photosynthesis. *The Journal of Experimental Biology,* 203**,** 3445-3457.

GATTUSO, J. P., ALLEMAND, D. & FRANKIGNOULLE, M. 1999. Photosynthesis and calcification at cellular, organismal and community levels in coral reefs: a review on interactions and control by carbonate chemistry. *American Zoologist,* 39**,** 160-183.

GATTUSO, J. P. & LAVIGNE, H. 2009. Technical Note: Approaches and software tools to investigate the impact of ocean acidification. *Biogeosciences,* 6**,** 2121-2133.

GAYLORD, B., KROEKER, K. J., SUNDAY, J. M., ANDERSON, K. M., BARRY, J. P., BROWN, N. E., CONNELL, S. D., DUPONT, S., FABRICIUS, K., HALL-SPENCER, J. M., KLINGER, T., MILAZZO, M., MUNDAY, P. L., RUSSELL, B. D., SANFORD, E., SCHREIBER, S. J., THIYAGARAJAN, V., VAUGHAN, M. L. H., WIDDICOMBE, S. & HARLEY, C. D. G. 2015. Ocean acidification through the lens of ecological theory. *Ecology,* In press.

GLYNN, P. W. 1996. Coral reef bleaching: facts, hypotheses and implications. *Global Change Biology,* 2**,** 495-509.

GOIRAN, C., AL-MOGHRABI, S. M., ALLEMAND, D. & JAUBERT, J. 1996. Inorganic carbon uptake for photosynthesis by the symbiotic coral/dinoflagellate association I. Photosynthetic performances of symbionts and dependence on sea water bicarbonate. *Journal of Experimental Marine Biology and Ecology,* 199**,** 207-225.

GUREVITCH, J. & HEDGES, L. V. 1999. Statistical issues in ecological meta-analyses. *Ecology,* 80**,** 1142-1149.

GUREVITCH, J. & HEDGES, L. V. 2001. Meta-analysis: Combining the Results of Independent Experiments. *In:* SCHEINER, S. (ed.) *Design and Analysis of Ecological Experiments.* New York: Oxford University Press.

GURNEY, G. G., MELBOURNE-THOMAS, J., GERONIMO, R. C., ALINO, P. M. & JOHNSON, C. R. 2013. Modelling coral reef futures to inform management: Can reducing local-scale stressors conserve reefs under climate change? *Plos One,* 8**,** e80137.

HALL, V. P. & HUGHES, T. P. 1996. Reproductive strategies of modular organisms: comparative studies of reef-building corals. *Ecology,* 77**,** 950-963.

HARLEY, C. D. G., ANDERSON, K. M., DEMES, K. W., JORVE, J. P., KORDAS, R. L. & COYLE, T. A. 2014. Effects of climate change of global seaweed communities. *Journal of Phycology,* 48**,** 1064-1078.

HARRINGTON, L., FABRICIUS, K., DE'ATH, G. & NEGRI, A. 2004. Recognition and selection of settlement substrata determine post-settlement survival in corals. *Ecology,* 85**,** 3428-3437.

HARVEY, B. P., GWYNN-JONES, D. & MOORE, P. J. 2013. Meta-analysis reveals complex marine biological responses to the interactive effects of ocean acidification and warming. *Ecology and Evolution,* 3**,** 1016-1030.

HELMUTH, B. S. T., SEBENS, K. P. & DANIELS, T. L. 1997. Morphological variation in coral aggregations: branch spacing and mass flux to coral tissue. *Journal of Experimental Marine Biology and Ecology,* 209**,** 233-259.

HENDRIKS, I. E., DUARTE, C. M. & ALVAREZ, M. 2010. Vulnerability of marine biodiversity to ocean acidification: A meta-analysis. *Estuarine, Coastal and Shelf Science,* 86**,** 157-164.

HOEGH-GULDBERG, O. 1999. Climate change, coral bleaching and the future of the world's coral reefs. *Mar. Freshwater. Res.,* 50**,** 839-866.

HOEGH-GULDBERG, O., MUMBY, P. J., HOOTEN, A. J., STENECK, R. S., GREENFIELD, P., GOMEZ, E., HARVELL, C. D., SALE, P. F., EDWARDS, A. J., CALDEIRA, K., KNOWLTON, N., EAKIN, C. M., IGLESIAS-PRIETO, R., MUTHIGA, N., BRADBURY, R. H., DUBI, A. & HATZIOLOS, M. E. 2007. Coral reefs under rapid climate change and ocean acidification. *Science,* 318**,** 1739-1742.

HOEKE, R. K., JOKIEL, P. L., BUDDEMEIER, R. W. & BRAINARD, R. E. 2011. Projected changes to growth and mortality of Hawaiian corals over the next 100 years. *Plos One,* 6**,** e18038.

HOLCOMB, M., MCCORKLE, D. C. & COHEN, A. L. 2010. Long-term effects of nutrient and CO_2 enrichment on the temperate coral *Astrangia poculata* (Ellis and Solander, 1786). *J. Exp. Mar. Biol. Ecol.,* 386**,** 27-33.

HOLCOMB, M., TAMBUTTE, E., ALLEMAND, D. & TAMBUTTE, S. 2014. Light enhanced calcification in Stylophora pistillata: effects of glucose, glycerol and oxygen. *PeerJ,* 2**,** DOI 10.7717/peerj.375.

HOOGENBOOM, M. O. & CONNOLLY, S. R. 2009. Defining fundamental niche dimensions of corals: synergistic effects of colony size, light, and flow. *Ecology,* 90**,** 767-780.

HOULBREQUE, F., RODOLFO-METALPA, R., JEFFREE, R., OBERHANSLI, F., TEYSSIE, J. L., BOISSON, F., AL-TRABEEN, K. & FERRIER-PAGES, C. 2012. Effects of increased pCO_2 on zinc uptake and calcification in the tropical coral *Stylophora pistillata*. *Coral Reefs,* 31**,** 101-109.

HUANG, H., YUAN, X. C., CAI, W. J., ZHANG, C. L., LI, X. & LIU, S. 2014. Positive and negative responses of coral calcification to elevated pCO_2: case studies of two coral species and the implications of their responses. *Marine Ecology Progress Series,* 502**,** 145-156.

HURD, C. L., CORNWALL, C. E., CURRIE, K., HEPBURN, C. D., MCGRAW, C. M., HUNTER, K. A. & BOYD, P. W. 2011. Metabolically induced pH fluctuations by some coastal calcifiers exceed projected 22nd century ocean acidification: a mechanism for differential susceptibility? *Global Change Biology,* 17**,** 3254-3262.

INCROPERA, F. P. & DEWITT, D. P. 1996. *Fundamentals of hear and mass transfer,* New York, Wiley.

IPCC 2007. Cross-chapter case study. *In:* PARRY, M. L., CANZIANI, O. F., PALUTIKOF, J. P., VAN DER LINDEN, P. J. & HANSON, C. E. (eds.) *Climate Change 2007: Impacts, Adaptation and Vulnerability. Contribution of Working Group II to the Forth Assessment Report of the Intergovernmental Panel of Climate Change.* Cambridge, UK: Cambridge University Press.

IPCC 2013. Declining coral calcification on the Great Barrier Reef. *In:* STOCKER, T. F., QIN, D., PLATTER, G. K., TIGNOR, M. M. B., ALLEN, S. K., BOSCHUNG, J., NAUELS, A., XIA, Y., BEX, V. & MIDGLEY, P. M. (eds.). Cambridge, United Kingdon and New York, NYm USA.

JACKSON, J. & HUGHES, T. P. 1985. Adaptive strategies of coral-reef invertebrates. *Am. Sci.,* 73**,** 265-274.

JACKSON, J., KIRBY, M. X., BERGER, W. H., BJORNDAL, K. A., BOTSFORD, L. W., BOURQUE, B. J., BRADBURY, R. H., COOKE, R., ERLANDSON, J., ESTES, J. A., HUGHES, T. P., KIDWELL, S., LANGE, C. B., LENIHAN, H. S., PANDOLFI, J. M., PETERSON, C. H., STENECK, R. S., TEGNER, M. J. & WARNER, R. R. 2001. Historical overfishing and the recent collapse of coastal ecosystems. *Science,* 293**,** 629-638.

JENNIONS, M. D., MOLLER, A. P. & PETRIE, M. 2001. Sexually selected traits and adult survival: a meta-analysis. *The Quarterly Review of Biology,* 76**,** 3-36.

JIMENEZ, I. M., KÜHL, M., LARKUM, A. W. D. & RALPH, P. J. 2011. Effects of flow and colony morphology on the thermal boundary layer of corals. *Journal of The Royal Society,* 8**,** 1785-1795.

JOKIEL, P. L. 2011a. Ocean acidification and control of reef coral calcification by boundary layer limitation of proton flux. *Bulletin of Marine Science,* 87**,** 639-657.

JOKIEL, P. L. 2011b. The reef coral two compartment proton flux model: a new approach relating tissue-level physiological processes to gross corallum morphology. *Journal of Experimental Marine Biology and Ecology,* 409**,** 1-12.

JOKIEL, P. L., RODGERS, K. S., KUFFNER, I. B., ANDERSSON, A. J., COX, E. F. & MACKENZIE, F. T. 2008. Ocean acidification and calcifying reef organisms: a mesocosm investigation. *Coral Reefs,* 27**,** 473-483.

JONES, R. J., HOEGH-GULDBERG, O., LARKUM, A. W. D. & SCHREIBER, U. 1998. Temperature-induced bleching of corals begins with impariment of the CO_2 fixation mechanism in zooxanthellae. *Plant, Cell & Environment,* 21**,** 1219-1230.

JONSSON, P. R., VAN DUREN, L. A., AMIELH, M., ASMUS, R., ASPDEN, R. J., DAUNYS, D., FRIEDRICHS, M., FRIEND, P. L., OLIVIER, F., POPE, N., PRECHT, E., SAURIAN, P. G. & SCHAAFF, E. 2006. Making water flow: a comparison of the hydrodynamic characteristics of 12 different benthic biological flumes. *Aquat. Ecol.,* 40**,** 409-438.

JØRGENSEN, B. B. & REVSBECH, N. P. 1985. Diffusive boundary layers and the oxygen uptake of sediments and detritus. *Limnol. Oceanogr.,* 30**,** 111-122.

JUMARS, P. A. & NOWELL, A. R. M. 1984. Fluid and sediment dynamic effects on marine benthic community structure. *Amer. Zool.,* 24**,** 45-55.

KELLY, M. W. & HOFMANN, G. E. 2013. Adaptation and the physiology of ocean acidification. *Functional Ecology,* 27**,** 980-990.

KLEYPAS, J. A., ANTHONY, K. R. N. & GATTUSO, J. P. 2011. Coral reefs modify their seawater carbon chemistry - case study from a barrier reef (Moorea, French Polynesia). *Global Change Biology,* 17**,** 3667-3678.

KLEYPAS, J. A., BUDDEMEIER, R. W., ARCHER, D., GATTUSO, J. P., LANGDON, C. & OPDYKE, B. N. 1999a. Geochemical consequences of increased atmospheric carbon dioxide on coral reefs. *Science,* 284**,** 118-120.

KLEYPAS, J. A., FEELY, R. A., FABRY, C., LANGDON, C., SABINE, C. L. & ROBBINS, L. L. 2006. Impacts of Ocean Acidification on Coral Reefs and Other Marine Calcifiers: A Guide for Future Research, a report of a workshop held 18-20 April 2005, St. Petersburg, FL, sponsored by NSF, NOAA and the U.S Geological Survey.

KLEYPAS, J. A. & LANGDON, C. 2006. Coral reefs and changing seawater chemistry. *In:* PHINNEY, J. T. & HOEGH-GULDBERG, O. (eds.) *Coral reefs and climate change: science and management.* Coastal Estuarine Studies ed. Washington, DC: American Geophysical Union.

KLEYPAS, J. A., MCMANUS, J. W. & MENEX, L. A. B. 1999b. Environmental limits to coral reef development: Where do we draw the line? *Amer. Zool.,* 39**,** 146-159.

KOCH, M., BOWES, G., ROSS, C. & ZHANG, X. H. 2013. Climate change and ocean acidification effects on seagrasses and marine macroalgae. *Global Change Biology,* 19**,** 103-132.

KRIEF, S., HENDY, E. J., FINE, M., YAM, R., MEIBOM, A., FOSTER, G. L. & SHEMESH, A. 2010. Physiological and isotopic responses of scleractinian corals to ocean acidification. *Geochimica et Cosmochimica Acta,* 74**,** 4988-5001.

KROEKER, K. J., KORDAS, R. L., CRIM, R. N., HENDRIKS, I. E., RAMAJO, L., SINGH, G. S., DUARTE, C. M. & GATTUSO, J. P. 2013. Impacts of ocean acidification on marine organisms: quantifying sensitivities and interaction with warming. *Global Change Biology,* 19**,** 1884-1896.

KROEKER, K. J., KORDAS, R. L., CRIM, R. N. & SINGH, G. G. 2010. Meta-analysis reveals negative yet variable effects of ocean acidification on marine organisms. *Ecology Letters,* 13**,** 1419-1434.

KÜHL, M., COHEN, Y., DALSGAARD, T., JØRGENSEN, B. B. & REVSBECH, N. P. 1995. Microenvironment and photosynthesis of zooxanthellae in scleractinian corals studied with microsensors for O_2, pH and light. *Marine Ecology Progress Series,* 117**,** 159-172.

LANGDON, C. & ATKINSON, M. J. 2005. Effect of elevated pCO_2 on photosynthesis and calcification of corals and interactions with seasonal change in temperature irradiance and nutrient enrichment. *Journal of Geophysical Research,* 110**,** C09S07, doi:10.1029/2004JC002576.

LANGDON, C., TAKAHASHI, T., SWEENEY, C., CHIPMAN, D. & GODDARD, J. 2000. Effects of calcium carbonate saturation state on the calcification rate of an experimental coral reef. *Global Biogeochemical Cycles,* 14**,** 639-654.

LAVIGNE, H. & GATTUSO, J. P. 2011. Seacarb: seawater carbonate chemistry with R. R package version 2.4.

LECLERCQ, N., GATTUSO, J. P. & JAUBERT, J. 2000. CO_2 partial pressure controls the calcification rate of a coral community. *Global Change Biology,* 6**,** 329-334.

LESSER, M. P., WEIS, V. M., PATTERSON, M. R. & JOKIEL, P. L. 1994. Effects of morphology and water motion on carbon delivery and productivity in the reef coral, *Pocillopora damicornis* (Linnaeus): Diffusion barriers, inorganic carbon limitation, and biochemical plasticity. *Journal of Experimental Marine Biology and Ecology,* 178**,** 153-179.

LOYA, Y. & RINKEVICH, B. 1980. Effects of oil polluion on coral reef communities. *Marine Ecology Progress Series,* 3**,** 167-180.

LOYA, Y., SAKAI, K., YAMAZATO, K., NAKANO, Y., SAMBALI, H. & VAN WOESIK, R. 2001. Coral bleaching: the winners and the losers. *Ecology Letters,* 4**,** 122-131.

MADIN, J. S., BAIRD, A. H., DORNELAS, M. & CONNOLLY, S. R. 2014. Mechanical vulnerability explains size-dependent mortality of reef corals. *Ecology Letters,* 17**,** 1008-1015.

MADIN, J. S., HUGHES, T. P. & CONNOLLY, S. R. 2012. Calcification, Storm Damage and Population Resilience of Tabular Corals under Climate Change. *Plos One,* 7**,** e46637.

MARSHALL, P. A. & BAIRD, A. H. 2000. Bleaching of corals on the Great Barrier Reef differential susceptibilities among taxa. *Coral Reefs,* 19**,** 155-163.

MARUBINI, F. & ATKINSON, M. J. 1999. Effects of lowered pH and elevated nitrate on coral calcification. *Mar. Ecol. Prog. Ser.,* 188**,** 117-121.

MARUBINI, F., BARNETT, H., LANGDON, C. & ATKINSON, M. 2001. Dependence of calcification on light and carbonate ion concentration for the hermatypic coral *Porites compressa*. *Mar. Ecol. Prog. Ser.,* 220**,** 153-162.

MARUBINI, F., FERRIER-PAGES, C. & CUIF, J. P. 2003. Suppression of skeletal growth in scleractinian corals by decreasing ambient carbonate-ion concentration: a cross-family comparison. *Proc. R. Soc. Lond. B,* 270**,** 179-184.

MARUBINI, F., FERRIER-PAGES, C., FURLA, P. & ALLEMAND, D. 2008. Coral calcification responds to seawater acidification: a working hypothesis towards a physiological mechanism. *Coral Reefs,* 27**,** 491-499.

MASS, T., BRICKNER, I., HENDY, E. & GENIN, A. 2011. Enduring physiological and reproductive benefits of enhanced flow for a stony coral. *Limnol. Oceanogr.,* 56**,** 2176-2188.

MASS, T., GENIN, A., SHAVIT, U., GRINSTEIN, M. & TCHERNOV, D. 2010. Flow enhances photosynthesis in marine benthic autotrophs by increasing the efflux of oxygen from the organism to the water. *PNAS,* 107**,** 2527-2531.

MCCLANAHAN, T. R., ATEWEBERHAN, M., GRAHAM, N. A. J., WILSON, S. K., RUIZ SEBASTIAN, C. & GUILLAUME, M. 2007. Western Indian Ocean coral communities: bleaching response and susceptibility to extinction. *Mar. Ecol. Prog. Ser.,* 337**,** 1-13.

MCCONNAUGHEY, T. A. & WHELAN, J. F. 1997. Calcification generates protons for nutrient and bicarbonate uptake. *Earth-Science Reviews,* 42**,** 95-117.

MCCULLOCH, M., FALTER, J. L., TROTTER, J. & MONTAGNA, P. 2012. Coral resilience to ocean acidification and global warming through pH up-regulation. *Nature Climate Change,* 2**,** 623-627.

MEHRBACH, C., CULBERSON, C. H., HAWLEY, J. E. & PYTKOWICZ, R. N. 1973. Measurement of the apparent dissociation constants of carbonic acid in seawater at atmospheric pressure. *Limnol. Oceanogr.,* 18**,** 897-907.

MOBERG, F. & FOLKE, C. 1999. Ecological goods and services of coral reef ecosystems. *Ecological Economics,* 29**,** 215-233.

MOLLER, A. P. & JENNIONS, M. D. 2001. Testing and adjusting for publication bias. *TRENDS in Ecology & Evolution,* 16**,** 580-586.

MORGAN, K. M. & KENCH, P. S. 2012. Skeletal extension and calcification of reef building corals in the central Indian Ocean. *Marine Environmental Research,* 81**,** 78-82.

NAKAMURA, M., OHKI, S., SUZUKI, A. & SAKAI, K. 2011. Coral larvae under ocean acidification: Survivla, metabolism, and metamorphosis. *Plos One,* 6**,** e14521.

NAKAMURA, T. & NAKAMORI, T. 2009. Estimation of photosynthesis and calcification rates at a fringing reef by accounting for diurnal variation and the zonation of coral reef communities on reef flat and slope: a case study for the Shiraho reef, Ishigaki Island, southwest Japan. *Coral Reefs,* 28**,** 229-250.

NEGRI, A., WEBSTER, N. S., RUSSELL, H. & HEYWARD, A. 2001. Metamorphosis of broadcast spawning corals in response to bacteria isolated from crustose algae. *Mar. Ecol. Prog. Ser.,* 223**,** 121-131.

NOBEL, P. S. 1983. *Biophysical plant physiology and ecology,* San Francisco, California, USA, W.H. Freeman.

OHDE, S. & HOSSAIN, M. M. M. 2004. Effects of $CaCO_3$ (aragonite) saturation state of seawater on calcification of *Porites* coral. *Geochemical Journal,* 38**,** 613-621.

PANDOLFI, J. M., CONNOLLY, S. R., MARSHALL, D. J. & COHEN, A. L. 2011. Projecting Coral Reef Futures Under Global Warming and Ocean Acidification. *Science,* 333**,** 418-422.

PATTERSON, M. R. 1992. A chemical engineering view of cnidarian symbioses. *American Zoologist,* 32**,** 566-582.

PATTERSON, M. R., SEBENS, K. P. & OLSON, R. R. 1991. In situ measurements of flow effects on primary production and dark respiration in reef corals. *Limnology and Oceanography,* 36**,** 936-948.

PINHEIRO, J., BATES, D., DEBROY, S., SARKAR, D. & TEAM, T. R. D. C. 2012. nlme: Linear and Nonlinear Mixed Effects Models.

PRICE, N. N., HAMILTON, S. L., TOOTELL, J. S. & SMITH, J. E. 2011. Species-specific consequences of ocean acidification for the calcarous tropical green algae Halimeda. *Mar. Ecol. Prog. Ser.,* 440**,** 67-78.

REIDENBACH, M. A., KOSEFF, J. R., MONISMITH, S. G. & GENIN, A. 2006. Effects of waves, currents and morphology on mass transfer in branched reef corals. *Limnol. Oceanogr.,* 51**,** 1134-1141.

RENEGAR, D. A. & RIEGL, B. M. 2005. Effect of nutrient enrichment and elevated CO_2 partial pressure on growth rate of Atlantic scleractinian coral *Acropora cervicornis*. *Mar. Ecol. Prog. Ser.,* 293**,** 69-76.

REYNAUD, S., LECLERCQ, N., ROMAINE-LIOUD, S., FERRIER-PAGES, C., JAUBERT, J. & GATTUSO, J. P. 2003. Interacting effects of CO_2 partial pressure and temperature on photosynthesis and calcification in a sclerectinian coral. *Global Change Biology,* 9**,** 1660-1668.

RIEGL, B. M., SHEPPARD, C. R. C. & PURKIS, S. J. 2012. Human impacts on atolls leads to coral loss and community homogenisation: A modeling study. *Plos One,* 7**,** e36921.

RIES, J. B., COHEN, A. L. & MCCORKLE, D. C. 2009. Marine calcifiers exhibit mixed responses to CO_2-induced ocean acidification. *Geology,* 37**,** 1131-1134.

RIES, J. B., COHEN, A. L. & MCCORKLE, D. C. 2010. A nonlinear calcification response to CO_2-induced ocean acidification by the coral *Oculina arbuscula*. *Coral Reefs,* 29**,** 661-674.

ROBBINS, L. L., HANSEN, M. E., KLEYPAS, J. A. & MEYLAN, S. C. 2010. CO2calc - A user-friendly seawater carbon calculator for Windows, Mac OS X, and iOS (iPhone): U.S. Geological Survey Open-File Report 2010-1280, 17p.

RODOLFO-METALPA, R., MARTIN, S., FERRIER-PAGES, C. & GATTUSO, J. P. 2010. Response of the temperate coral *Cladocora caespitosa* to mid- and long-term exposure to pCO_2 and temperature levels projected for the year 2100 AD. *Biogeosciences,* 7**,** 289-300.

ROSENTHAL, R. 1991. *Meta-analytic Procedures for Social Research,* Newbury Park, California, Sage.

ROTH, L., KOKSAL, S. & VAN WOESIK, R. 2010. Effects of thermal stress on key processes driving coral-population dynamics. *Mar. Ecol. Prog. Ser.,* 411**,** 73-87.

SABINE, C. L., FEELY, R. A., GRUBER, N., KEY, R. M., LEE, K., BULLISTER, J. L., WANNINKHOF, R., WONG, C. S., WALLACE, D. W. R., TILBROOK, B., MILLERO, F. J., PENG, T. H., KOZYR, A., ONO, T. & RIOS, A. F. 2004. The oceanic sink for anthropogenic CO_2. *Science,* 205**,** 367-371.

SCHLICHTING, H. & GERSTEN, K. 2000. *Boundary layer theory,* Berlin, Springer.

SCHNEIDER, K. & EREZ, J. 2006. The effect of carbonate chemistry on calcification and photosynthesis in the hermatypic coral *Acropora eurystoma*. *Limnology and Oceanography,* 51**,** 1284-1293.

SCHNEIDER, K., LEVY, O., DUBINSKY, Z. & EREZ, J. 2009. In situ diel cycles of photosynthesis and calcification in hermatypic corals. *Limnol. Oceanogr.,* 54**,** 1999-2002.

SCHOEPF, V., GROTTOLI, A. G., WARNER, M. E., CAI, W. J., MELMAN, T. F., HOADLEY, K. D., PETTAY, D. T., HU, X., LI, Q., XU, H., WANG, Y., MATSUI, Y. & BAUMANN, J. H.

2013. Coral energy reserves and calcification in a high-CO_2 world at two temperature. *Plos One,* 8**,** e75049.
SCHRAMEYER, V., WANGPRASEURT, D., HILL, R., KÜHL, M., LARKUM, A. W. D. & RALPH, P. J. 2014. Light respiratory processes and gross photosynthesis in two scleractinian corals. *Plos One,* 9**,** e110814.
SCHULZ, K. G., BARCELOS E RAMOS, J., ZEEBE, R. E. & RIEBESELL, U. 2009. CO2 pertubation experiments: similarities and differences between dissolved inorganic carbon and total alkalinity manipulations. *Biogeosciences,* 6**,** 2145-2153.
SEBENS, K. P., GRACE, S. P., HELMUTH, B. S. T., MANEY, E. J. & MILES, J. S. 1997. Water flow and prey capture by three scleractinian corals, *Madracis mirabilis*, *Montastrea cavernosa* and *Porites porites* in a field enclosure. *Marine Biology,* 131**,** 347-360.
SHAPIRO, O. H., FERNANDEZ, V. I., GARREN, M., GUASTO, J. S., DEBAILLON-VESQUE, F. P., KRAMARSKY-WINTER, E., VARDI, A. & STOCKER, R. 2014. Vortical ciliary flows actively enhance mass transport in reef corals. *PNAS,* 111**,** 13391-13396.
SHASHAR, N., COHEN, Y. & LOYA, Y. 1993. Extreme diel fluctuations of oxygen in diffusive boundary layers surrounding stony corals. *Biological Bulletin,* 185**,** 455-461.
SHASHAR, N., KINANE, S., JOKIEL, P. L. & PATTERSON, M. R. 1996. Hydromechanical boundary layers over a coral reef. *Journal of Experimental Marine Biology and Ecology,* 199**,** 17-28.
SILVERMAN, J., LAZAR, B., CAO, L., CALDEIRA, K. & EREZ, J. 2009. Coral reefs may start dissolving when atmospheric CO_2 doubles. *Geophysical Research Letters,* 36**,** L05606.
SILVERMAN, J., LAZAR, B. & EREZ, J. 2007. Effect of aragonite saturation, temperature, and nutrients on the community calcification rate of a coral reef. *Journal of Geophysical Research,* 112**,** C05004, doi:1029/2006JC003770.
SMITH, S. V. 1978. Coral-reef area and the contributions of reefs to processes and resources of the world's oceans. *Nature,* 273**,** 225-226.
SMITH, S. V. & KINSEY, D. W. 1978. Calcification and organic carbon metabolism as indicated by carbon dioxide. *In:* STODDART, D. R. & JOHANNES, R. E. (eds.) *Coral Reefs: Research Methods.* Unesco.
STIMSON, J. 1985. The effect of shading by the table coral Acropra hyacinthus on understory corals. *Ecology,* 66**,** 40-53.
STUMM, W. & MORGAN, J. J. 1981. *Aquatic chemistry. An introduction emphasizing chemical equilibria in natural water, 2nd edn.,* New York, John Wiley & Sons.
SUGGETT, D. J., DONG, L. F., LAWSON, T., LAWRENZ, E., TORRES, L. & SMITH, D. J. 2012. Light availability determines susceptibility of reef building corals to ocean acidification. *Coral Reefs,* 32**,** 327-337.
TANS, P. 2009. An accounting of the observed increase in oceanic and atmospheric CO_2 and an outlook for the future.
TEAM, R. D. C. 2011. R: A language and environment for statistical computing. Vienna, Austria: R Foundation for Statistical Computing.
THOMAS, F. I. M. & ATKINSON, M. 1997. Ammonium uptake by coral reefs: Effects of water velocity and surface roughness on mass transfer. *Limnol. Oceanogr.,* 42**,** 81-88.

TRENCH, R. K. 1987. Dinoflagellates in non-parasitic symbiosis. *In:* TAYLOR, F. J. R. (ed.) *The biology of dinoflagellates.* Oxford: Blackwell.

VAN HOOIDONK, R. V., MAYNARD, J. A., MANZELLO, D. & PLANES, S. 2013. Opposite latitudinal gradients in projected ocean acidification and bleaching impacts on coral reefs. *Global Change Biology,* 20**,** 103-112.

VAN WOESIK, R., IRIKAWA, A., ANZAI, R. & NAKAMURA, T. 2012. Effects of coral colony morphologies on mass transfer and susceptibility to thermal stress. *Coral Reefs,* 31**,** 633-639.

VENN, A., TAMBUTTE, E., HOLCOMB, M., ALLEMAND, D. & TAMBUTTE, S. 2011. Live Tissue Imaging Shows Reef Corals Elevate pH under Their Calcifying Tissue Relative to Seawater. *Plos One,* 6**,** e20013.

VIECHTBAUER, W. 2010. Conducting meta-analyses in R with the metafor package. *Journal of Statistical Software,* 36**,** 1-48.

WANGPRASEURT, D., LARKUM, A. W. D., FRANKLIN, J., SZABO, M., RALPH, P. J. & KUHL, M. 2014. Lateral light transfer ensures efficient resource distribution in symbiont-bearing corals. *The Journal of Experimental Biology,* 217**,** 489-498.

WANGPRASEURT, D., WEBER, M., ROY, H., POLERECKY, L., DE BEER, D., SUHARSONO & NUGUES, M. M. 2012. In situ oxygen dynamics in coral-algal interactions. *Plos One,* 7**,** e31192.

WEBSTER, N. S., UTHICKE, S., BOTTE, E. S., FLORES, F. & NEGRI, A. 2013. Ocean acidification reduces induction of coral settlement by crustose coralline algae. *Global Change Biology,* 19**,** 303-315.

WEIL, E., SMITH, G. & GIL-AGUDELO, D. L. 2006. Status and progress in coral reef disease research. *Diseases of Aquatic Organisms,* 69**,** 1-7.

WIJGERDE, T., JURRIAANS, S., HOOFD, M., VERRETH, J. A. J. & OSINGA, R. 2012. Oxygen and heterotrophy affect calcification of the scleractinian coral *Galaxea fascicularis*. *Plos One,* 7**,** doi:10.1371/journal.pone.0052702.

WIJGERDE, T., SILVA, C. I., SCHERDERS, V., VAN BLEIJSWIJK, J. & OSINGA, R. 2014. Coral calcification under daily oxygen saturation and pH dynamics reveals the important role of oxygen. *Biology Open,* 3**,** 489-493.

WILKINSON, C. R. 1999. Global and local threats to coral reef functioning and existence: review and predictions. *Mar. Freshwater. Res.,* 50**,** 869-878.

WILLAIMS, S. L. & CARPENTER, R. C. 1988. Nitrogen-limited primary productivity of coral reef algal turfs: Potential contibution of ammonium excreted by Diadema antillarum. *Mar. Ecol. Prog. Ser.,* 47**,** 145-152.

WOLF-GLADROW, D., BIJMA, J. & ZEEBE, R. E. 1999. Model simulation of the carbonate chemistry in the microenvironment of symbiont bearing foraminifera. *Marine Chemistry,* 64**,** 181-198.

YATES, K. K. & HALLEY, R. B. 2006. CO32- concentration and pCO2 thresholds for calcification and dissolution on the Molokai reef flat, Hawaii. *Biogeosciences Discussions,* 3**,** 123-154.

ZEEBE, R. E. & WOLF-GLADROW, D. 2001. *CO_2 in Seawater: Equilibrium, kinetics, isotopes,* Amsterdam.

ZUUR, A. F., IENO, E. N., WALKER, N. J., SAVELIEV, A. A. & SMITH, G. M. 2009. *Mixed effects models and extensions in ecology with R,* New York, Springer.

Reference	Type	Genus species	Study specimen origin	Carbonate manipulation method	Calcification measurement method	Growth rate classification	Reference for growth rate	Duration of study	Range of $\Omega_{aragonite}$ used	Temperature	Salinity	Light	Nutritional state	Slope	Standard deviation of residual variation
Holcomb, M. et. al. 2010. J. Exp. Mar. Biol. Ecol. 386:27-33	Single species	Astrangia poculata	Field collected	CO_2 bubbling	Both	Slow	Holcomb et al 2010	6 mths	1.82-2.94	25.8	31	40 - 115 umol/m2/s-1	Fed	44.42	32.91
Rodolfo-Metalpa, R. et. al. 2010. Biogeosciences 7:289-300	Single species	Cladocora caespitosa	Field collected	CO_2 bubbling	Alkalinity anomaly	Slow	Rodolfo-Metalpa et al 2006	1 mth	2.68-3.77	21.7	38	15 - 60 umol/m2/s-1	Naturally fed	6.30	6.22
Rodolfo-Metalpa, R. et. al. 2010. Biogeosciences 7:289-300	Single species	Cladocora caespitosa	Field collected	CO_2 bubbling	Alkalinity anomaly	Slow	Rodolfo-Metalpa et al 2006	1 mth	2.78-3.86	24.5	38	15 - 60 umol/m2/s-1	Naturally fed	9.13	4.36
Rodolfo-Metalpa, R. et. al. 2010. Biogeosciences 7:289-300	Single species	Cladocora caespitosa	Field collected	CO_2 bubbling	Buoyant weighing	Slow	Rodolfo-Metalpa et al 2006	1 yr	1.8-3.8	19	38	15 - 60 umol/m2/s-1	Naturally fed	25.67	15.94
Jury, C.P. et. al. 2010. Global Change Biology 16:1632-1644	Single species	Madracis auretenra	Field collected	CO_2 bubbling	Alkalinity anomaly	Slow	Harriott 1999	2 hrs	1.74-4.26	28	36	200 umol/m2/s-1	Not fed	16.20	1.57
Krief, S. et. al. 2010. Geochimica et Cosmochimica Acta 74: 4988-5001	Single species	Porites porites	Field collected	CO_2 bubbling	Buoyant weighing	Slow	Clark and Edwards 1995	13 mths	0.72-4.23	25	40.7	200 umol/m2/s-1	Naturally fed	24.37	25.02
Krief, S. et. al. 2010. Geochimica et Cosmochimica Acta 74: 4988-5001	Single species	Stylophora pistillata	Field collected	CO_2 bubbling	Buoyant weighing	Fast	Gomez et al 1985	13 mths	0.72-4.23	25	40.7	200 umol/m2/s-1	Naturally fed	9.09	6.71
Bates, N.R. et. al. 2010. Biogeosciences 7:2509-2530	Field study	Mixed			Buoyant weighing			2 yrs	1.25-2.56	24	36.5		Naturally fed	24.44	8.25
Reis, J.B. et. al. 2010. Coral Reefs 29:661-674	Single species	Oculina arbuscula	Field collected	CO_2 bubbling	Buoyant weighing	Slow	Rodolfo-Metalpa et al 2006	8 wks	0.8-2.6	25	31.6	426 Watts /m2	Fed	25.63	6.03
Hii, Y.S. et. al. 2009. Journal of Marine Biology 2009:1-7	Single species	Porites cylindrica	Field collected	CO_2 bubbling	Alkalinity anomaly	Slow	Clark and Edwards 1995	15 days	1.56-2.6	27	35	392 umol/m2/s-1	Not fed	66.04	44.26
Anthony, K.R.N. et. al. 2008. PNAS 105:17442-17446	Single species	Acropora intermedia	Field collected	CO_2 bubbling	Buoyant weighing	Fast	Gomez et al 1985	8 wks	1.65-4.61	25	35	700 - 1200 umol/m2/s-1	Naturally fed	11.24	2.72
Anthony, K.R.N. et. al. 2008. PNAS 105:17442-17446	Single species	Porites lobata	Field collected	CO_2 bubbling	Buoyant weighing	Slow	Clark and Edwards 1995	8 wks	1.65-4.61	25	35	700 - 1200 umol/m2/s-1	Naturally fed	14.15	5.20
Marubini, F. et. al. 2008. Coral Reefs 27:491-499	Single species	Stylophora pistillata	Field collected	Acid addition	Buoyant weighing	Fast	Gomez et al 1985	8 days	1.35-5.37	26.5	38.3	300 umol/m2/s-1	Not fed	9.66	2.91
Schneider, K. & Erez, J. 2006. Limnol. Oceanogr. 51:1284-1293	Single species	Acropora eurystoma	Field collected	Acid addition	Alkalinity anomaly	Fast	Gomez et al 1985	2 hrs	0.78-6.77	24	40.7	350 umol/m2/s-1	Not fed, but naturally fed between runs	20.81	5.74
Renegar, D.A. & Riegl, B.M. 2005. Mar. Ecol. Prog. Ser. 293:69-76	Single species	Acropora cervicornis	Field collected	CO_2 bubbling	Buoyant weighing	Fast	Gomez et al 1985	4 wks	1.24-3.19	25.3	35.6	Not measured	Not disclosed	34.51	26.46
Langdon, C. & Atkinson, M.J. 2005. J. Geophys. Res. 110:C09S07	Mesocosm	Mixed	Field collected	Acid addition	Alkalinity anomaly			1.5 hrs	1.65-3.01	23.8	35	450 umol/m2/s-1	Not disclosed	39.59	7.68
Ohde, S. & Hussain, M.M.M. 2004. Geochemical Journal 38:613-621	Single species	Porites lutea	Field collected	Acid addition	Alkalinity anomaly	Slow	Clark and Edwards 1995	6 hrs	2.3-8.76	25	34.6	13 umol/m2/s-1	Not disclosed	36.70	8.14
Reynaud, S. et. al. 2003 Global Change Biology 9:1660-1668	Single species	Stylophora pistillata	Aquaria raised	CO_2 bubbling	Buoyant weighing	Fast	Gomez et al 1985	5 wks	2.85-3.96	25	38	380 umol/m2/s-1	Not disclosed	-25.25	7.16
Marubini, F. et. al. 2003. Proc. R. Soc. Lond. B 270:179-184	Single species	Acropora verweyi	Aquaria raised	Acid addition	Buoyant weighing	Fast	Gomez et al 1985	8 days	2.24-4.3	26.5	35	300 umol/m2/s-1	Not disclosed	7.70	2.77
Marubini, F. et. al. 2003. Proc. R. Soc. Lond. B 270:179-184	Single species	Galaxea fascicularis	Aquaria raised	Acid addition	Buoyant weighing	Slow	Orejas et al 2011	8 days	2.24-4.3	26.5	35	300 umol/m2/s-1	Not disclosed	8.77	3.26
Marubini, F. et. al. 2003. Proc. R. Soc. Lond. B 270:179-184	Single species	Pavona cactus	Aquaria raised	Acid addition	Buoyant weighing	Slow	Guzman and Cortes 1989	8 days	2.24-4.3	26.5	35	300 umol/m2/s-1	Not disclosed	9.62	1.71
Marubini, F. et. al. 2003. Proc. R. Soc. Lond. B 270:179-184	Single species	Turbinaria reniformis	Aquaria raised	Acid addition	Buoyant weighing	Fast	Orejas et al 2011	8 days	2.24-4.3	26.5	35	300 umol/m2/s-1	Not disclosed	6.49	1.25
Marubini, F. et. al. 2001. Mar. Ecol. Prog. Ser. 220:153-162	Single species	Porites compressa	Field collected	Acid addition	Buoyant weighing	Slow	Clark and Edwards 1995	6 wks	2.56-5.94	26.2	35	150 umol/m2/s-1	Not disclosed	11.61	2.58
Leclercq, N. et. al. 2000. Global Change Biology 6:329-334	Mesocosm	Mixed		CO_2 bubbling	Alkalinity anomaly			1 day	1.52-5.41	26	38	230 umol/m2/s-1	Naturally fed	8.08	2.84
Langdon, C. et. al. 2000. Global Biogeochemical Cycles 14:639-654	Mesocosm	Mixed		Acid addition	Alkalinity anomaly			3.8 yrs	1.58-4.4	25	35	92 - 289 umol/m2/s-1	Naturally fed	64.89	7.01

References

Clark S. and Edwards A.J. (1995) Coral transplantation as an aid to reef rehabilitation: evaluation of a case study in the Malidvies Islands. Coral Reefs 14:201-213

Gomez E.D., Acala A.C., Yap H.T., Alcala L.C., and Alino P.M. (1985) Growth studies of commercialy important scleractinians. Proceedings of the 5th International Coral Reef Symposium, Tahiti 6:199-204

Harriot V.J. (1999) Coral growth in subtropical eastern Australia. Coral Reefs 18:291-291

Holcomb M, McCorkle DC, Cohen AL (2010) Long-term effects of nutrient and CO2 enrichment on the temperate coral Astrangia poculata (Ellis and Solander, 1786). Journal of Experimental Marine Biology and Ecology 386: 27-33

Orejas C, Ferrier-Pages C, Reynaud S, Tsounis G, Allemand D, Gili JM (2011) Experimental comparison of skeletal growth rates in the cold-water coral Madrepora oculata Linnaeus, 1758 and three tropical scleractinian corals. Journal of Experimental Marine Biology and Ecology 405: 1-5

Rodolfo-Metalpa R, Richard C, Allemand D, Ferrier-Pages C (2006) Growth and photosynthesis of two Mediterranean corals, Cladocora caespitosa and Oculina patagonica, under normal and elevated temperatures. Journal of Experimental Marine Biology and Ecology 209: 4546-4556

List of studies included in the meta-analysis, including references, species, study specimen origin, carbonate manipulation method, calcification measurement method, growth rate classification, reference for the growth rate classification (if different from the study reference), duration of study, range of Ω_{Arag} used, temperature, salinity, slope and standard deviation.

Appendix B

Procedure for random effects meta-analysis

Random-effects meta-analysis is a two step process. Step one involves conducting a fixed effects meta-analysis to determine the between study variance. Step two produces the random effects estimates, which involves using the estimate in step one to partition the total variance into among-study and within-study components.

In the first step, the combined slope, m_c is expressed as a weighted average of slopes:

$$m_c = \sum_{i=1}^{k} w_i m_i \Big/ \sum_{i=1}^{k} w_i$$

where k is number of studies, m_i is the estimated slope of the calcification-Ω_{arag} relationship from the ith study, and w_i is the study-specific weight of study i (Borenstein et al 2009). Weights are simply the reciprocal of the variance (i.e. the square of the slope standard error) of the slope estimate, $w_i=1/v_i$. The variance of the combined slope, m_c, is thus given by:

$$S^2_{m_c} = 1/\sum_{i=1}^{k} w_i$$

(note that this represents measurement uncertainty around the mean slope, not the total amount of among-study variation).

The Q statistic, which is used to test for heterogeneity of variance, was then calculated by:

$$Q = \sum_{i=1}^{k} w_i m_i^2 - \frac{\left(\sum_{i=1}^{k} w_i m_i\right)^2}{\sum_{i=1}^{k} w_i}$$

And the between-study variance, τ^2, was calculated as:

$$\tau^2 = \begin{cases} \dfrac{Q - df}{C} \; if \; Q > df \\ 0 \; if \; Q \leq df \end{cases}$$

where C is a scaling factor to ensure that τ^2 has the same units as the within-study variance, and calculated by

$$C = \sum w_i - \frac{\sum w^2_i}{\sum w}$$

and *df* (degrees of freedom) is number of studies minus 1.

In the second step, the combined (within and between study) variance for each study is

$$^{*} v_i = v_i + \tau^2$$

Combined slope, variance and 95% confidence intervals are then re-calculated as done in step one but with the study weights w_i^* set equal to $1/v_i$, instead of $1/v_i$, as in step one.

Quantifying variance between studies

The I^2 statistic, the ratio of excess dispersion to total dispersion, was calculated by

$$I^2 = \left(\frac{Q - df}{Q}\right) \times 100\%$$

I^2 values of 25%, 50% and 75% have been suggested as indicative of low, moderate and high variance respectively (Higgins et al 2003).

Testing for between-group differences

The estimated difference between two effects is

$$\mu_{Diff} = M_B - M_A$$

where M_A & M_B are the mean estimated slopes for groups A & B, calculated according to eq. 1

The standard error of this estimated difference is

$$\sigma_{Diff} = \sqrt{V_{M_A} + V_{M_B}}$$

And thus the Z-statistic is

$$Z_{Diff} = \frac{\mu_{Diff}}{\sigma_{Diff}}$$

Under the null hypothesis that the true mean effect size μ is the same for both groups

$$H_0: \mu_A = \mu_B$$

Z_{Diff} would follow the normal distribution. For a two-tailed test the *p*-value is given by

$$p = 2\,[1 - (\Phi(|Z_{Diff}|))]$$

Meta-regression procedure

As with the original meta-analysis, meta-regression involves, first, a fixed effects meta-regression to determine the between study variance, followed by a random effects step that partitions the total variance into among-study and within-study components.

In step one, the fixed effects weighted regression uses the model:

$$m_i \sim \mathrm{N}(\alpha + \hat{\beta} x_i, v_i)$$

Where m_i is the estimated slope of the calcification-Ω_{arag} relationship from study i, x_i is the value of the explanatory variable (log(study duration) or log(irradiance level), depending on the meta-regression) in study i, v_i is the variance of the estimated slope within study i, β represents the change in the calcification-Ω_{arag} slope per unit change in the explanatory variable, and $\hat{\alpha}$ is the intercept of the relationship between the calcification-Ω_{arag} slope, and the explanatory variable (Thompson & Sharp 1999). $N(\hat{\alpha}+\hat{\beta}x_i, v_i)$ denotes a normal distribution with mean $\hat{\alpha}+\hat{\beta}x_i$ and variance v_i. Maximum likelihood estimates of $\hat{\alpha}$ and β were obtained by weighted least squares regression (glm() in R) of m_i on x_i, with weights $w_i = 1/v_i$

The moment estimator of between-study variance, τ^2, was calculated as

$$\tau^2 = \frac{Q-(k-2)}{F(w,x)} \text{ if } Q > k-2, \text{ or 0 otherwise}$$

where

$$Q = \sum w_i (y_i - \hat{\alpha} - \hat{\beta}x_i)^2$$

k is the number of studies, and

$$F(w,x) = \sum w_i - \frac{\sum w_i^2 x_i^2 - 2\sum w_i^2 x_i \sum w_i x_i + \sum w_i \left(\sum w_i x_i\right)^2}{\sum w_i \sum w_i x_i^2 - \left(\sum w_i x_i\right)^2}$$

In step two, the random effects weighted regression uses the model

$$m_i \sim N(\hat{\alpha}^* + \hat{\beta}^* x_i, v_i^*)$$

Where $v_i^* = v_i + \tau^2$, and estimates of $\hat{\alpha}^*$ and $\hat{\beta}^*$ were obtained in the same way as $\hat{\alpha}$ and $\hat{\beta}$, except with weights $w_i^* = 1/(v_i + \tau^2)$ used in place of $w_i = 1/v_i$.

Publication Bias

The fail-safe number (X) is:

$$X = \frac{(\sum Z_j)^2}{2.706} - K$$

where $Z_j = Z_{rj}\sqrt{(N_j - 3)}$, Z_{rj} is Fisher's z-transformed correlation coefficient for the relationship between calcification and $\Omega_{Aragonite}$ for sample j, N_j is sample size for sample j and K is the number of studies (Moller and Jennions 2001). The z-test value 2.706 (=1.645^2) is based on a one-tailed p value of 0.05 (Moller and Jennions 2001). Fisher's z-transformed correlation coefficient is:

$$Z_{rj} = \frac{1}{2} ln \frac{1+r}{1-r}$$

where r is the correlation coefficient between calcification and Ω_{Arag}.

References

Borenstein M, Hedges LV, Higgins JPT, Rothstein HR (2009) Introduction to Meta-Analysis. John Wiley & Sons, Hoboken, NJ, USA

Higgins J, Thompson SG, Deeks JJ, Altman DG (2003) Measuring inconsistency in meta-analysis. BMJ 327: 557-560

Moller AP, Jennions MD (2001) Testing and adjusting for publication bias. TRENDS in Ecology & Evolution 16: 580-586

Thompson SG, Sharp SJ (1999) Explaining heterogeneity in meta-analysis: A comparison of methods. Statist. Med. 18: 2693-2708

Appendix C

Slow growing (decreased mortality) model

Demographic functions for the slow growing species (decreased mortality) (a) survival plotted against area at year t and (b) colony size structure at year 2014

(a)

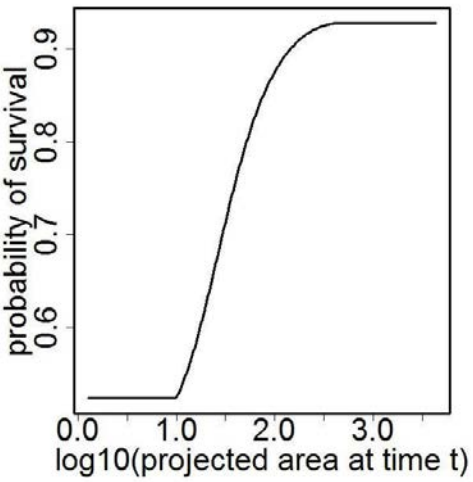

(b)

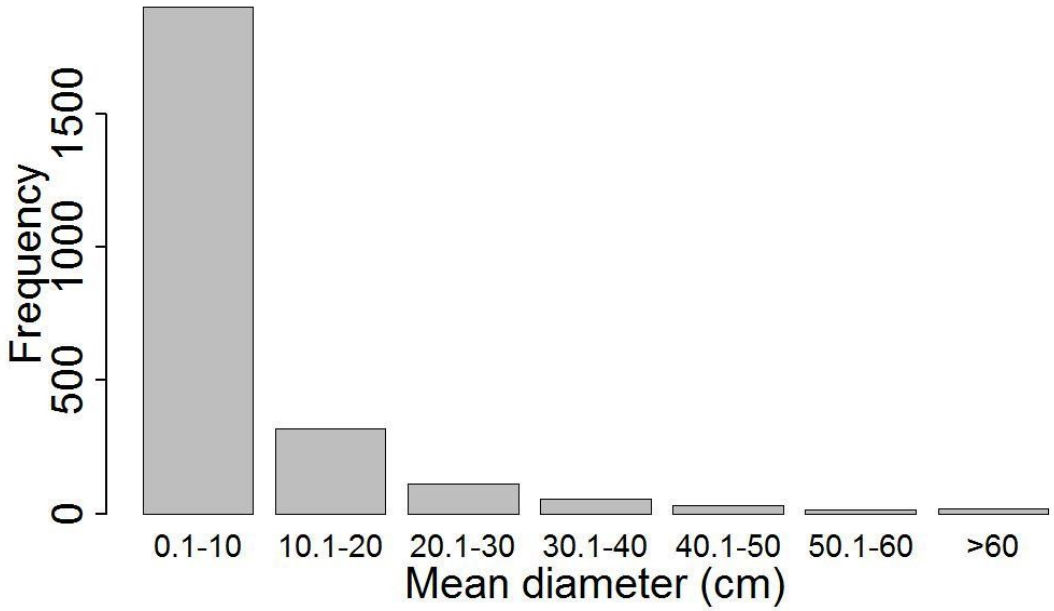

Results from the slow growing (decreased mortality) model. (a) Model projections of the effects of ocean acidification under RCP 6.0 on the long term population growth rate. (b) Sensitivity of λ to ±10% changes in growth and recruitment/fecundity. (c) Sensitivity of λ to conversion factor for calcification to growth. (d) Comparison of long term population growth rate produced by model with effect of ocean acidification on both growth and reproduction against the sum of the results from models with effect of ocean acidification on either growth and reproduction

(a) (b)

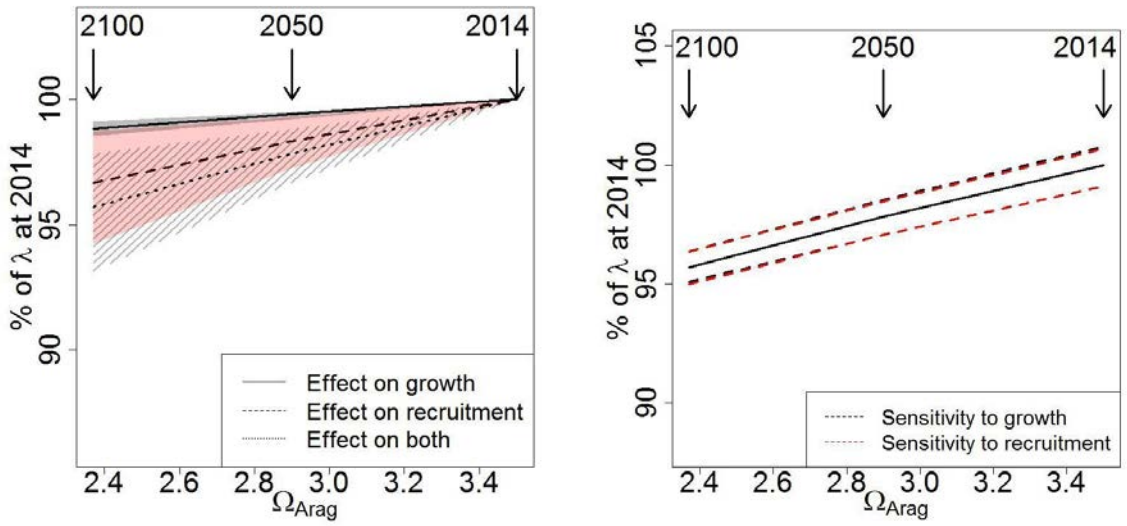

(c)

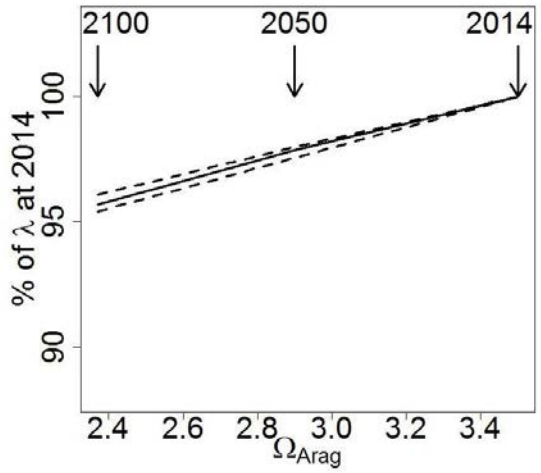
2100
2050
2014
% of λ at 2014
90
95
100
2.4
2.6
2.8
3.0
3.2
3.4
Ω_{Arag}

(d)

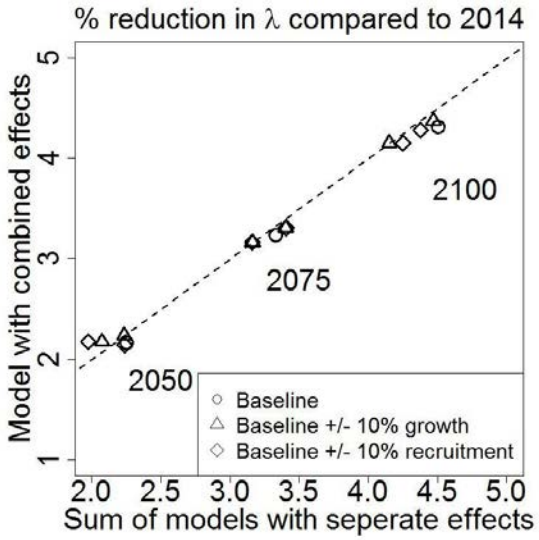
% reduction in λ compared to 2014
Model with combined effects
1
2
3
4
5
2100
2075
2050
Baseline
Baseline +/- 10% growth
Baseline +/- 10% recruitment
2.0
2.5
3.0
3.5
4.0
4.5
5.0
Sum of models with seperate effects

Appendix D

Model selection for flow-ocean acidification experiments (Chapter 4)

Flow diagram of model selection for calcification (a), photosynthesis, and calcification/photosynthesis (c) based on Likelihood Ratio statistics. We first tested for temporal auto-correlation (using REML estimation) and then tested for a significant tank effect (using ML estimation). For temporal auto-correlation, we fit a number of structures (compound symmetry & auto-regressive moving average (ARMA) models) and the best-fitting structure was then compared with a model including no temporal autocorrelation. Likelihood ratio test statistics comparing models with and without temporal autocorrelation shown on the Figure are those for this latter comparison. To test for the tank effect, we included tank in the model as a fixed effect, and starting with the most complex model (with three way interaction between Ω_{Arag}/DIC, flow and tank), selected for the optimal fixed effects structure. Values on arrows represent the Likelihood ratio when comparing the two alternative models connected by the arrow. Asterisks (*) indicate $p < 0.05$; the arrow indicates the direction of preference i.e. points to the favoured model. Solid lines indicate that the more complex model is significantly better (at $\alpha = 0.05$); dashed lines indicate that the more complex model is not significantly better (in which case the simpler model is preferred).

(a)

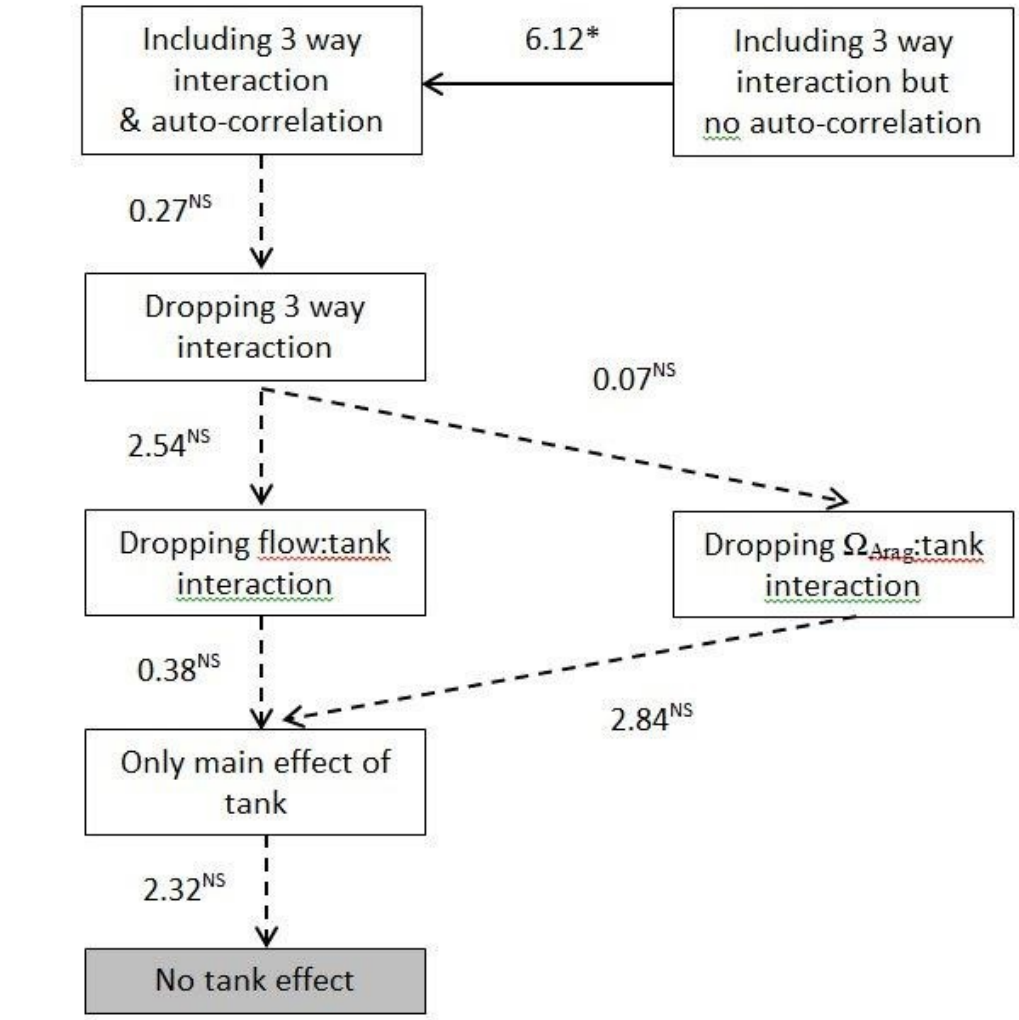
Including 3 way interaction & auto-correlation
6.12*
Including 3 way interaction but no auto-correlation
0.27NS
Dropping 3 way interaction
0.07NS
2.54NS
Dropping flow:tank interaction
Dropping ΩArag:tank interaction
0.38NS
2.84NS
Only main effect of tank
2.32NS
No tank effect

(b)

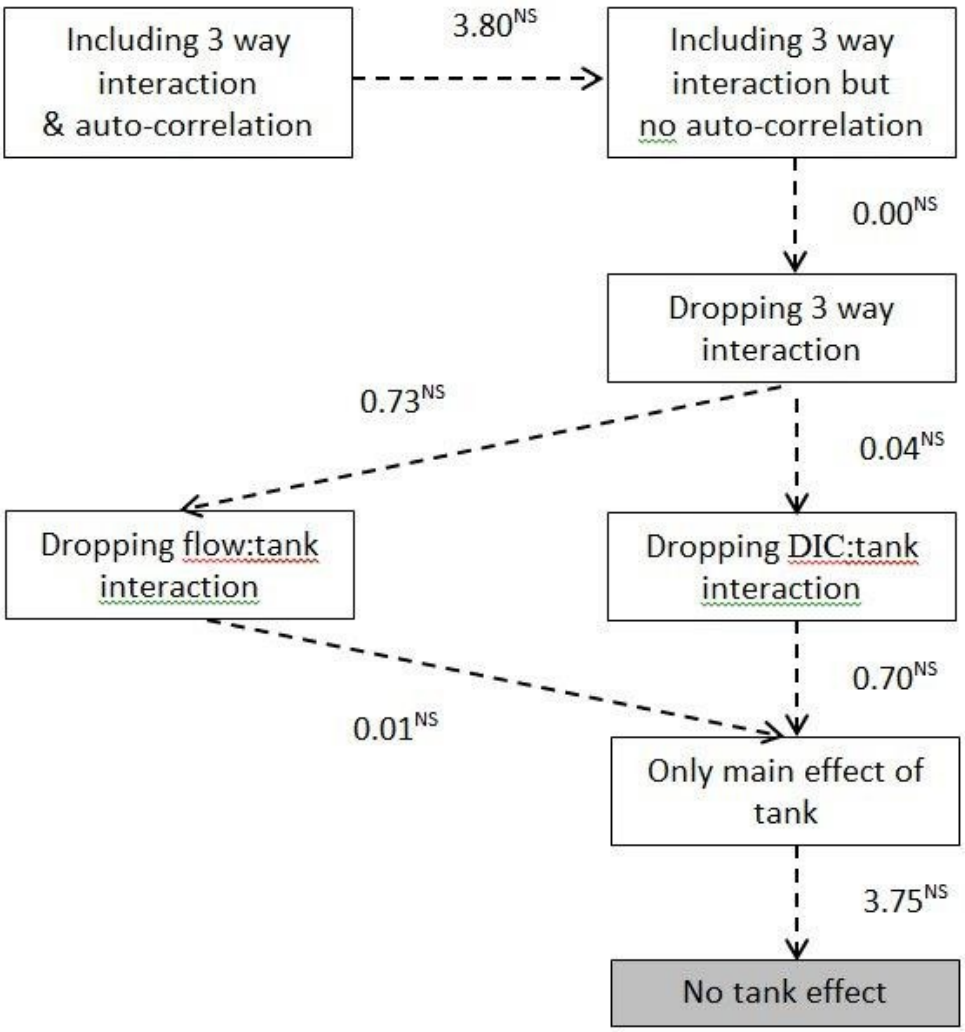
Including 3 way interaction & auto-correlation
3.80NS
Including 3 way interaction but no auto-correlation
0.00NS
Dropping 3 way interaction
0.73NS
0.04NS
Dropping flow:tank interaction
Dropping DIC:tank interaction
0.70NS
0.01NS
Only main effect of tank
3.75NS
No tank effect

(c)

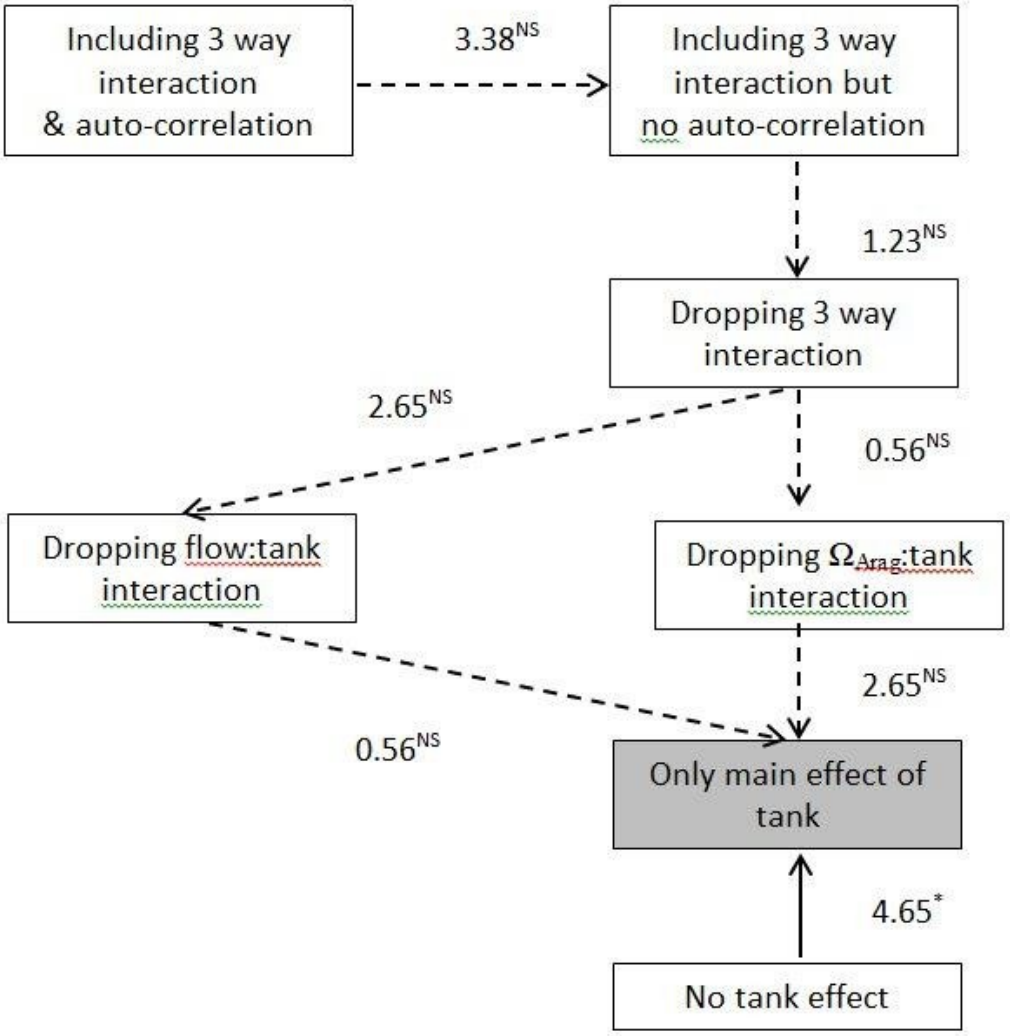
Including 3 way interaction & auto-correlation
3.38NS
Including 3 way interaction but no auto-correlation
1.23NS
Dropping 3 way interaction
2.65NS
0.56NS
Dropping flow:tank interaction
Dropping ΩArag:tank interaction
2.65NS
0.56NS
Only main effect of tank
4.65*
No tank effect

Appendix E

Methods for pilot study on Heron Island (Chapter 5)

The study was carried out over 2 weeks from mid to late September 2013 at Heron Island (151°55'E, 23°26'S) on the Great Barrier Reef, Australia. Colonies of *Goniastrea aspera* and *Stylophora pistillata* (~5cm diameter) were collected at low tide from Shark Bay. Colonies were returned to the Heron Island Research Station and allowed to recover in the outdoor aquaria for a day before the start of experiments. Holding tanks were shaded by shade cloth. Colonies were then placed in a 0.15m wide by 0.15m deep by 1m long recirculating flumes (see Chapter 4 for details). O_2 profiles within the boundary layer were measured under 4 flow velocities (2, 5, 10 & 15 cms^{-1}) using Clark type O_2 microsensors (as described in Chapter 5). Visible light was provided by a tungsten-halogen lamp of constant colour temperature (Schott KL1500). All measurements were carried out at an irradiance of 800 μmol photons $m^{-2}s^{-1}$. Measurements were done with the microelectrodes mounted at a 25° angle and light mounted vertically. Measurements were carried out at a temperate of 24°C and in water salinity of 36 ppt. Measurements were taken at branch tips for branching species and on the coenosarc for massive species as these regions of the coral have been shown to have the highest calcification rate for each morphology respectively (de Beer et al 2000, Jokiel 2011).

a) b)

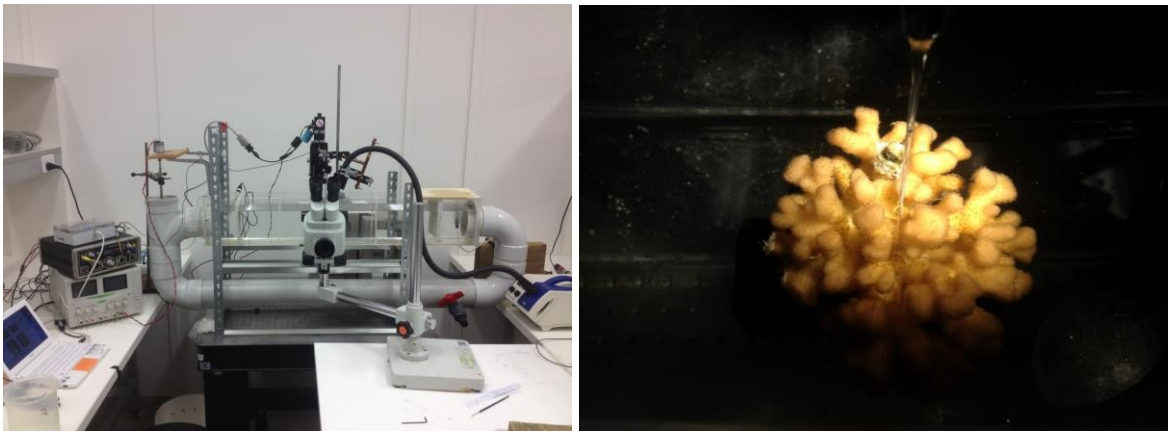

Figure AE.1 Images of the experimental setup. a) The flume b) Example of a colony used